Mechanical Analysis for New and Spent Fuel Storage Racks

Revision 2

Non-Proprietary

January 2017

REVISION HISTORY

Revision	Date	Page	Description
0	December 2014	All	First Issue
1	April 2015	38 44 45 50 to 51	The following item was revised to incorporate result of the drop analysis of transport container handling tool. Added transport container handling tool Added transport container handling tool Added container handling tool drop evaluation Revised references
2	January 2017	All	Complete revision to: • Incorporate in the responses to NRC Section 9.1.2 Requests for Additional Information pertaining to fuel racks and add Appendix A as a cross-reference. • Present revised seismic analysis based on use of ANSYS Version 15. • Present revised fuel assembly drop analysis based on use of finite element analysis.

ABSTRACT

This report documents the structural integrity of the new and the spent fuel storage racks under operating conditions including the accident scenarios for the APR1400 design. All analyses have been performed based on NRC guidance (e.g., Standard Review Plan Section 3.8.4, Appendix D).
This report describes the design features and geometry, fabrication sequence, structural and seismic analysis, and mechanical accident analysis for the new and the spent fuel storage racks for the APR1400 design.

The nonlinear dynamic analysis for the new and the spent fuel storage racks under operating conditions is performed using a single or a whole pool multi-rack analysis model with time-history seismic loads. The loads and the displacements are calculated to demonstrate the structural integrity of the new and the spent fuel storage racks. Overturning is evaluated by showing that the rack does not exhibit a rotation sufficient to bring the center of mass over a corner pedestal. The lateral impact load on the spent fuel assembly is evaluated for two acceptance criteria: fuel spacer grid buckling and fuel rod cladding yield stress. All stress evaluations for the fuel racks are performed based on the worst-case results from dynamic simulations in accordance with ASME Code Section III, Division 1, Subsection NF requirements for Class 3 component supports.

The mechanical accidents analyses for the spent fuel storage racks are performed based on each of the following scenarios: a stuck fuel assembly and drops of the fuel assembly along with the handling tool on a top edge of the rack, into an interior cell away from the support pedestals either along the outer edge or in the center, or into a cell located above a support pedestal. The new fuel storage racks are analyzed for a drop into an interior cell. For the drop accidents, the deformations of the cell wall and the baseplate are calculated by using dynamic finite element analysis. This will ensure that the configuration analyzed in the criticality evaluation remains valid and the deformed baseplate of the rack does not impact the pool liner (or underlying concrete for the new fuel storage racks). For the postulated stuck fuel uplift event, the structural integrity of the spent fuel storage racks is evaluated by using the classical strength of materials equation. This analysis is performed to demonstrate that the damage of the cell wall is limited to the portion of the rack structure above the neutron absorber.

Based results of the structural and seismic analysis, the spent fuel storage rack design is satisfactory:
(1) The rack pedestals do not slide off the embedment plates onto the spent fuel pool liner;
(2) The racks do not impact the spent fuel pool wall;
(3) Overturning of the racks does not occur;
(4) The fuel spacer grid does not buckle and the bending stress induced in the fuel rod cladding is well below the yield strength of the fuel rod clad; and
(5) The calculated stresses on the racks are below the allowable stress limits of the ASME Boiler and Pressure Vessel Code (B&PVC) Section III, Division 1, Subsection NF requirements for Class 3 component supports.

Similarly, the structural and seismic performance of the new fuel storage rack design is satisfactory:
(1) The racks do not impact the new fuel storage pit wall;
(2) The fuel spacer grid does not buckle and the bending stress induced in the fuel rod cladding is well below the yield strength of the fuel rod clad;
(3) Calculated stresses on the racks are below the allowable stress limits of the ASME B&PVC Section III, Division 1, Subsection NF requirements for Class 3 component supports; and
(4) The studs holding the racks in place are not overstressed.

The mechanical accident analysis demonstrates that the new and spent fuel storage racks meet the applicable regulatory acceptance criteria for structural integrity and prevention of damage to underlying structure.

Therefore, the new and the spent fuel storage racks for the APR1400 design are consistent with the acceptance criteria of the NRC Standard Review Plan.

Page intentionally blank

TABLE OF CONTENTS

Contents

LIST OF TABLES

LIST OF FIGURES

ACRONYMS AND ABBREVIATIONS

ASME	American Society of Mechanical Engineers
COF	coefficient of friction
E-W	east-west
KEPCO	Korea Electric Power Corporation
KHNP	Korea Hydro & Nuclear Power Co., Ltd.
NFP	new fuel storage pit
NFSR	new fuel storage rack
N-S	north-south
NRC	U.S. Nuclear Regulatory Commission
OBE	operating basis earthquake
PSD	power spectra density
PWR	pressurized water reactor
RG	regulatory guide
SFP	spent fuel pool
SFSR	spent fuel storage rack
SRP	standard review plan
SRSS	square root of the sum of the squares
SSE	safe shutdown earthquake
WPMR	whole pool multi-rack

Page intentionally blank

1 INTRODUCTION

The purpose of this report is to evaluate the structural adequacy of the APR1400 new fuel storage racks (NFSRs) and the spent fuel storage racks (SFSRs) under normal operating conditions and postulated accident scenarios. All analyses are performed based on U.S. Nuclear Regulatory Commission (NRC) guidance (e.g., Standard Review Plan (SRP) Section 3.8.4, Appendix D (Reference 1)).

Section 2 describes the design features and fabrication process for the APR1400 NFSRs and the SFSRs. Section 3 includes the analysis methods, acceptance criteria, modeling assumptions, significant results of dynamic simulations, and stress evaluations for a seismic loading. Section 4 presents the methodology, assumptions, and significant results of accident scenarios involving dropped and stuck fuel assemblies.

2 FUEL RACKS

2.1 Description of New Fuel Storage Racks

Figure 2-1 shows the layout and the plan view of the two NFSR modules in the dry, unlined new fuel storage pit (NFP). Each rack module consists of a 7 x 8 array of storage cells that are bolted to the pit floor and supported by top, middle, and base plates and stiffeners as shown in Figure 2-2 and Figure 2-3. The NFSR modules have 112 storage cells, which provide more than enough locations to store a refueling batch. The center-to-center spacing between adjacent fuel assemblies is 35.5 cm (14 in) to maintain subcriticality without the use of neutron absorbers. The NFSR cell wall thickness is 6 mm (0.236 in). SA-240 Type 304L material is used for the cell walls, plates, stiffeners, and pedestals, and SA-564 Grade 630 is used for the stud bolt. The basic dimensions of the NFSR modules are summarized in Table 2-1.

2.2 Description of Spent Fuel Storage Racks

Figure 2-4 shows the layout of the SFSR modules in the spent fuel pool (SFP), which consists of two regions, Region I and Region II. Fresh fuel assemblies, spent fuel assemblies, and damaged fuel in canisters can be stored in Region I, which has the capacity to store one full core, one refueling batch, and five damaged fuel canisters. Region I consists of four 8 x 8 cell modules (A1-1, A1-2, A1-3 and A1-4) and two 6 x 8 cell modules (A2-1 and A2-2). Module A2-1 has five cells that can each contain a damaged fuel canister. Region II consists of nineteen 8 x 8 cell modules (B1, B2-1, B2-2, B2-3, B3, B4, B5-1, B5-2, B5-3, B5-4, B5-5, B5-6, B6-1, B6-2, B6-3, B7, B8, B9 and B10) and four 8 x 7 cell modules (C1, C2, C3 and C4). Figure 2-5 gives the dimensions of the gaps between cell walls when the rack baseplates are installed touching, as indicated in Figure 2-6.

As shown in Figure 2-7 through 2-10, the SFSR modules are free-standing with pedestals resting on embedment plates (the SFSRs do not rest on the liner or use bearing pads), which distribute the dead weight of the loaded racks to the reinforced concrete structure of the floor. Each SFSR module is supported by four pedestals, and each pedestal has a 7-inch diameter leveling foot that can be adjusted with a long-handled tool. The SFSR modules are submerged in borated water with space between the racks and the cell walls. Therefore, the motions of racks and the fuel assemblies will be influenced by fluid-structure interactions.

To maintain subcriticality, the center-to-center spacing between adjacent fuel assemblies is 27.5 cm (10.83 in) for Region I racks and 22.5 cm (8.86 in) for Region II racks. The cell wall thickness of the SFSRs is 2.5 mm (0.098 in). SA-240 Type 304L material is used for the cell walls, baseplate, and pedestal; SA-564 Grade 630 is used for the leveling foot; and a hot-rolled composite plate material (METAMIC^{TM}) is used as a neutron absorber. The basic dimensions of the SFSRs are summarized in Table 2-2.

2.3 Fuel Storage Rack Fabrication

As described above, all of the fuel storage racks are similar in concept. However, the NFSRs and the SFSRs for Regions I and II have slightly different fabrication sequences. Note that welds are visually inspected in each step before access to perform a weld inspection is blocked due to addition of subsequent parts.

2.3.1 Fabrication Procedure of NFSR and SFSR

The NFSRs and SFSRs are fabricated in accordance with a design specification (Reference 22) and manufacturing drawings. The following describes the expected fabrication sequence but actual work may differ, provided design specification and drawing requirements (e.g., dimensions, inspection acceptance criteria, quality assurance) are met.

TS

2.3.2 General Requirements

Fabrication of the new and spent fuel racks is in accordance with the requirements of Subsection NF of Section III of the ASME B&PV Code for component supports.

The fuel storage racks meet the guidance in NRC RG 1.29 (Reference 2) and ANSI/ANS 57.3 (Reference 3).

2.3.3 Quality Control and Quality Assurance

The new and spent fuel racks are Seismic Category I structures that are treated as safety-related components for determining Quality Assurance requirements (10 CFR 50, Appendix B) and periodic condition monitoring requirements (10 CFR 50.65 “Maintenance Rule”). The quality control requirements for the fuel storage racks are in accordance with 10 CFR 50, Appendix B.

The quality control procedures for the new and spent fuel storage racks are prepared in accordance with the requirements of:

- ASME B&PV Code, Section III, Div. 1, NF
- ASME NQA-1
- US Code of Federal Regulations, 10 CFR 50
- US NRC Regulatory Guide 1.28

2.3.4 Welding Requirements

Welding materials are selected and controlled to contain between 8 and 25 percent ferrite, as determined by Subsection NB-2433 of the ASME Code. Electrodes must conform to ASME SFA 5.4 or 5.9, Type 308. Processes are established for avoidance of sensitization of austenitic stainless steel, Type 308L is used as electrodes.

Austenitic stainless steel items are not allowed to be heated above 177°C (350°F) (except during welding), unless they are subsequently given a full solution anneal at temperatures recommended for the individual types of stainless steel followed by water quenching or spraying from the solution heat treating temperature to below 427°C (800°F) (or black metal) within three minutes.

The acceptance criteria for visual examination of all fuel rack welds comply with the ASME B&PV Code NF-5360 of Section III and T-952 of Section V.

2.3.5 Cleanliness

All internal and external surfaces are thoroughly cleaned of scale, dirt, chips, nonadherent weld spatter (which can be removed by power wire brushing), oil, grease, organic matter, loose particles, and all other potentially harmful materials. Adherent weld spatter on the interior surface of a fuel storage location must be removed, such that the function of the mock fuel assembly inspection gage is not hindered by weld spatter.

Components, parts and subassemblies that will have crevices or inaccessible surfaces after assembly, are required to be cleaned prior to assembly. Acidic materials are prohibited for use on items containing crevices or inaccessible areas where complete drainage, neutralization, or removal of residuals cannot be accomplished.

Cleaning of corrosion-resistant materials is required to be in accordance with ASME NQA-1 to the extent specified herein. The surfaces of cleaned components meet the requirements of ASME NQA-1, Part II, Subpart 2.1, Class C.

Table 2-1 NFSR Dimensions

No.	Description	Dimensions(*), mm (in)
1	Cell Length	4,570 (179.9)
2	Cell Thickness	6.0 (0.236)
3	Cell Inside Dimension (Width)	220.0 (8.66)
4	Cell Center-to-Center Pitch	355 (13.98)
5	Baseplate Thickness	25.0 (0.984)
6	Baseplate Flow Hole Diameter	127.0 (5.0)
7	Distance from Baseplate Bottom to Pit Floor	185.0 (7.28)
8	Intermediate Plate Thickness	50.0 (1.97)
9	Rack Pedestal Dimensions	380 x 380 x 135 (15 x 15 x 5.3)
10	Stud Bolt Diameter	90.0 (3.54)

(*) All of the dimensions are nominal values and taken from Reference 5.

Table 2-2 SFSR Dimensions

No.	Description		Dimensions(*), mm (in)
1	Cell Height from Baseplate Top to Rack Top		4,590 (180.7)
2	Cell Wall Thickness		2.5 (0.098)
3	Cell Inside Dimension(Width)		220.0 (8.66)
4	Damaged Fuel Canister Inside Dimension		242.0 (9.53)
5	Cell Pitch	Region I	275.0 (10.83)
		Region II	225.0 (8.86)
6	Baseplate Thickness		25.0 (0.984)
7	Baseplate Hole Diameter		133.0 (5.24)
8	Distance from Baseplate Bottom to Liner		160.0 (6.30)
9	Rack Female Pedestal Dimensions	Region I	297.5 x 297.5 x 145 (11.7 x 11.7 x 5.7)
		Region II	285 x 285 x 140 (11.2 x 11.2 x 5.5)
10	Male Pedestal Dia.		177.8 (7.0)
11	Neutron Absorber Material		METAMIC™
12	Neutron Absorber Length		
13	Neutron Absorber Width		
14	Neutron Absorber Thickness		
15	Neutron Absorber Sheathing Thickness	Inside	
		Outside	
16	Distance from Top of Rack Baseplate to Bottom of Neutron Absorber		

TS

(*) All of the dimensions are nominal values and taken from Reference 6.

TS

Figure 2-1 Layout and Plan View of NFSR

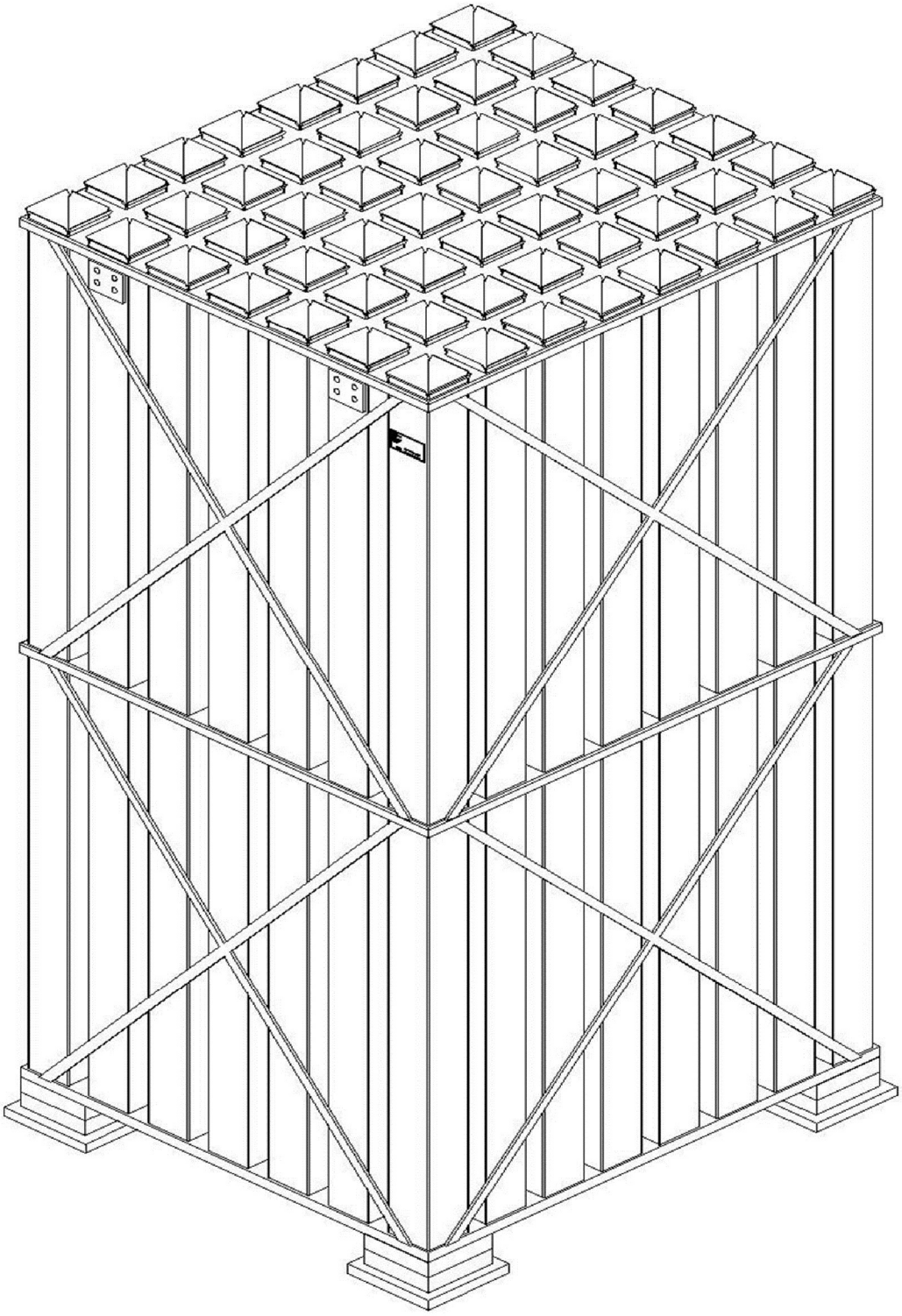

Figure 2-2 Isometric Schematic of NFSR

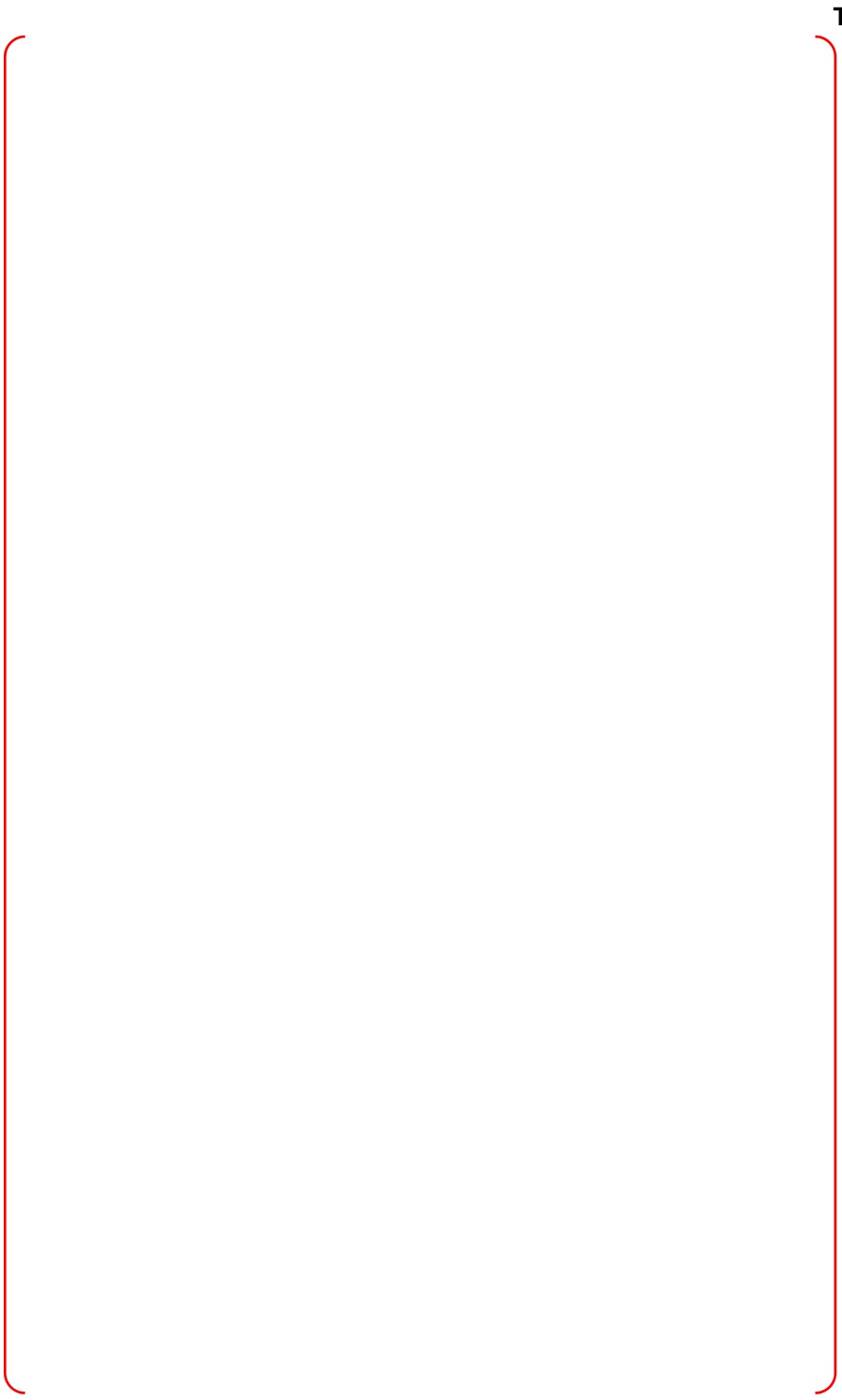

Figure 2-3 Configuration of NFSR

TS

Figure 2-4 Layout of SFSR

TS

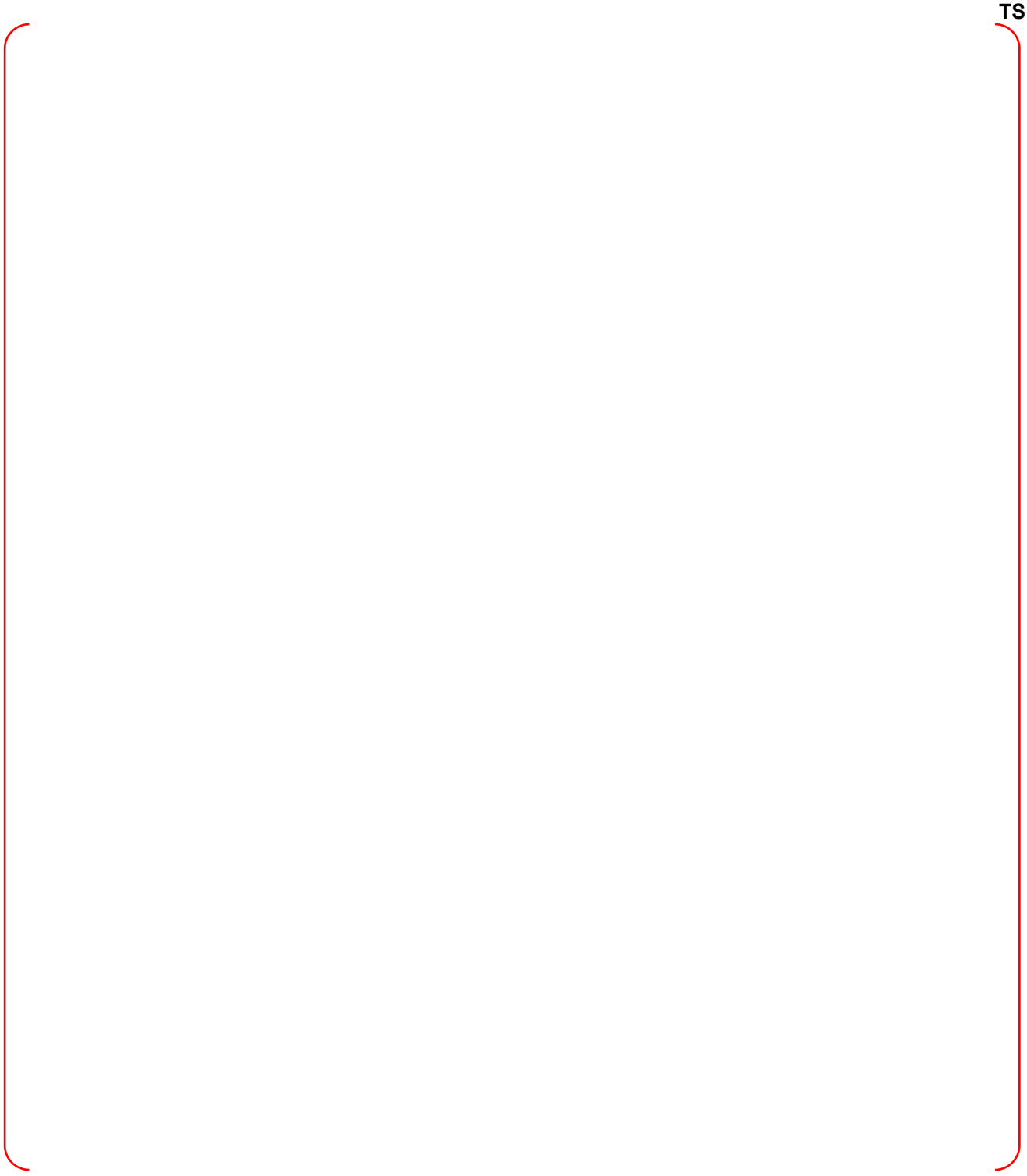

Figure 2-5 Plan View of SFSR Showing Rack Gaps above Baseplate Level

TS

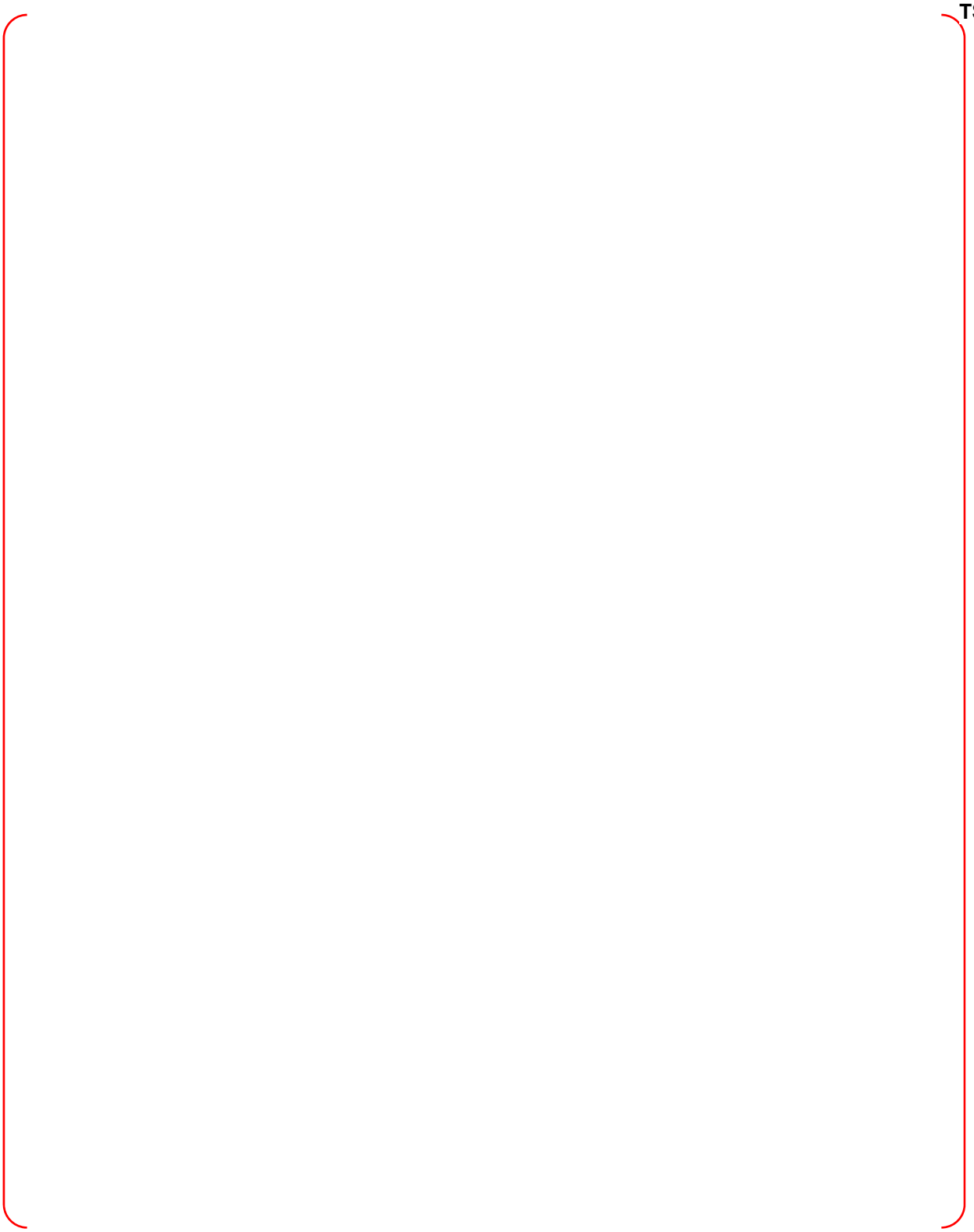

Figure 2-6 Plan View of SFSR Showing Rack Gaps at Baseplates

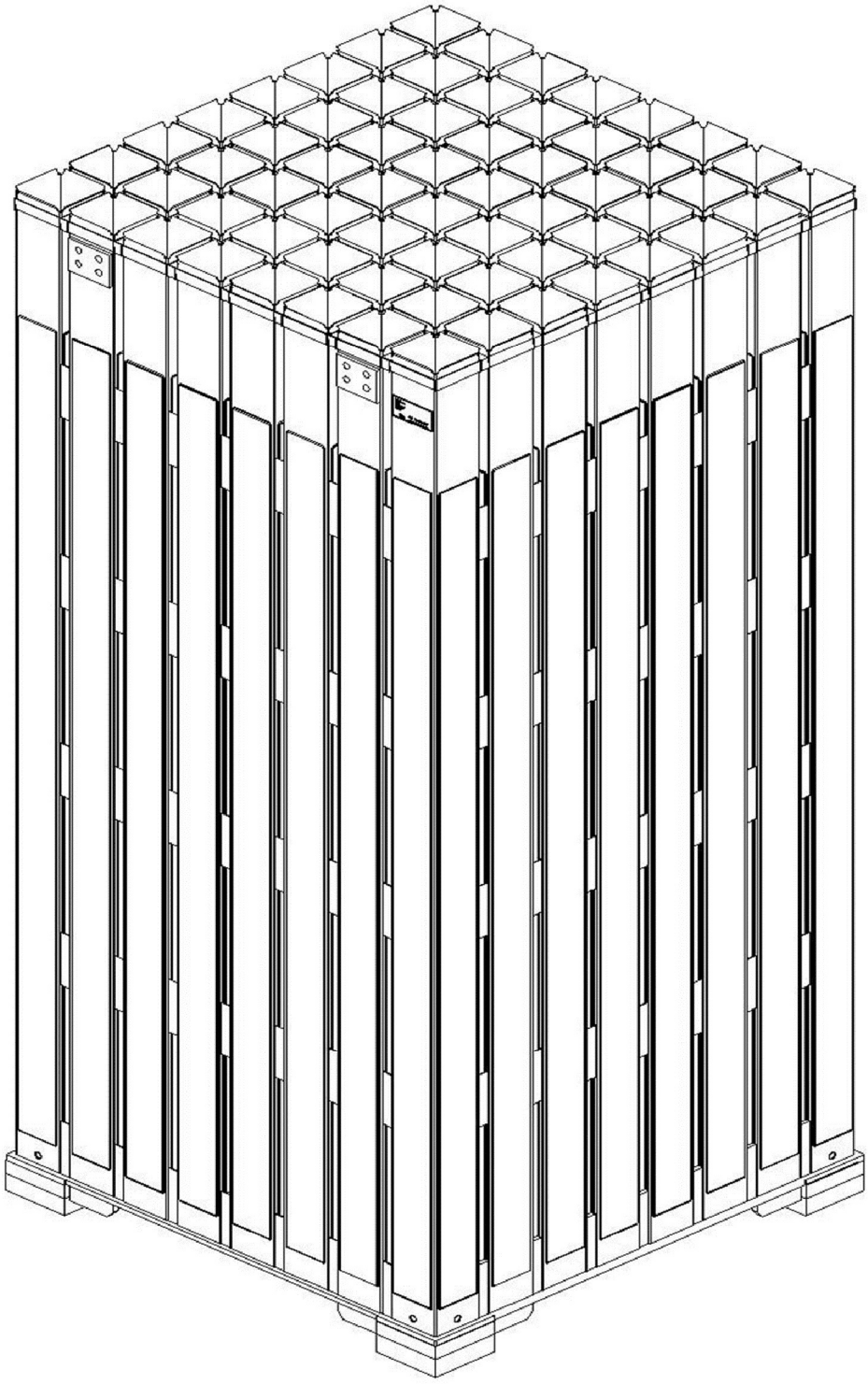

Figure 2-7 Isometric Schematic of SFSR (Region I)

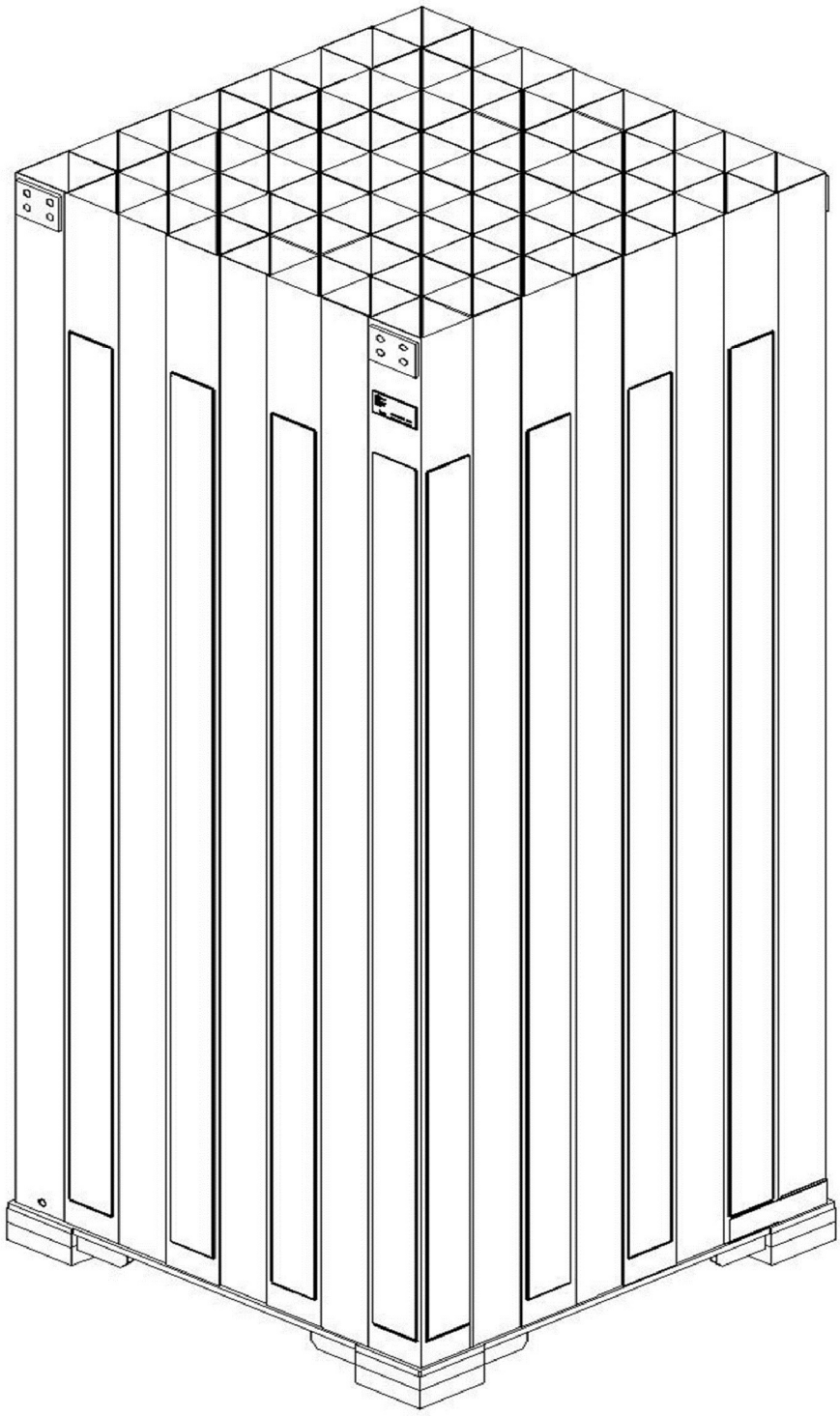

Figure 2-8 Isometric Schematic of SFSR (Region II)

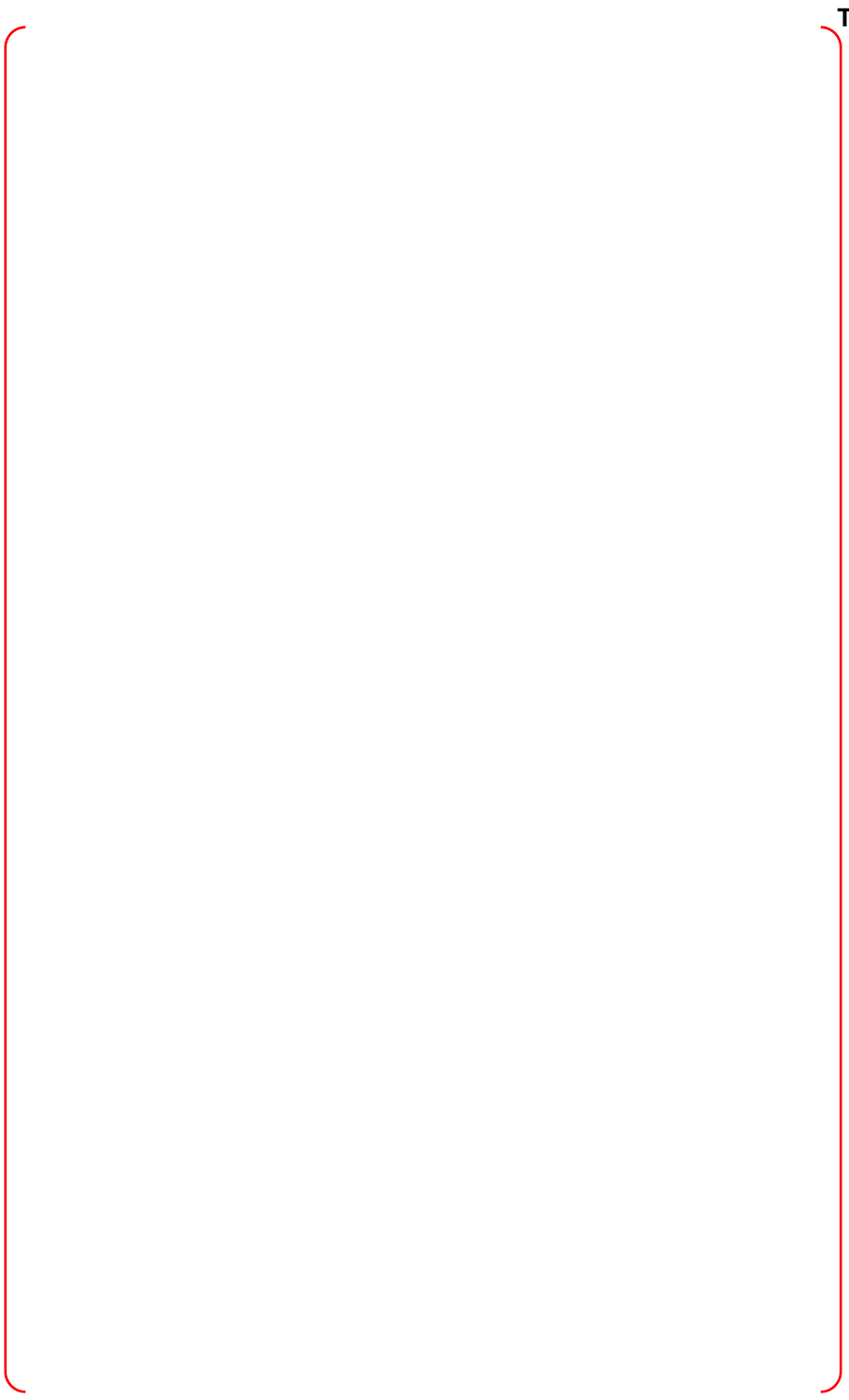

Figure 2-9 Configuration of SFSR (Region I)

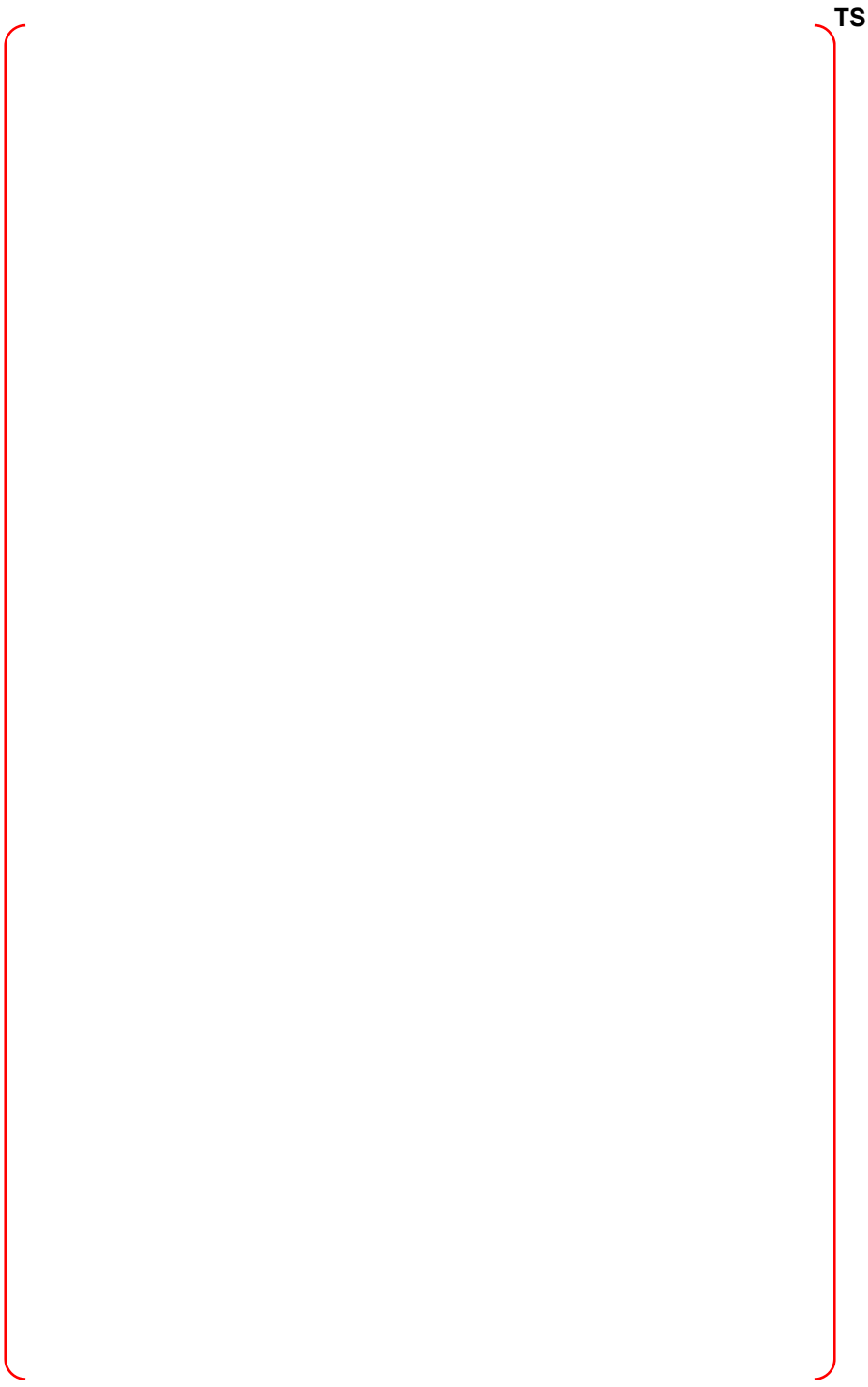

Figure 2-10 Configuration of SFSR (Region II)

TS

Figure 2-11 Region I SFSR Fabrication

TS

Figure 2-12 Region II SFSR Fabrication

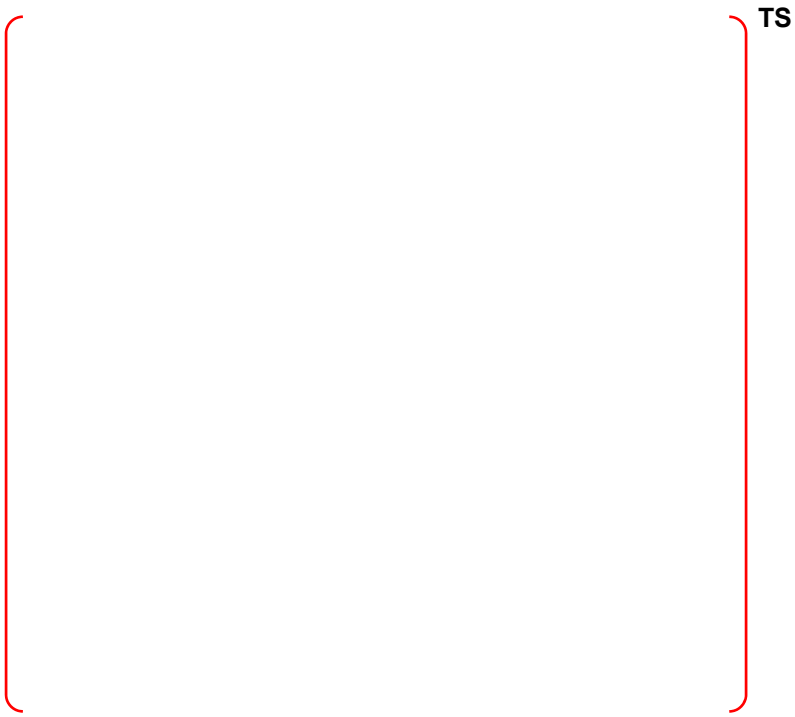

Figure 2-13 Position of “Inaccessible” Box Assembly to Baseplate Weld

Figure 2-14 Steps to Make “Inaccessible” Box Assembly to Baseplate Weld

TS

Figure 2-15 Visual Inspection of “Inaccessible” Cell to Baseplate Welds

3 STRUCTURAL AND SEISMIC ANALYSIS

The structural and seismic analysis for the NFSRs and the SFSRs described below includes dynamic analysis methodology, modeling details, acceptance criteria for kinematic and structural evaluation, assumptions, input data for racks and fuel assembly, and significant results of dynamic simulations under seismic loading.

3.1 Methodology

The response of a free-standing SFSR module to seismic input is highly non-linear and involves a complex combination of motions such as sliding, rocking, twisting, impacts, and friction effects. Linear methods, such as response spectrum analysis, cannot accurately simulate the structural response of such a highly non-linear structure to seismic excitation. An accurate evaluation of non-linear response requires a three dimensional time history analysis to establish the proper response during a seismic loading. The analysis method used to evaluate the new and spent fuel storage racks is summarized as follows:

- Synthetic acceleration time history input was developed to represent the seismic motion of the new fuel storage pit floor and the spent fuel pool floor and walls (Section 3.1.1).
- Adequacy of the time histories was checked (References 7 and 8) in accordance with SRP Section 3.7.1 (Reference 9).
- Detailed three dimensional finite element shell models were developed for each fuel rack type listed in Table 3-2 to determine overall stiffness parameters.
- A three-dimensional beam model of each rack type listed in Table 3-2 was developed based on the shell model stiffness parameters. In these models, the array of fuel assemblies within a single rack was represented by a single equivalent three dimensional beam model coupled to the rack beam model (Figure 3-1 and Figure 3-2).
- For the spent fuel pool, the individual rack-fuel models were duplicated and assembled into an array of rack models referred to as the Whole Pool Multi-Rack (WPMR) model (Figure 3-3).
- Analyses apply the three orthogonal time histories simultaneously. Multiple time history analyses were performed, each with a variation in a significant input parameter such as the friction coefficient between the rack pedestals and embedment plates (Table 3-5).
- Maximum displacements and loads were extracted from each case run (Table 3-6 through Table 3-8).
- The maximum loads were evaluated statically by calculating stresses in the rack components with traditional strength of materials methods (hand calculations) and compared to ASME code allowable stresses.

Although behavior of the NFSRs is not as complex since they are anchored to the embedment plates and not submerged in water, the same analysis method was used.

3.1.1 Acceleration Time Histories Generation

Five sets of artificial acceleration time histories for three orthogonal directions were developed specific to the NFSRs and SFSRs.

The fully-synthetic acceleration time histories were developed to match the safe shutdown earthquake (SSE) in-structure response spectra (ISRS) (i.e., no time history seed was used). For the NFSRs, the auxiliary building ISRS at elevation 137’-6” were used. For the SFSRs, response spectra were selected to envelope the ISRSs at the elevation of the spent fuel pool base (114'-0'') and the pool wall (132'-0''). The top of the SFSRs is at approximately elevation 130' with the bottom at about 115’.

Although previous versions did not discuss it, guidance in Revision 4 of SRP 3.7.1 discusses the need for artificial time histories to be corrected to remove displacement drift, which often occurs with recorded and

fully-synthetic acceleration time histories. The Lagrange multiplier method developed by Borsoi and Ricard (Reference 10) was used to change the initial accelerogram into a corrected accelerogram that is very close to the first one, but corrects unrealistic velocity and displacements shifts. Note that this same method has been implemented in the P-CARES (Probabilistic - Computer Analysis for Rapid Evaluation of Structures) code developed by Brookhaven National Laboratory for the NRC staff to use to perform evaluations of the seismic response of relatively simplified soil and structural models (Reference 11). NUREG/CR-6983 (Reference 12) discusses using the baseline correction method for shake table data analysis showing a large displacement drift. It points out that "the modification to the acceleration time history is small […]. More importantly, the change in the input motions due to baseline correction has virtually no effect in the analytical responses."

Figure 3-5 through Figure 3-7 for the NFSRs and Figure 3-8 through Figure 3-10 for the SFSRs show the five time histories (after spectral matching and displacement drift correction (Reference 13)) applied in each of the three orthogonal directions (N-S, E-W, and vertical). These artificial time histories have a duration of 25 seconds and meet the guidelines set forth in SRP 3.7.1, as discussed in the next section.

Consistent with Regulatory Guide 1.61, the 4% damped SSE response spectra were used to generate the synthetic time histories for the APR1400 fuel storage racks.

3.1.1.1 Adequacy Checks of Time Histories

The seismic analyses for the NFSRs and SFSRs consider five sets of artificial seismic time histories. Suitability of time-histories is verified according to SRP Section 3.7.1 Option 2 criteria for multiple sets of time histories. Option 2 identifies an acceptable method for time-history verification is through Approach 2 (Section II.1.B.ii of SRP 3.7.1) with certain criteria evaluated based on the average of the suite of multiple time histories.

The APR1400 DCD was docketed in March 2015. According to 10 CFR 52.47(a)(9), regulatory guidance formally issued up to six months prior to docketing is applicable, which would be Revision 3 of SRP 3.7.1. APR1400 DCD Tier 2 Section 1.9.2 acknowledges this regulatory provision. However, Tier 2 Table 1.9-2 identifies the applicable revision of SRP 3.7.1 as draft Revision 4. In general, a draft licensing document is not an appropriate reference since the NRC could alter guidance or acceptance criteria, but Revision 4 was not issued until December 2014, after the cutoff per 10 CFR 52.47(a)(9).

As documented in References 7 and 8, the time histories meet the acceptance criteria of SRP 3.7.1 Revision 3 as follows:

- ✓ A total duration of at least 20 seconds – met, duration is 25 seconds.
- ✓ Time increment of at most 0.010 seconds – met, increment is 0.010 seconds.
- ✓ Spectral acceleration computed at a minimum of 100 points per frequency decade – met, 100 points per frequency decade,
- ✓ Uniformly spaced over the log frequency scale from 0.1 Hz to 50 Hz frequency – met.
- ✓ Average of computed 5% damped[1] response spectra from the suite of multiple time histories:
  - Not more than 10% below target response spectrum at any one frequency – met, lowest value is 5.5% below for NSFR.
  - Not below target response spectrum at more than 9 adjacent frequency points – met for NFSR (7 points) but not for SFSR (11).
  - Not more than 30% above target response spectrum at any frequency in the frequency range of interest. If exceedances are larger than 30%, the average power spectral density (PSD) of the suite of multiple accelerograms needs to be computed and shown not to have significant gaps in energy at any frequency over the frequency range of interest, with a frequency band width of ±20%, centered on the frequency – met,

[1] 4% damping is appropriate per RG 1.61 for seismic analysis, but SRP 3.7.1 specifies doing adequacy checks at 5%.

because the PSDs shown in Figure 3-17 and Figure 3-18 have no abrupt dip or low points in power that could indicate insufficient energy input at a frequency in the range of interest.

- ✓ The time history for each of the three orthogonal directions is statistically independent from the others, as demonstrated by the absolute value of their correlation coefficient not exceeding 0.16 – met, largest value is 0.08 for both NFSR and SFSR.

Figure 3-11 through Figure 3-14 show the comparison between the target response spectrum (red) and the computed average response spectrum (black) for the five time histories for the E-W, N-S, and vertical directions for NFSR and SFSR, respectively. The two areas where the adequacy checks are not consistent with the guidance are the 30% exceedance and number of consecutive points below the target. Since the PSD check was performed for the each average of all time histories and showed no gaps (Figure 3-17 and Figure 3-18), the points of exceedance just result in additional energy input, which is conservative and judged acceptable.

In addition, a comparison of predicted results was performed to confirm that none of the time histories provided unexpected or inconsistent behavior, as described in Section 3.7.5.

The average of the generated response spectra is shown to envelope the corresponding target spectra (Figure 3-11 through Figure 3-14), meeting the intent of SRP 3.7.1 (Reference 9).

Based on the above, the use of the five time artificial histories shown in Figure 3-5 to Figure 3-10 is considered satisfactory for the nonlinear structural analysis of the fuel storage rack response to seismic conditions.

3.1.2 Modeling

3.1.2.1 General Considerations

Reliable assessment of the kinematic behavior of the rack modules requires suitable dynamic models that incorporate the key attributes of the structures. The SFSR model must have the ability to execute concurrent sliding, rocking, bending, twisting, and other motions associated with free-standing racks. Additionally, the SFSR model must possess the capability to simulate fuel assembly rattling, rack lift-off, and subsequent impact of support pedestals, while also considering the effect of the water mass in and around the rack modules. Similarly, the NFSR model must be able to simulate fuel assembly rattling and other motions associated with fixed-base racks.

The sections below describe individual features of the 3-D dynamic analysis model for the fuel racks.

(1) Seismic Input and Response Combination

Seismic inputs for the three orthogonal directions (east-west, north-south, and vertical) are applied simultaneously to the rack modules. The horizontal loads are combined using the square root sum of the squares (SRSS) method in the analysis of the fuel assembly, rack structure, welded connections, and rack supports.

(2) Fuel Loading

The dynamic analysis of the NFSR assumes the racks are fully loaded; the SFSR analysis considers various loading configurations (in most cases fully loaded, but also mixed/partially loaded and empty). When fuel assemblies are present in a rack, they are assumed to be fully seated (lowered all the way into a cell).

(3) Contact Elements

Gaps between fuel assemblies and rack cell walls/baseplate, adjacent rack baseplates, and pedestals and embedment plates are modeled with contact elements in the WPMR analysis, as described in Section 3.1.2.4.

(4) Coefficient of Friction

Because the SFSRs are free-standing, they may slide during an earthquake. The pedestal-to-embedment plate interface is assigned a coefficient of friction (COF) that represents contact between stainless steel surfaces in a wet environment. Based on experimental data (Reference 14), the COF is bounded within the range from 0.2 to 0.8 with a mean value of 0.5.

Since the NFSRs are attached to the floor, COF is not applicable as long as the stud bolts remain intact.

For both the NFSRs and SFSRs, a COF of 0.5 between the fuel assembly and the rack was used.

(5) Fluid Coupling

For seismic conditions, the submerged SFSR is influenced by fluid coupling as well as by mechanical contact. When the racks displace toward each other and the gaps between them are reduced, the fluid coupling effect increases. Because the racks are densely arranged in the spent fuel pool, the fluid coupling effect can be significant. Fluid coupling is included in the SFSR models by use of hydrodynamic mass based on the potential flow theory of Fritz (References 15 and 16).

Hydrodynamic masses are defined at fuel assembly-to-cell wall gaps, rack-to-rack gaps, rack-to-pool wall gaps, and rack baseplate-to-pool floor gaps based on the size of the gaps at those locations. Figure 2-5 and Figure 2-6 show the installation gaps for the SFSRs.

As gap size is increased, the hydrodynamic mass decreases. The hydrodynamic mass is calculated based upon the initial gap sizes. The initial SFSR rack-to-rack baseplate gaps are the minimum physically possible. Although the hydrodynamic mass increases as the rack moves to close the gap, the increase is not meaningful until the gap becomes very small. Therefore, hydrodynamic mass is not updated during a seismic response run because the maximum displacement of the outermost rack is small in comparison with the gap size of the outermost rack and the pool wall. If applied, the increase in hydrodynamic mass would reduce the sliding response of the racks. Therefore, it is conservative for maximizing the amount of rack sliding and the potential for rack-to-pool wall and rack-to-rack impacts to not increase the hydrodynamic mass. This is also consistent with the discussion of fluid effects in NUREG/CR-5912, Section 6.4.3, Fluid Effects, which states "...the change was not significant and that the practice of using a constant hydrodynamic mass based on initial gaps is reasonable."

Therefore, a sensitivity analysis of variation in gaps (i.e., installation tolerances for the gap) was not performed.

Hydrodynamic mass is calculated based on Fritz's classical two-body fluid coupling model (Reference 16) extended to multiple bodies. In its simplest form, the fluid coupling effect can be explained by considering the proximate motion of two bodies (such as a rack and a wall) under water.

The effect of hydrodynamic mass is implemented through the use of the ANSYS MATRIX27 element as discussed in Section 3.1.2.3.

The NFSRs have no hydrodynamic effect because they are installed in air.

3.1.2.2 Details for Rack and Fuel Assembly Model

The sections below provide details on the rack and fuel assembly modeling.

(1) New Fuel Storage Rack Model

The dynamic analysis model for the NFSR and fuel assemblies are shown in Figure **3**-**1**. The NFSR and fuel assembly model are of a single rack and includes 3-D elastic beam elements (ANSYS BEAM4) and lumped mass elements (ANSYS MASS21) with properties derived from the dynamic characteristics of the detailed 3-D shell model of the NFSR. Effective structural properties for the dynamic model are determined from the natural frequencies and mode shapes of the detailed model (see Section 3.1.2.7). Details of effective structural properties for fuel racks are shown in Appendix H of Reference 17. Structural properties (i.e. Young's modulus and flexural rigidity) for fuel assemblies are shown in Table 3-3.

Vertical portions of the NFSR cells and fuel assemblies are each represented by five nodes. Nodes are located at the rack baseplate, ¼ H, ½ H, ¾ H, and H (where H is the rack height measured above the baseplate). Each rack node has six degrees of freedom (three translations and three rotations) and a lumped mass associated with it. The nodes for the rack and the fuel assembly are connected by contact elements (ANSYS CONTAC52) in the horizontal direction. There is a single contact element in the vertical direction between the fuel assembly bottom node and the baseplate node.

Lumped masses of the NFSR and fuel assemblies are distributed among the five nodes for rack cells and fuel assemblies as shown in the table below:

Node No. (Figure 3-1)		Location	Total Mass Distribution
Rack	Fuel Assembly		
13	18	Top of Rack	12.5 %
12	17	3/4 Height	25 %
11	16	1/2 Height	25 %
10	15	1/4 Height	25 %
9	14	Bottom (Baseplate) of Rack	12.5 %

(2) Spent Fuel Storage Rack Model

To model the interaction among the multiple SFSRs, the WPMR shown in Figure 3-3 is comprised of a dynamic analysis model for individual SFSRs, as shown in Figure 3-2. This model is similar to the NFSR model and is composed of elastic beam elements and lumped mass elements with properties derived from the dynamic characteristics of the detailed 3-D shell model of the SFSR. An underlying assumption in the modeling of the rack as a single beam using the overall bending stiffness of the entire rack is that the cell-to-cell welds remain intact and can carry the internal forces. This assumption is confirmed by structural evaluation of the welds (see Section 3.7.3.3).

Effective structural properties for the dynamic model are determined from the natural frequencies and mode shapes of the detailed model (see Section 3.1.2.7).

Figure 3-2 shows a schematic depicting five nodes representing masses of fuel and rack cells and their associated elements, which are used to represent the interactions and vertical and horizontal motions of support pedestals, respectively. Contact (i.e., gap) elements are used in the representation of rack sliding and impact. A directional stiffness is assigned to the contact element. The pool floor is assumed to be a rigid body initially in contact with the rack pedestals. The contact elements are used to represent potential impact of a rack pedestal on the pool floor. The coefficient of friction between the rack pedestals and pool floor is incorporated into a contact (gap) element.

The hydrodynamic masses for the fuel assembly-to-cell wall, rack-to-rack and rack-to-pool wall are modeled as ANSYS mass MATRIX27 elements. The hydrodynamic masses for rack baseplate-to-pool floor are considered as added masses to each rack baseplate.

Lumped masses of the rack and fuel assemblies are distributed among the five nodes for spent fuel storage rack cells and fuel assemblies as shown in the table below.

Node No. (Figure 3-2)		Location	Total Mass Distribution
Rack	Fuel Assembly		
13	18	Top of Rack	12.5 %
12	17	3/4 Height	25 %
11	16	1/2 Height	25 %
10	15	1/4 Height	25 %
9	14	Bottom (Baseplate) of Rack	12.5 %

All the fuel assemblies in each storage rack module are modeled as one beam of which the mass equals the sum of the masses of all the fuel assemblies in a rack module. Structural properties (i.e. Young's modulus and flexural rigidity) for fuel assemblies are shown in Table 3-3. Because the fuel assemblies in a rack module are modeled together, all fuel assemblies move simultaneously in one direction. This assumption results in larger impact forces on the rack module than the actual case and results in conservative loads on the storage rack. Because the fuel assembly is modeled with five nodes, the calculated impact loads on the nodes will be larger than the actual value because the fuel assembly actually has eleven spacer grids. The maximum fuel assembly grid horizontal impact load is determined by dividing the maximum impact load at each node by the number of grids associated with that node (2.75 for Nodes 10, 11, and 12, and 1.375 for Nodes 9 and 13).

Fluid damping and form drag are conservatively omitted.

Figure 3-3 shows the WPMR analysis model, which combines the single rack models described above to represent the entire spent fuel pool.

3.1.2.3 Hydrodynamic Mass

In addition to the structural mass of racks and fuel assemblies, hydrodynamic masses are included in the SFSR model to account for fluid coupling. Hydrodynamic mass is included in the SFSR model with the ANSYS MATRIX27 element and added mass, which represents an arbitrary element whose geometry is undefined but whose kinematic response can be specified by mass coefficients. Details of hydrodynamic masses are shown in Appendix H of Reference 17.

(1) Fuel Assembly-to-Cell Wall

A fuel assembly consists of fuel rods, guide tubes, top and bottom nozzles, and spacer grids. The hydrodynamic mass coefficients between the rack cell wall and the fuel assembly are calculated assuming the rack cell and fuel assembly are long coaxial cylinders. Hydrodynamic masses acting at the centers of two rigid cylinders with a fluid-filled annulus are represented using the following formula in Reference 15:

$$\begin{pmatrix} F_1 \\ F_2 \end{pmatrix} = \begin{bmatrix} -M_H & M_1 + M_H \\ M_1 + M_H & -(M_1 + M_2 + M_H) \end{bmatrix} \begin{pmatrix} X_1'' \\ X_2'' \end{pmatrix}$$

$$M_H = \left[\frac{R_2^2 + R_1^2}{R_2^2 - R_1^2} \right] \pi \rho R_1^2 h$$

Where,

F_1, F_2 = Fluid reaction forces on the inner and outer bodies, respectively,
M_H = Hydrodynamic mass that depends on the fluid flow when the two bodies move relative to each other,
M_1 = Mass of fluid displaced by inner body,
M_2 = Mass of fluid inside the outer body in the absence of the inner body,
X''_1 = Absolute acceleration of the inner body,
X''_2 = Absolute acceleration of the outer body,
R_1 = Equivalent radius of fuel assembly,
R_2 = Equivalent radius of storage cell,
h = Length of fuel assembly, and
ρ = Density of fluid.

Hydrodynamic mass is assigned to the five nodes of the rack cell and the fuel assembly as shown in the table below:

Node No. (Figure 3-2)		Location	Total Mass Distribution
Rack	Fuel Assembly		
13	18	Top of Rack	12.5 %
12	17	3/4 Height	25 %
11	16	1/2 Height	25 %
10	15	1/4 Height	25 %
9	14	Bottom (Baseplate) of Rack	12.5 %

The hydrodynamic mass calculated with the formula above is the mass between one cell and one fuel assembly. Therefore, the hydrodynamic mass used in a single rack model is multiplied by the number of fuel assemblies assumed to be present in that rack.

(2) Rack-to-Rack and Rack-to-Pool Wall

The hydrodynamic mass matrices for rack-to-rack and rack-to-pool wall fluid gaps are calculated based on the height of the rack, density of fluid, and distance between adjacent racks, assuming the centers are eccentric as shown below. Figure 2-5 and Figure 2-6 show the dimensions of rack-to-rack and rack-to-pool wall gaps. An example calculation is included in Appendix H of Reference 17.

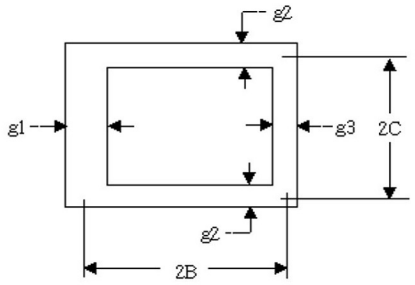

$$M_{H(horiz)} = 2\rho hC^2\left[\frac{C}{3g_1}+\frac{C}{3g_3}+\frac{2B}{g_2}\right]$$

$$M_1 = \rho h\,(2C - g_2)\left[2B - \left(\frac{g_1+g_3}{2}\right)\right]$$

$$M_2 = \rho h (2C + g_2) \left[2B + \left(\frac{g_1 + g_3}{2} \right) \right]$$

Where,

M_H = Hydrodynamic mass that depends on the fluid flow when the two bodies move relative to each other,
M_1 = Mass of fluid displaced by inner body,
M_2 = Mass of fluid inside the outer body in the absence of the inner body,
h = height of the storage rack,
ρ = density of the fluid, and
g_1, g_2, g_3 = initial gaps between the two bodies.

If g_2 is not the same on both sides, an average value of g_2 is used. If two or more racks overlap each other, the hydrodynamic mass is calculated using a weighted average gap.

(3) Rack Baseplate-to-Pool Floor

The hydrodynamic mass under the baseplate of each rack is calculated using the following formula in accordance with Table 1 of Reference 16.

$$M_{baseplate} = K \cdot (\pi \cdot \rho \cdot a^2 \cdot b / 4)$$

Where,
K = hydrodynamic mass coefficient (K = 0.478 is used for the SFSR),
a, b = length a and width b dimensions of the rack, and
ρ = density of the fluid.

3.1.2.4 Stiffness of Model

Two types of stiffness are used in the SFSR model: 3-D elastic beam elements, as discussed above, and contact elements. The contact elements are used to calculate horizontal loads due to friction (between the rack pedestal and embedment plate) and impacts (fuel-to-cell wall, rack-to-rack, and pedestal-to-embedment plate). The contact element used is ANSYS CONTAC52.

CONTAC52 represents two surfaces that may maintain or break physical contact and may slide relative to each other. This element is capable of supporting only compression in the direction normal to the surfaces and shear (coulomb friction) in the tangential direction. The element has three degrees of freedom at each node (x, y, and z). A specified stiffness acts in the normal and tangential directions when the gap is closed. The stiffness values (i.e., spring constants) for the rack baseplates and pedestal are calculated in Appendix E of Reference 17. For these contact elements, the location of the element determines which values are used:

TS

(1) Fuel Assembly-to-Cell Wall

Each node of the fuel assembly beam and the corresponding node of the rack beam is connected using a contact element in order to represent impact between the fuel assembly and the rack cell wall. The normal direction stiffness of this element is calculated assuming a series spring connection of the stiffness of the fuel assembly spacer grid and the local stiffness of the cell in the horizontal direction. To be conservative, the cell wall local stiffness is neglected. The fuel assembly/rack cell contact element has a local stiffness (K_i) to account for impact phenomena of the

fuel assembly-to-cell wall. The grid stiffness for a fuel assembly beam is multiplied by the number of fuel assemblies assumed to be in the rack. The stiffness of fuel assembly grid is applied by dividing the total grid stiffness at each node by number of grid associated with node (K_i/4 for Nodes 15, 16, and 17, and K_i/8 for Nodes 14 and 18).

(2) Pedestal-to-Embedment Plate

Four nodes corresponding to the rack pedestals are connected to the pool floor using contact elements. The stiffness of these elements is a series spring connection of the vertical stiffness of the rack baseplate and pedestal. The baseplate vertical stiffness is calculated from FEM analysis. The stiffness values for the rack baseplates and pedestal are calculated in Appendix F of Reference 17. Therefore, pedestal-to-embedment plate stiffness value is calculated using the following formula:

TS

(3) Rack-to-Rack and Rack-to-Pool Wall

The stiffness for the rack-to-rack contact element is based on connections of the horizontal rack stiffness at the base plate. Analysis results show that the rack-to-rack and rack-to-pool wall displacements are less than the available rack-to-rack and rack-to-pool wall clearances. Consequently, contact elements are not included on the racks except for baseplate-to-baseplate and pedestal rack-to-floor interaction.

Because rack-to-rack impact other than at the baseplates does not occur, no sensitivity is performed. Therefore, the sensitivity of the impact force to the impact spring constant is evaluated for rack baseplate-to-rack baseplate only. A sensitivity analysis is performed in which the spring constant value is uniformly decreased or increased by 20%, respectively.

3.1.2.5 Friction Coefficient

Because SFSRs are not fixed to the storage pool, sliding could occur between the rack pedestals and the embedment plates or pool floor. The contact element is used to model this effect. Based on experimental data (Reference 14), the COF is bounded within the range from 0.2 to 0.8 with a mean value of 0.5. A low friction coefficient may increase sliding distance, while a high friction coefficient may increase rack load.

3.1.2.6 Buoyant Force

The SFSRs are submerged in water; therefore, buoyant forces are calculated and applied to the applicable nodes as concentrated loads in the vertical direction as follows:

$$\text{Buoyant force acting on rack} = W_{rack} - [\ (\rho_{rack} - \rho_{water}) / \rho_{rack}\ ] \times W_{rack}$$

$$\text{Buoyant force acting on fuel assembly} = W_{FA} - V_{FA} \times \rho_{water} \times \text{gravity}$$

Where,

ρ_{rack} = Density of storage rack, 8,000 kg/m^3 (0.289 lbm/in^3),
ρ_{water} = Density of fluid, 1,000 kg/m^3 (0.036 lbm/in^3),
W_{rack} = Weight of rack in air, and

V_{FA} = Volume of water displaced by fuel assembly, 0.743 m^3 (2.625 ft^3).

The calculated buoyant forces were applied as follows:

Buoyant Force Acting on Rack and Fuel Assembly		
	Node(s) (See Figure 3-2)	Buoyant Force Applied to Each Node
Rack	1,2,3,4	Buoyant Force acting on rack /8
	9	Buoyant Force acting on rack /2
Fuel Assembly	18	Buoyant Force acting on fuel assembly

3.1.2.7 Natural Frequencies

The dynamic analysis models for the NFSR and SFSRs are generated using simplified beam elements. Each simplified beam model is developed to have dynamic characteristics (1st and 2nd mode of natural frequency and mode shapes) similar to the detailed finite element model. Appendix H of Reference 17 documents the comparison of the simplified and detailed three-dimensional models.

The fundamental frequencies of the NFSR are above 20 Hz and of the SFSR are above 30 Hz.

The range of frequencies considered is from 1 to 100 Hz according to the floor response spectra of design specification (Reference 22).

3.1.3 Simulation and Solution Methodology

The SFSR WPMR analysis is performed to calculate the displacements and loads for each rack and determine the presence or absence of specific rack-to-rack or rack-to-pool wall impacts during the seismic event. The analysis of the SFSR is performed as follows:

(1) Use the ANSYS program (Reference 18) to prepare a 3-D WPMR model that includes hydrodynamic effects and nonlinear elements to produce realistic simulations of rack and fuel assembly motion during a seismic event.

(2) Perform transient dynamic analyses for various combinations of friction coefficient values and rack loading conditions (full, partially full, and empty) with multiple input motion time histories to determine the response of the rack and fuel assemblies.

The basic equation of motion solved by a transient dynamic analysis is

$$(M)\{\ddot{u}\} + (C)\{\dot{u}\} + (K)\{u\} = \{F(t)\}$$

Where,

(M) = mass matrix,
(C) = damping matrix,
(K) = stiffness matrix,
$\{\ddot{u}\}$ = nodal acceleration vector,
$\{\dot{u}\}$ = nodal velocity vector,
{u} = nodal displacement vector, and
{F(t)} = load vector.

At any given time, t, these equations can be thought of as a set of “static” equilibrium equations that also take into account inertia forces and damping forces. Displacement and loads of each storage rack are obtained by post-processing the results of the WPMR analysis.

(3) Apply a constant time step size and a single computer processor to ensure repeatability. Repeatability of the solution results was confirmed by rerunning one of the base transient cases with unaltered input and confirming the same results would be obtained if the case were rerun.

(4) Perform stress analyses of the racks using the loads from the transient dynamic analyses. Evaluate calculated stresses based on the criteria in ASME Code Section III, Subsection NF (Reference 4) and perform local evaluation for the bounding case to show that the structural integrity of the fuel is maintained under all impact loads.

The analysis for the NFSR is performed in a similar manner except that only a single rack module is modeled. This simplification is appropriate because of the large separation between the two rack modules (approximately 24 inches) and the absence of water.

3.2 Acceptance Criteria

The composite dynamic simulation wherein all racks in the pool are modeled is used 1) to determine the loads and displacements for each fuel storage rack in the pool and the relative motion between racks, and 2) to evaluate the potential damage and consequences of inter-rack and rack-wall impact phenomena in the racks.

The NFSRs and the SFSRs are designed as seismic Category I. The structural analysis of fuel storage rack is performed for all load conditions of the fuel storage rack in accordance with NRC SRP 3.8.4 (Reference 1) and NRC SRP 3.8.5 (Reference 20). This includes loads on the racks when fuel assemblies are normally stored in the racks; when a SSE occurs; and when the fuel assembly or other permitted items handled over the racks falls down onto or into them. The principal design criteria of the racks are shown in Sections 3.2.1 and 3.2.2.

Per Section I.3 of SRP 3.8.4 (Reference 1), the impact loads on the fuel assembly should not lead to damage of the fuel. Damage of the fuel is evaluated for structural elements of a fuel assembly including the fuel rod cladding to verify they are not stressed beyond the material allowable limits such that the fuel rods are no longer able to provide confinement for contained radioactive fission materials. In addition, an evaluation considering pertinent failure modes such as buckling should be performed to demonstrate that when subject to the consequent loads resulting from the load combinations described in Table 3-1, the structural elements of the fuel assembly will not exceed the material allowable limits.

3.2.1 Kinematic Criteria

Because the SFSRs are not fixed, overturning or sliding could happen due to external load. According to the NRC SRP 3.8.5 (Reference 20), the minimum acceptable factor of safety against overturning under the seismic event is 1.5. This ensures that the rack does not exhibit a rotation sufficient to bring the center of mass over the corner pedestal. Because NFSRs are attached to the floor, they were confirmed not susceptible to overturning by showing that their stud bolt stresses are acceptable (Section 3.2.2.4).

3.2.2 Stress Limit Criteria

Stress limits must not be exceeded under the required load combinations. The applicable loads and load combinations of structural analysis for the rack are defined in the Table 3-1, based on NRC SRP 3.8.4, Appendix D (Reference 1). For the APR1400, the operating basis earthquake (OBE) ground motion is defined as one-third the SSE ground motion design response spectra. Therefore, in accordance with 10 CFR Part 50, Appendix S, an OBE design analysis is not required and load combinations involving “E” have been removed. The acceptance limits are defined in ASME Code Section III, Subsection NF (Reference 4), as applicable for Class 3 component supports.

The APR1400 SFSRs are free-standing; thus, there is no or minimal restraint against free thermal expansion at the base of the rack. Moreover, stresses induced due to thermal expansion will be secondary stresses since they are self-limiting, and have no stipulated stress limits in Class 3 structures or components when acting in concert with seismic loadings. Therefore, thermal loads applied to the racks are not included in the stress combinations involving seismic loadings. ASME Code Section III, Division 1, Subsection NF and Appendix F are applied as stress limits criteria of fuel storage rack for service conditions.

Material properties for analysis and stress evaluation are provided in subsection 3.4.4.

3.2.2.1 Normal Conditions (Level A)

(1) Stress in Tension

The allowable stress in tension on a net section (F_t) is given in NF-3321.1(a)(1).

$$F_t = 0.6\ S_y \text{ [but not more than } 0.5\ S_u\text{]}$$

Where,

S_y = yield strength of material at a given temperature, and
S_u = ultimate strength of material at a given temperature.

(2) Stress in Shear

The allowable stress in shear on a net section (F_v) is given in NF-3322.1(b)(1).

$$F_v = 0.4\ S_y$$

(3) Stress in Compression

The allowable stress in compression on a net section (F_a) of austenitic stainless steel is given in NF-3322.1(c)(2).

$$F_a = S_y\ (0.47 - k \cdot l/444r)$$

Where,

kl/r is less than or equal to 120 for all sections,
l = unsupported length of component,
k = length coefficient which gives influence of boundary conditions, e.g.,
k = 1; simple support both ends,
k = 2; cantilever beam, conservatively used for evaluations,
k = 0.5; clamped at both ends, and
r = radius of gyration of component.

(4) Stress in Bending

The allowable bending stress (F_b) resulting from tension and compression on extreme fibers of box-type flexural members is given in NF-3322.1(d)(4).

$$F_b = 0.60\ S_y$$

(5) Combined Stress (Combined Bending and Compression Loads)

Combined bending and compression load on a net section per NF-3322.1(e)(1) satisfies the following equation.

$$f_a/F_a + C_{mx}f_{bx}/D_xF_{bx} + C_{my}f_{by}/D_yF_{by} \leq 1.0$$

Where,

f_a = Direct compressive stress in the section,
f_{bx} = Maximum bending stress along x-axis,
f_{by} = Maximum bending stress along y-axis,
C_{mx} = 0.85,
C_{my} = 0.85,
D_x = $1 - (f_a/F'_{ex})$,
D_y = $1 - (f_a/F'_{ey})$,
F'_{ex}, F'_{ey} = $(\pi^2 E)/(2.15 (kl/r)_{x,y}^2)$,
and subscripts x and y reflect the particular bending plane.

(6) Combined Stress (Combined Flexure and Tension Loads)

Combined flexure and tension/compression load on a net section satisfies the following equation given in NF-3322.1(e).

$$(f_a/0.6\ S_y) + (f_{bx}/F_{bx}) + (f_{by}/F_{by}) \leq 1.0$$

(7) Welds

The allowable maximum shear stress on the net section of a weld (F_w) is given in Table NF-3324.5(a)-1.

$$F_w = 0.3\ S_u$$

Where, S_u is the weld material ultimate strength at temperature. For the area in contact with the base metal, the shear stress on the gross section is limited to 0.4 S_y. Where, S_y is the yield strength of material at a given temperature.

3.2.2.2 Upset Conditions (Level B)

The stress limits for Level B are those for Level A multiplied by the stress limit factor specified in Table NF-3523(b)-1 (Reference 4).

3.2.2.3 Faulted/Abnormal (Level D)

Article F-1334 (ASME Section III, Appendix F (Reference 4), states that limits for the Level D condition are the smaller of 2 or 1.167 S_u/S_y times the corresponding limits for the Level A condition if $S_u > 1.2\ S_y$, or 1.4 if $S_u \leq 1.2\ S_y$ except for requirements specifically listed below. S_u and S_y are the ultimate strength and yield strength at the specified rack design temperature. Examination of material properties for 304L stainless demonstrates that 1.2 times the yield strength is less than the ultimate strength. Since 1.167 x (66,100/21,400) = 3.60, the multiplier of 2.0 controls.

Exceptions to the above general multiplier are the following:

(1) The tensile stress on the net section shall not exceed the lesser of 1.2 S_y and 0.7 S_u.

(2) The shear stress on the gross section shall not exceed the lesser of 0.72 S_y or 0.42 S_u. In the case of the austenitic stainless steel material used here, 0.72 S_y governs.

(3) Combined axial compression and bending - The equations for Level A conditions shall apply except that F_a = 2/3 x Buckling Load, and F'_{ex} and F'_{ey} may be increased by the factor 1.65.

(4) For welds, the Level D allowable weld stress is not specified in Appendix F of the ASME Code. Therefore, a limit for weld throat stress is used conservatively as follows:

$$F_w = (0.3\ S_u) \times \text{Factor}$$

Where,

Factor = (Level D shear stress limit)/(Level A shear stress limit) = $0.72 \times S_y / 0.4 \times S_y = 1.8$

3.2.2.4 Stress Limit for NFSR Stud Bolt

The allowable tensile and shear stresses in the stud bolt are in accordance with ASME Code Section III, Subsection NF and Appendix F for Service Level A and D, respectively. The appropriate stress limit factors K_{bo} are given in Table NF-3225.2-1 in accordance with the load condition. The NFSR stud bolt subjected to combined shear and tension shall be proportioned so that the combined effects of shear and tensile stress satisfy the ellipse equation as shown below.

Load Condition	Tensile (F_{tb})	Shear (F_{vb})	Combined(1)
Level A	$S_u/3.33$	$0.62S_u/5$	$\frac{f_t^2}{F_{tb}^2} + \frac{f_v^2}{F_{vb}^2} \le 1$
Level D(2)	$\text{Min}(0.7S_u, S_y)$	$\text{Min}(0.42S_u, 0.6S_y)$	

(1) f_t and f_v are calculated tensile and shear stresses, respectively.
(2) Specified in Appendix F-1335 of ASME Code, Section III, Division 1.

3.2.3 Dimensionless Stress Factors

Dimensionless stress factors are calculated by the ratio of the calculated stress to the allowable stress for the combined and the individual loads according to ASME Code Section III, Division 1, Subsection NF. When the calculated stress factor does not exceed 1.0, it is considered to meet stress limit requirements for each service condition. In this report, a stress factor as described below is calculated using the load combination for each service condition.

FACT1 = Stress factor of member subject to combined bending and compression (as defined in subsection 3.2.2.1(5)).
FACT2 = Stress factor of member subject to combined flexure and tension (or compression) (as defined in subsection 3.2.2.1(6)).
FACT3 = Stress factor of gross shear on a net section.

3.3 Assumptions

The following assumptions are used in the WPMR dynamic analysis:

(1) Fluid damping is conservatively neglected.
(2) Sloshing of the SFP water during a seismic event does not influence the dynamic response of the racks in either horizontal direction because the height of the racks is approximately equal to 3/8 times the depth of water in the spent fuel pool (see Reference 21).
(3) The fuel assembly is considered as 3-D elastic beam with concentrated masses at the upper and lower ends and at three equally spaced intermediate points of the rack (total of 5 nodes).
(4) When the SSE occurs, the rack is affected by irregular movement of every single fuel assembly. For conservative evaluation, all the fuel assemblies within the rack rattle in unison (model as a single beam) throughout the seismic event, which exaggerates the impact against the cell wall.

3.4 Input Data

3.4.1 Rack Data

Dimensions and mass of the new and the spent fuel storage racks used in the analysis are in accordance with the design drawings (References 5 and 6) and are summarized in the Tables 2-1, 2-2 and 3-2.

3.4.2 Fuel Assembly Data

Dimensions and mass of the fuel assembly used in the analysis are based on the pressurized water reactor (PWR) PLUS7 fuel assembly data (References 22 and 23) and are summarized in the Table 3-3.

3.4.3 Structural Damping

Rayleigh damping is used to specify mass (M) and stiffness (K) proportional damping (C):

$$C = \alpha \times M + \beta \times K$$

The constants α and β are calculated in the range of the lowest and highest frequencies of interest in the dynamic analysis (Reference 17). M corresponds to real mass of the rack-fuel system and does not include any hydrodynamic mass. Only material damping for the fuel and rack is used in calculating the damping matrix C. The design basis damping value for the NFSRs and the SFSRs is 4% for a SSE event in accordance with the regulatory guide (RG) 1.61 (Reference 24) for welded steel. The frequency range from 20 Hz to 100 Hz is applied to NFSR, while 2 Hz to 65 Hz is applied to SFSR considering installation in the water. The frequencies selected bound the natural frequencies of interest (e.g., for the SFSRs, frequencies of the fuel assemblies and rack structure in water). The damping model underpredicts damping (i.e., is conservative) at intermediate frequencies where the highest input accelerations occur.

3.4.4 Material Data

Material properties of a fuel assembly are taken from the PWR PLUS7 fuel assembly data (References 22 and 23) as shown in the Table 3-3. In addition, those of the racks are obtained from ASME Code Section II, Part D (Reference 19). The values listed correspond to a design temperature of 93.3 ºC (200 ºF); higher temperatures reduce material strength compared to normal conditions.

3.5 Computer Codes

3.5.1 ANSYS

A benchmarking study (Reference 25) was performed to demonstrate that ANSYS Version 15.0 (Reference 18) is an acceptable computer code for the seismic analysis of the SFSR and NFSR. While the SRP Section 3.8.1 Subsection II.4.F (Reference 26) states that meeting any one of the following methods is sufficient to validate computer programs used for design analysis, the benchmarking study addressed all three:

1) The computer program is recognized in the public domain and has had sufficient history of use to justify its applicability and validity without further demonstration.
2) The computer program's solutions to a series of test problems have been demonstrated to be substantially identical to those obtained from classical solutions or from accepted experimental tests or to analytical results published in technical literature. The test problems should be demonstrated to be similar to or within the range of applicability of the classical problems analyzed to justify acceptance of the program.
3) The computer program's solutions to a series of test problems have been demonstrated to be

substantially identical to those obtained by a similar and independently written and recognized program in the public domain. The test problems should be demonstrated to be similar to or within the range of applicability of the problems analyzed by the public domain computer program.

ANSYS has been used in the nuclear energy industry for nearly 40 years. The ANSYS software is developed within an ISO 9001 quality program that meets both ASME NQA-1 and 10 CFR 50 Appendix B. ANSYS software has previously been accepted by the NRC for SFSR seismic structural analysis.

Five test cases were run with ANSYS Version 15.0 to provide a comparison of ANSYS results to analytical results published in technical literature. These test cases exercised the ANSYS elements (MASS21, COMBIN14, CONTAC52, BEAM4, and MATRIX27) and features (direct integration time history, mass, spring, friction, impact and hydrodynamic coupling) used for the ARP1400 fuel rack seismic analysis. The five test cases involved coulomb friction, a two degree of freedom system with inertial coupling, mass impact on a beam, mass impact on a flexible surface, and the Fritz methodology for modeling hydrodynamic mass. The results of these five test problems compared very well to the published analytical results.

To further validate the use of ANSYS for APR1400 fuel rack seismic analysis, a single SFSR was analyzed with both ANSYS and LS-DYNA for five different sets of acceleration time histories. ANSYS is an implicit finite element code used for structural analysis with the capability to perform both static and dynamic simulations, while LS-DYNA is an explicit finite element code used for transient analysis. The results showed good agreement between ANSYS and LS-DYNA, thereby providing confidence that both codes correctly solve the equations of motion and produce reasonable results.

3.6 Dynamic Simulations

The simulations listed in Table 3-5 are performed for the new and the spent fuel racks to investigate the structural integrity of each rack. The loading conditions for the racks are based on the SSE event.

The SFSR configurations at the full, empty, and mixed loadings are considered in the dynamic simulations. To consider the effect of the friction coefficient between pedestal and embedment plate as discussed in Section 3.1.2.5, simulations are performed by using the friction coefficient with upper and lower bound values and a mean value.

The nonlinear dynamic analyses for dynamic simulations of the NFSRs and the SFSRs are performed using the ANSYS (Reference 18) finite element program. The results of the simulations are compared to the stress and kinematic criteria in Section 3.2.

Run numbers 1 through 5 are dynamic simulations of the NFSR. For the SFSR, run numbers 6 through 10 use the coefficient of friction (COF) value 0.2, run numbers 11 through 15 are with the COF value 0.5, and run numbers 16 through 20 are with the COF value 0.8.

Run numbers 21 through 36 are sensitivity runs. The inputs (e.g., which time history, which COF for the SFSRs) for the sensitivity analysis were chosen from those used for base runs 1 to 5 for the NFSRs and 6 to 20 for the SFSRs, using the following rationale:

- Maximum vertical load on a single pedestal and fuel-to-cell wall impact load among the base runs.
- Maximum rack-to-rack baseplate impact load from among the base runs.
- Maximum horizontal load on a single pedestal load among the base runs.
- Maximum stress factor from among the base runs.

Table 3-5 identifies the conditions (e.g., COF) used in various base runs and the sensitivity runs

performed to verify that fuel rack response is reasonably bounded. These sensitivities were:

- Run numbers 21 and 22 are identical to the NFSR bounding run but vary the value of the rack elastic modulus times the moment of inertia (i.e., EI) ±20%.
- Run numbers 23 and 24 are identical to the bounding run but vary the value of the rack elastic modulus times the moment of inertia (i.e., EI) ±20%.
- Run numbers 25 through 32 vary impact spring constants of rack-to-floor, rack-to-rack baseplate, and fuel-to-cell wall by ±20%.
- Run number 33 evaluates EOL fuel elastic modulus times the moment of inertia (i.e., EI)
- Run numbers 34 and 35 assume empty racks and a mix of full, 50%, 25%, and empty racks (see Figure 3-4).
- Run number 36 was performed with a fixed time step of one half that used for all other runs in order to demonstrate convergence.

Conclusions from these sensitivity cases are discussed in Section 3.7.4.

3.7 Results of Analyses

This section discusses the results, which are presented in tables and figures at the end of the section. Detailed results are provided in Reference 17. Structural evaluation results according to load combination of Table 3-1 are meet the ASME Code Section III, Subsection NF.

Although runs are performed with five different time histories, note that individual runs shown are not independent. For example, runs 6, 11, and 16 are identical inputs except for the rack pedestal coefficient of friction. Also, sensitivities runs were performed using the base runs (i.e., runs 6 through 20 for the SFSR and 1 through 5 for the NFSR) giving the most limiting results. For example, the sensitivity on rack-to-rack stiffness (i.e., runs 31 and 32) used base run 12 since it had the highest baseplate-to-baseplate impact load, leading to results of runs 31 and 32 being biased high. Since all sensitivities were performed this way, the sensitivity run loads will average higher than the loads from the base runs.

For the SFSRs, each run was performed for all racks, and results are reported separately for region I and region II. The heaviest region I rack weighs almost twice as much as the lightest in region II (see Table 3-2), leading to different magnitudes of some responses between regions.

The following results are presented in the identified tables:

- Displacements of racks:
  (1) SFSR baseplates relative to pool floor (i.e., where they were at start of transient)[Table 3-6]
  (2) NFSR and SFSR tops in relation to their bases (i.e., flexing of rack upper structure that could lead to contact even if bases are not touching)[Table 3-6]
- Loads on supports:
  (1) NFSR and SFSR pedestal loads in vertical direction and horizontal directions [Table 3-7]
- Loads on structure:
  (1) Impact loads on SFSR baseplates (i.e., adjacent racks bump into each other) – used to assess integrity of baseplate to cell welds [Table 3-8]
  (2) Impact loads on cell walls (i.e., fuel assemblies rattle against walls of cell containing them) – used to assess integrity of cell-to-cell welds [Table 3-8]
  (3) Impact loads on fuel assembly grids (i.e., not all grids along the height impact cell walls uniformly) [Table 3-8]
- Margin to overturning – used to verify rack does not tip [Table 3-10]
- Stress factors – used to compare calculated loads to allowable stresses (i.e., values <1.0 have margin to allowable [Table 3-9]

- Rack weld stresses and safety factors – used to confirm racks maintain their structural integrity [Table 3-12]
- Stress on fuel assembly – used to confirm fuel assemblies are not damaged to the extent that cladding is breached [Table 3-11]
- Stresses on the threads of the SFSR pedestal leveling feet – used to assess damage to threads [Table 3-13]
- Stresses on the NFSR stud bolt - used to confirm NFSR stud bolts maintain their structural integrity [Table 3-14]

The seismic responses in the horizontal directions are combined using the square root of the sum of the squares (SRSS) method in the analysis of the fuel assembly, rack structure, welded connections, and the rack supports of NFSR and SFSR. For all horizontal loads except fuel assembly grid impact, the SRSS combination uses the maximum E-W and the maximum N-S load at any time during the transient, even if they do not occur during the same time step. The grid impact loads use the values during the same time step to find the maximum.

3.7.1 Time History Simulation Results

The loads and the displacements by dynamic simulations are summarized in Table 3-6 through Table 3-8 and in Figure 3-20 through Figure 3-26. Note that the values shown are maximum values found for any of the racks for each run. Where horizontal loads are reported, they are for the same rack, but the vertical load reported for that run may be from a different rack. For the SFSRs, results are reported for both Region I and Region II racks since they are slightly different structurally and have different rack-to-rack spacing.

3.7.1.1 Displacements of Rack

The NFSRs are fixed and not subject to displacement at their bases provided their stud bolts remain intact, as shown in Figure 2-3. The displacement of the NFSRs at their top is determined to confirm there is no contact between adjacent cells or with the new fuel storage pit walls.

The SFSRs are specified to be installed with pedestals and baseplates as close as possible, as shown in Figure 2-6. Therefore, during a seismic event they will initially move apart, although they could again slide together during the transient. Due to the random nature of the seismic acceleration, the racks will move in different directions by different amounts, and this can be affected by the time step and COF used in the analysis. This randomness would be true even if experiments were run repeatedly using different time histories. The initial movement can determine the ultimate relative position of racks to each other. As discussed in Section 3.1.1, a baseline correction process has been used to eliminate unrealistic cumulative displacement leading to large final displacements. The use of five independent time histories with sensitivities for COF and rack loading provides a reasonable range of possible displacements. Since none of the runs predicted displacements of more than a small fraction of the gap between the outermost racks to SFP wall, contact of cells between SFSRs and the SFP walls is not expected. The baseplates of adjacent racks can come into contact at some velocity if they initially move apart and then back together, as discussed in Section 3.7.1.3.

Presuming that the racks are in contact at their bases, flexure of the racks along their height could cause the top ends of adjacent racks to come into contact. The maximum reduction in gap between adjacent racks (i.e., larger values indicate the rack upper structures to be closer to each other) are shown in Table 3-6. The minimum gap for the cell-to-cell contact in Region I is 60.0 mm (2.36 in), and that of Region II is 30.0 mm (1.18 in), as shown in Figure 2-5. Therefore, there is no impact on the rack cells by each other, because the maximum relative displacements of racks are smaller than the cell wall separation with baseplates touching.

The maximum relative displacement of the rack pedestal from its starting point is 104.3 mm (4.1 in) as shown in Table 3-6. The minimum size of the embedment plate is about 610 mm (24 in) x 610 mm (24 in) (Reference 27). Therefore, rack pedestals do not slide off the embedment plates onto the spent fuel pool liner because the maximum displacement of rack pedestal is not large enough to move off of the embedment plate.

The maximum rotations of the rack are obtained from a post-processing of the rack time history response output. The SFSR should not exhibit rotations sufficient to cause the rack to overturn (i.e., the rack does not exhibit a rotation sufficient to bring the center of mass over the corner pedestal). Based on the width and height of a 8x7 rack, the rotation required to produce incipient tipping for this rack is approximately equal to:

$$\tan^{-1}[(1/2*\text{Distance to bring center of gravity over pedestal}) / (1/2*\text{Height of rack})]$$

$$\tan^{-1}[(1{,}610/2) / (4{,}775/2)] = 18.5^{o}$$

As shown in Table 3-10, the safety factor for allowable angle is greater than the acceptance criteria of 1.5 from SRP 3.8.5. Therefore, overturning of a rack module does not occur.

3.7.1.2 Support Pedestal Loads of Rack

The maximum horizontal and vertical loads generated on support pedestal with the application of SSE loads are shown in Table 3-7 and Figure 3-22 and are used to perform structural integrity evaluation of support pedestal and rack. The dynamic simulations of the racks give results for the vertical and two horizontal forces (i.e., E-W and N-S directions) throughout the transient. From those values, the maximum axial force in the vertical direction and the maximum shear forces of the two horizontal directions per pedestal are determined. The resultant shear force for each run is conservatively calculated by combining the maximum horizontal loads on any single pedestal as shown in Table 3-7 using the square root of the sum of the squares (SRSS) method. The maximum bending moment at the bottom baseplate-to-pedestal interface is computed by multiplying the maximum shear force and the distance from the bottom baseplate to the contact point surface underneath of the NFSRs and SFSRs, which is 185 mm (7.28 inches) and 160 mm (6.3 inches) as shown in Tables 2-1 and 2-2, respectively. Additional detail is provided in Appendix F of Reference 17.

3.7.1.3 Impact Loads

The impact loads for fuel-to-cell wall, rack-to-rack and rack-to-pool wall of the NFP and SFP are calculated as follows:

(1) Fuel-to-Cell Wall

For purposes of assessing the effect on rack structural integrity, the maximum impact loads of fuel assembly-to-cell wall for the NFSRs and the SFSRs are as shown in Table 3-8. These loads are determined by dividing the maximum total fuel assembly beam to cell wall load by the number of fuel assemblies in the rack under evaluation (e.g., divide by 64 for a full rack, 32 for a half full rack).

For purposes of determining the effect on the fuel assembly grids, the impact load on each of the fuel support grids at each time step is determined by dividing the maximum calculated impact load per cell at each of the five nodes by number of spacer grids at each of the nodes. For each run, the impact loads in the East-West and North-South directions are combined using the SRSS method at the same time. The combined maximum impact loads on fuel support grid of the NFSRs and the SFSRs are shown in Table 3-8.

(2) Impacts of Rack-to-Rack and Rack-to-Pool Wall

SFSRs are installed as closely as possible with the protruding baseplate intended to be in contact with the adjacent baseplates. If the racks were initially installed with slight separation, conclusions would not change since it would be no different than a few time steps into a transient when the rack bases have moved slightly apart. As reported in Section 3.7.1.1, the upper part of the racks do not come into contact. Therefore, the only rack-to-rack contact is between the baseplate of racks. The maximum impact load at the SFSR baseplates is shown in Table 3-8.

Also as reported in Section 3.7.1.1, the racks do not contact the SFP wall. Therefore, no rack to pool wall impact loads are calculated. This is consistent with SRP Section 3.8.4, Appendix D, Structural Acceptance Criteria, which states:

> "In the consideration of the effects of seismic loads, factors of safety against gross sliding and overturning of racks and rack modulus [sic] under all probable service conditions should be in accordance with SRP Section 3.8.5, Subsection II.5. This position on factors of safety against sliding and tilting need not be met provided that the applicant meets any one of the following conditions:
>
> "a. Detailed nonlinear dynamic analyses show that the amplitudes of sliding motion are minimal and impact between adjacent rack modules or between a rack module and the pool walls is prevented provided that the factors of safety against tilting are within the allowable values provided in SRP Section 3.8.5, Subsection II.5…."

3.7.2 Fuel Structural Evaluation

Lateral impact load on the spent fuel assembly is evaluated for two acceptance criteria: fuel spacer grid buckling and fuel cladding yield stress.

The maximum impact load per cell applied to fuel assembly is evaluated for the peak load shown in Table 3-8. Therefore, the maximum acceleration load that the rack imparts on the fuel assembly can be conservatively calculated as follows:

$$a = \frac{F}{w}$$

Where,

a = Maximum lateral acceleration in g's,
F = Maximum fuel-to-cell wall impact load per cell, and
w = Weight of one fuel assembly (6.27 kN (1408.6 lbf)).

The structural integrity of fuel assembly cladding is evaluated for the maximum lateral acceleration load, obtained by combining (i.e., SRSS) the simultaneous impact load in the E-W and N-S directions to find the maximum value at any time step. The fuel assembly spacer grid is evaluated for the maximum grid impact load, obtained by combining (i.e., SRSS) the simultaneous impact load in the E-W and N-S directions at the same time.

3.7.2.1 Structural Integrity Evaluation of Fuel Spacer Grid

The lateral impact loads on a single fuel spacer grid is compared against its buckling load capacity, which is shown in the Table 3-3. The critical buckling load of the fuel spacer grid for the APR1400 design is 24.8 kN (5,567 lbf) and compared with the combined fuel grid impact load as shown in Table 3-8. The resulting safety factor on fuel assembly spacer grid is as summarized in Table 3-11.

3.7.2.2 Stress Evaluation of Fuel Cladding

The maximum lateral acceleration acting on the fuel mass is used to calculate a load uniformly distributed

over a single fuel rod modeled as a beam simply supported by the spacer grids, and the maximum fuel rod length between the spacer grids is 359.4 mm (14.148 in) as shown in Table 3-3.

The uniformly distributed load on the fuel rod is calculated as follows:

$$q = a \times W_{fuel}$$

Where,

a = Maximum lateral acceleration in g's, and
W_{fuel} = Fuel assembly rod mass per unit length (0.61 kg/m).

The maximum bending moment for uniform load is calculated as

$$M = (q \times L_{spacer}^2) / 8$$

Where,

L_{spacer} = Maximum fuel rod length between spacer grids (359.4 mm (14.148 in)).

The resulting maximum bending stress in the fuel cladding is calculated from equation below.

$$\sigma_b = \frac{M \cdot R_o}{I}$$

Where,

R_o = Outer radius of fuel rod (4.75 mm (0.187 in)), and
I = Moment of inertia of fuel rod cladding (160.4 mm^4 (3.853 x 10^{-4} in^4)).

This bending stress is compared to the yield stress of 540.3 MPa (78,365 psi) per Table 3-3 for fuel rod cladding, the resulting safety factor is given in Table 3-11. The strain associated with this maximum stress is

$$\varepsilon = \sigma_b / E$$

The maximum impact load on an individual fuel grid spacer cell, the bending stress and the strain induced in the fuel rod cladding due to the maximum lateral acceleration are summarized in Table 3-11. The structural integrity of the stored fuel assemblies under the SSE event is maintained, because the safety factors are greater than 1.0.

3.7.3 Rack Structural Evaluation

To ensure that the fuel racks have adequate safety margins, all stress evaluations for the fuel racks are performed based on the worst-case results in any rack at any time during multiple simulations. In this section, the structural integrity of welds and racks is evaluated by using the maximum loads in vertical and horizontal direction calculated by time-history analysis of the racks.

3.7.3.1 Stress Factors for Racks

Using the time-history analysis results for pedestal normal and lateral interface forces, the limiting bending moment and shear force at the baseplate-to-pedestal interface may be computed as a function of time. In particular, maximum values for the stress factors which are defined in Section 3.2.2 can be determined for each pedestal in each rack. Using this information, the structural integrity of the pedestals can be assessed.

The net section maximum bending moments and shear forces can also be determined at the bottom of the rack structure. From these loads, the stress factors for the NFSRs and the SFSR cell walls just above the baseplate can be also determined in the rack. Because they are at the end of fuel rack beam, these locations are the most heavily loaded net sections in the structure so that satisfaction of the stress factor criteria at these locations ensures that the overall structural criteria set forth in Section 3.2 are met.

As shown in Table 3-9:

- Maximum pedestal stress factors for the NFSRs and SFSRs are less than the allowable of 1.0.
- Maximum cell wall stress factors for the NFSRs and SFSRs are less than the allowable of 1.0.

Therefore, the rack cells and the support pedestals are able to maintain their structural integrity under the worst loading conditions.

3.7.3.2 Pedestal Thread Stress Evaluation

The integrity for the support pedestal thread is evaluated using the maximum load on the support pedestal in vertical direction as shown in Table 3-7. Using this load, the maximum shear stress of thread in the engagement region is calculated. The allowable shear stress of SA-240 Type 304L material for Level D condition is the lesser of 0.72 S_y = 106.2 MPa (15,408 psi) or 0.42 S_u = 191.4 MPa (27,762 psi) as stated on Section 3.2.2. Therefore, the former criteria controls, and the calculated shear stress of pedestal thread is acceptable, as shown on Table 3-13.

3.7.3.3 Stresses on Welds

Weld locations of the NFSRs subjected to SSE loading are at the bottom of the rack at the cell-to-baseplate connection, and at the top of the pedestal support at the baseplate connection.

SFSR welds are at the bottom of the rack at the cell-to-baseplate connection, at the top of the pedestal support at the baseplate connection, and at cell-to-cell connections. The maximum values of resultant loads are used to evaluate the structural integrity of these welds. The calculated stresses on fuel rack welds are summarized in Table 3-12.

(1) Cell-to-Baseplate Weld

As given in ASME Code Section III, Subsection NF, for Level A or B conditions, an allowable shear stress of a weld is 0.3 S_u = 136.7 MPa (19,830 psi) conservatively based on the base metal material. As stated in Section 3.2.2.3, the allowable weld stress may be increased for Level D by a factor of 1.8, giving an allowable of 0.54 S_u = 246.1 MPa (35,694 psi).

Stresses in the cell-to-baseplate welds are determined through the use of a simple conversion factor (ratio) applied to the corresponding stress factor in the adjacent rack material. This stress factor is discussed in Section 3.2.3, and given in Table 3-9. The conversion factor (ratio) values are developed from consideration of the differences in material thickness and length versus weld throat dimension and length, as follows:

Ratio = [(220 + 2.5) x 2.5)] / (180 x 2.5 x 0.707) = 1.75 (for the SFSRs)

Where,
Inner cell dimension (220 mm (8.66 in)),
Cell wall thickness (2.5 mm (0.098 in)),
Weld length (180 mm (7.09 in)), and
Weld thickness (= 2.5 x 0.707 = 1.767 mm (0.069 in)) are used.

For the NFSRs, the cell wall thickness and weld thickness are 6.0 mm (0.236 in) and 4.24 mm (0.167 in), respectively. The conversion factor (ratio) for the NFSRs is calculated as 1.54.

The highest predicted cell-to-baseplate weld stress is conservatively calculated based on the highest FACT2 for the rack cell region tension stress factor and FACT3 for the rack cell region shear stress factor. The maximum stress factors used do not all occur at the same time instant and the shear stress factors are the maximum for all load conditions. These cell wall stress factors are converted into actual stress on the weld of cell-to-cell as follows:

$$(FACT2 + FACT3) \times (2 \times 0.6 \times S_y) \times Ratio$$

The 2.0 multiplier value is used to adjust the Level A allowable to the Level D allowable, as discussed in Section 3.2.2.3.

The calculated stress value is less than the allowable weld stress value of 246.1 MPa (35,694 psi). Therefore, all weld stresses between the cell wall and the baseplate are acceptable.

(2) Baseplate-to-Pedestal Weld

The stress in the baseplate-to-pedestal weld is conservatively evaluated using the maximum horizontal pedestal load for the NFSR, the maximum compressive vertical load for the NFSR, and the dimensions of the SFSR support pedestal welds. This provides a conservative combination of parameters. The weld stress is derived from simultaneous application of the maximum tensile force obtained from ANSYS and the maximum pedestal friction forces in the horizontal directions in Table 3-7. The calculated maximum stress identified in Table 3-12 is well below the Level D allowable of 246.1 MPa (35,694 psi). Therefore, all weld stresses between baseplate and support pedestal are acceptable.

(3) Cell-to-Cell Weld

Cell-to-cell connections are a series of connecting welds along the cell height. Stresses in the SFSR cell-to-cell welds develop due to fuel assembly impacts with the cell wall. Weld stress is calculated based on the maximum fuel-to-cell wall impact load and shear stress, which is obtained by using the cell wall shear stress coefficient under Level D conditions from the dynamic analysis results. These weld stresses are conservatively considered by assuming that fuel assemblies in adjacent cells are moving out of phase with one another so that impact loads in two adjacent cells are in opposite directions and are applied simultaneously. This load application tends to separate the two cells from each other at the weld. Stress in the cell-to-cell weld is combined by the square root of the sum of the squares (SRSS) method for the shear stress due to horizontal load acting on rack and the shear stress due to impact load of rack fuel-to-cell wall, and the stress due to cell wall axial shear load.

The maximum fuel-to-cell wall impact load is taken from Table 3-8. The shear stress on the cell wall is calculated by multiplying shear allowable stress under Level D conditions and the cell wall stress coefficient, FACT3 from Table 3-9. The total shear stress acting on the weld is calculated by combining the shear stress acting on cell wall with the fuel-to-cell impact stress using the SRSS method. The calculated stresses of the cell-to-cell weld and the base metal shear are well below the allowable, and the results are summarized in Table 3-12.

Figure 3-19 shows a free-body diagram explaining how the loads were transferred and used to evaluate the cell-to-cell welds.

In summary, the stress on the cell-to-cell weld is calculated using the following formulas as described in Reference 17.

1) Stress calculation of base metal adjacent to weld due to impact load:

$$S_{impact} = \frac{F_{impact}}{A_{weld}}$$

Where,

F_{impact} : Maximum fuel assembly to cell impact load in Table 3-8, and
A_{weld} : Total area of weld.

2) Shear stress calculation of the cell wall:

$$S_{shear} = FACT3 * V_{sse}$$

Where,

FACT3 : Shear stress factor of cell wall in Table 3-9, and
V_{sse} : Allowable stress of cell wall under Level D condition.

3) Axial shear stress calculation of the cell wall:

$$S_{a\_shear} = \frac{F_{a\_shear}}{A_{weld}}$$

Where,

F_{a_shear} : Axial shear force of cell wall,
$= \mathrm{FACT2} * V_{sse_{axial}} * A_{cell}$
FACT2 : Tensile or bending stress factor of cell wall in Table 3-9,
V_{sse_axial} : Allowable stress of cell wall under Level D condition, and
A_{cell} : Area of cell.

4) Total shear stress calculation acting at cell-to-cell weld:

$$S_{combined} = \sqrt{S_{impact}^2 + S_{shear}^2 + S_{a\_shear}^2}$$

3.7.3.4 Stress Evaluation of Stud Bolt for NFSR

The integrity for the stud bolt is evaluated for the maximum loads on NFSR module. Detailed calculation is provided in Appendix F (Reference 17). Stud bolt stress is evaluated against the criteria for Level D. The calculated stresses of stud bolt are well below the allowable, and the results are summarized in Table 3-14.

3.7.3.5 Local Stress Evaluation

(1) Cell Wall Impact

The maximum fuel-to-cell wall impact loads for the NFSRs and the SFSRs are as shown in Table 3-8. The evaluation for cell wall for impact is performed to guarantee that local impact does not affect criticality of stored fuel. Integrity of local cell wall is evaluated conservatively using the peak impact load. The limiting impact load to induce overall permanent deformation is calculated by plastic analysis. The cell walls of the new and the spent fuel storage racks can withstand a side load of a maximum of 273.2 kN (61,410 lbf) and 47.4 kN (10,660 lbf), respectively (Reference 17). Therefore, the cell wall of racks satisfies the requirement with the maximum impact loads less than the allowable loads.

(2) Cell Wall Buckling

The allowable local buckling stresses of the cell walls for the fuel storage rack are obtained by using classical plate buckling analysis on the lower portion of the cell walls. A critical buckling stress for cell walls can be calculated by following equation (Reference 28).

$$\sigma_{cr} = K \frac{E}{(1 - \nu^2)} (\frac{t}{b})^2$$

Where,

E (Young's modulus) = 1.896E+05 N/mm^2 (27.5E+06 psi),
ν (Poisson's ratio) = 0.3,
t (Cell Thickness) = 2.5 mm (0.098 in),
b (Cell width) = 220 mm (8.66 in), and
a (Unreinforced height) = 130 mm (5.10 in).

The K factor varies depending on the plate length/width ratio and the boundary support conditions at the side of the plate. At the base of the rack, the cell wall acts alone in compression for a length of about 5.1 inch up to the point where the cover plate for the neutron absorber sheathing is attached. Above this level, the cover plate for the neutron absorber sheathing provides additional strength against buckling, which is not considered here. Therefore, the length/width ratio for the 220 mm (8.66 in) wide cell wall will be taken as 0.59. From Table 35 of Roark's Formulas for stress & strain (Reference 28), the value of K is taken as 5.80, which is the corresponding value for a/b (length/width ratio) = 0.6, for two edges simply supported and two opposite edges clamped.

For the given data above, two-thirds of the critical buckling stress (σ_{cr}) as the limit under Service Level D condition is calculated as 103.2 MPa (14,964 psi) for all racks. It should be noted that this calculation is based on the applied stress being uniform along the entire length of the cell wall. In the actual fuel rack, the compressive stress comes from consideration of the overall bending of the rack structures during a seismic event and as such is negligible at the rack top. In the simulation, the maximum compressive stress due to overall bending is generated near the baseplate. This local buckling stress limit is not violated anywhere in the body of the rack modules since the peak calculated stress is within the allowable value of 103.2 MPa (14,964 psi). Therefore, a buckling of the rack cell wall does not occur.

(3) Secondary Stress by Temperature Effects

The temperature gradients across the rack structure caused by differential heating effects between one or more filled cells and one or more adjacent empty cells are considered. The worst thermal stress in a fuel rack is obtained when a storage cell has a fuel assembly generating heat at the maximum postulated rate and the surrounding storage cells contain no fuel. The thermal stress stresses that occur in this scenario are secondary stresses as defined by the ASME Code Section III, Division 1. Therefore, it is independently evaluated without combining with primary stress of other load conditions.

A conservative estimate of the weld stresses along the length of an isolated hot cell is obtained by considering a beam strip uniformly heated by ΔT = 36 ^{o}C (65 ^{o}F), and restrained from growth along one long edge. The temperature rise envelops the difference between the maximum local spent fuel pool water temperature (76.2 ^{o}C (169 ^{o}F) bounding) inside a storage cell and the bulk pool temperature (48.9 ^{o}C (120 ^{o}F)) based on the thermal-hydraulic analysis of the spent fuel pool (Reference 29). This analysis assumes an almost full SFP to which freshly discharged fuel with worst case decay heat is added in adjacent cells and SFP thermal capacity of only the water above the top of the SFRs. The maximum shear stress due to temperature change for isolated hot cell weld is calculated as follows:

$$\tau_{max} = E \times \alpha \times \Delta T$$

Where,

E = 1.896E+05 N/mm^2 (27.5E+06 psi),
α = 9.5E-06 in/in-^{o}F, and
ΔT = 36 ^{o}C (65 ^{o}F).

The maximum shear stress due to the temperature gradient for an isolated hot cell is calculated given that

this thermal stress is classified as secondary stress, the allowable shear stress criteria for Level D condition (0.42 S_u = 191.4 MPa (27,762 psi)) is used as the limit of allowable. Therefore, the maximum shear stress due to the temperature gradient is acceptable.

Another possible source of temperature induced stress is expansion of adjacent SFSRs with increased temperature resulting in a contact load between pedestals and baseplates of adjacent racks or relatively different expansion for a fuel assembly and the cell surrounding it. For the former, it is likely that a fuel assembly would cool over time so that it would not generate an increase stress. However, in the event of a loss of SFP cooling, the fuel and the surrounding cell could heat up at different rates. The fuel assembly grid typical dimension is 206.45 mm (8.128 in) square, and a SFSR cell inner dimension is 220.0 ±3 mm square, for a gap of 10.55 mm (0.415 in). Assuming that thermal expansion of the fuel assembly and the rack material is identical, the elongation of SA-240 Type 304L material due to thermal expansion is:

$$\epsilon = \alpha\,(T_2 - T_1) = 0.001\ in/in$$

Where,

ε: Differential thermal expansion elongation (in/in),
α: Thermal expansion coefficient of SA-240 Type 304L = 8.9E-6 (in/in-°F),
T_2: Temperature = 223.7°F [Maximum fuel clad cladding temperature of spent fuel assembly at abnormal condition per thermal-hydraulic analysis], and
T_1: Temperature = 115.5 °F [Bulk temperature on normal condition of spent fuel pool].

Given the fuel assembly dimensions, the total differential expansion is 0.21 mm (0.008 in), which is a small fraction of the available gap.

As for the load due to expansion of each SFSR causing a contact stress, assuming the racks are installed touching at 21°C (70°F) and heat up to 48.9°C (120°F), the expansion of each rack is about 0.43 mm (0.017 in). In order to develop a load due to constraint of free end displacement, more than two adjacent racks must be in hard contact this is extremely unlikely. Therefore, the development of any significant thermal load due to restraint of free end displacement is not considered credible. Any incidental forces that might develop if some baseplates are in contact are self-limiting as a very small displacement, or shifting of the racks, relieves the stress. Self-limiting stresses developed by constraint of the structure and relieved by minor deformation are, by definition (NF-3121.3), secondary stresses.

According SRP Section 3.8.4, Appendix D, Section I.2, “Design, fabrication, and installation of fuel racks of stainless steel material may be performed based on ASME Code, Section III, Division 1, Subsection NF requirements for Class 3 component supports.” For the design of Class 3 component supports, Table NF-3251.2-1, does not require the evaluation of secondary stresses. Based on this, it is concluded that the development of significant thermal loads due to constraint of the baseplates is not credible and any postulated incidental loads need not be considered since they result in secondary stresses. Therefore, loads from the restraint of adjacent racks do not need to be explicitly considered in the design analysis.

(4) Punching Shear Analysis of Rack Baseplate

a. Punching due to Vertical Pedestal Load

A punching shear analysis has been performed for the rack baseplate under seismic loading conditions. The analysis demonstrates that the maximum vertical load on a single support pedestal is less than the force necessary for the 285 mm (11.2 in) square pedestal block to punch through the 25 mm (0.984 in) thickness of the baseplate. The punching shear capacity of the baseplate (F_v) can be calculated by following equation.

$$F_V = \frac{S_y}{\sqrt{3}} \times 4 \times L \times t$$

Where,

$\frac{S_y}{\sqrt{3}}$ (shear stress limit according to the distortion energy theory of yielding),
S_y (yield strength of baseplate) = 147.5 MPa (21,400 psi),
L (side length of the pedestal block) = 285 mm (11.2 in), and
t (thickness of the baseplate) = 25 mm (0.984 in).

The punching shear capacity of the baseplate calculated using the above equation exceeds the maximum pedestal load per Table 3-7 as shown in Table 3-15. Therefore, a punching shear failure of the rack baseplate will not occur.

b. Punching due to Fuel Impact Load

A punching shear analysis due to the maximum impact load of fuel assembly-to-baseplate is performed for the rack baseplate under seismic loading conditions and compared with the allowable stress limit (0.72 x S_y = 106.2 MPa (15,408 psi)) for the Level D condition as follows:

$$\sigma_{shear} = F_{impact} / (4 \times L \times t/2)$$

Where,
F_{impact} (Maximum fuel assembly-to-baseplate impact load in vertical direction)
= 55.7 kN (12,516 lbf) per Table 3-8,
L (Side length of the square cross-section of fuel assembly) = 206.5 mm (8.128 in), and
t (Thickness of the baseplate) = 25 mm (0.984 in).

The resultant stress (σ_{shear}) does not exceed the allowable stress limit as shown in Table 3-15. Therefore, a punching shear failure of the rack baseplate will not occur.

3.7.4 Sensitivity Studies

Since the NFSRs are secured in place and do not slide, the following sensitivities (except for the first, rack EI) are not considered applicable. Therefore, discussion of these sensitivities is for the SFSRs only.

3.7.4.1 Rack EI

For both the NFSR and SFSR, sensitivities of ±20% of the product of rack elastic modulus and moment of inertia are evaluated in runs 21 through 24. For the NFSR, fuel assembly grid to cell impact loads were similar. For the SFSR, all loads were similar to those for the base case.

3.7.4.2 Coefficient of Friction

Each of the five time histories was applied to both Region I and Region II racks at COF values of 0.2, 0.5, and 0.8, as shown in Table 3-5 and Figure 3-20. The following trends were noted:

- For loads on a single pedestal, horizontal loads increase with increasing COF
- Baseplate-to-baseplate impact loads increase with increasing COF
- COF does not affect the other loads.

3.7.4.3 Spring constant

Three sensitivities were performed on spring constants (i.e., stiffness) in the model, as shown in:

- The rack-to-floor stiffness was evaluated at ±20% of the nominal value.
- The rack-to-rack stiffness was evaluated at ±20% of the nominal value.
- The fuel-to-rack stiffness was evaluated at ±20% of the nominal value.

The effect of the sensitivities was a change in predicted loads within the variation found for different time histories and less than the variation for different COFs. Figure 3-24 show the effect on pedestal and baseplate impact loads, respectively.

3.7.4.4 Fuel Assembly EI

One case (Run 33) evaluates the effect of end of life fuel assembly properties. Fuel-to-cell wall and fuel assembly grid impact loads were consistent with those of the BOL case.

3.7.4.5 Rack Loading

The free standing SFSRs do slide and different fuel loading arrangements were considered, as shown in Table 3-5 and described in most runs used fully loaded racks, but one sensitivity involved all racks being empty (Run 34) and another (Run 35) had one quarter full rack and also two half full racks loaded uniformly (see Figure 3-4). The results for these runs were as would be expected in comparison with those done with all racks fully loaded.

3.7.4.6 Calculational Time Step

Comparison of a run at one half the fixed time step used for all other runs showed small changes in calculated results comparable to the run to run variation with different time histories. Small differences, vice identical results, are expected because the time step used affects where in each time history the acceleration is taken and how long it is applied. Convergence criteria for both force and displacement were 5%.

3.7.5 Conservatisms in Seismic Analysis

The APR1400 fuel rack seismic analytical approach includes significant conservatisms:

- All of the fuel mass at each elevation in the rack is assumed to move as a unit, resulting in a conservative impact force and rack response.
- The damping applied in the time history analyses is a conservative value. The ANSYS analyses are based on full integration of the equations of motion and necessarily use frequency dependent damping. For frequency dependent damping, the damping curve is anchored at the lower and upper bounds of the frequency range of interest. For all frequencies between the lower and upper bound, a conservative, lower damping value will then be applied.
- When evaluating stresses, the calculated loads are combined conservatively. For all horizontal loads except fuel assembly grid impact, the combination uses the maximum E-W and the maximum N-S load at any time during the transient, even if they do not occur during the same time step. The grid loads use the values during the same time step to find the maximum. The times of maximum load in the two directions are in general not the same.
- Fluid drag in the spent fuel pool is conservatively neglected. If considered, fluid drag would result in lower impact loads.

Consequently, the reported results include considerable conservatisms that are not quantified.

3.7.6 Review of Results

Following completion of the analyses described above, results were reviewed for unexpected or inconsistent behavior. The following high level conclusions were noted.

The analyses performed for loads results from a SSE show satisfactory performance to regulatory acceptance criteria.

For the SFSRs, a comparison of each time history at each of the three COF values was made for each of the loading conditions for Region I and Region II.

- Loads on a single pedestal within a region
  - SRSS of horizontal loads are all within about 25% of their means for each COF
  - Horizontal loads increase linearly with increasing COF (see Figure 3-20)
  - Vertical loads are also within 25% of their means for each COF (excludes empty rack runs)
  - Vertical loads are not affected by the COF (see Figure 3-20)

- Rack to rack baseplate impact loads
  - Values increase with increasing value of the COF
  - For a single value of COF (excluding the empty rack case), results vary from about two-thirds to about five-thirds of the average for that COF.

- The fuel assembly to cell impact loads are independent of COF, and the means of E-W and N-S loads are within 16% of each other.

Figure 3-22 and Figure 3-23 provide graphs of the pedestal and baseplate loads for SFSR runs, for the two different fuel rack regions. Figure 3-24 compares SFSR baseplate impact loads for stiffness sensitivity variations of ±20%. Figure 3-25 shows the effect of fuel-to-rack stiffness on grid impact load. Finally, Figure 3-26 is a chart of maximum single pedestal loads for all NFSR runs. The magnitude of variability in loads over the ±20% range used in these sensitivities is similar to that across different time histories with the same assumed conditions.

For the NFSRs, there are very few variable factors to consider. The range of result variation is comparable to that noted for the SFSRs.

The trends described above are physically reasonable and show no discrepancies that would indicate non-physical behavior is predicted by the model.

Table 3-1 Load Combinations for Rack Analysis

Load Combination	Acceptance Limit
D + L D + L + T_o	ASME Code Section III, Subsection NF Level A service limits for Class 3
D + L + T_o + P_f	ASME Code Section III, Subsection NF Level B service limits for Class 3
D + L + T_a + E'	ASME Code Section III, Subsection NF Level D service limits for Class 3
D + L + F_d	The functional capability of the fuel racks should be demonstrated.

Where,

D : Dead weight including fuel assembly weight.

L : Live load (not applicable for the fuel rack, since there are no moving objects in the rack load path). Note that it is accepted practice to consider the fuel weight as a dead weight.

E' : Safe Shutdown Earthquake (SSE).

T_o= Differential temperature induced loads, based on the most critical transient or steady state condition under normal operation or shutdown conditions.

T_a= Highest temperature associated with the postulated abnormal design conditions.

F_d= Force caused by the accidental drop of the heaviest load from maximum possible height.

P_f= Upward force on the racks caused by a postulated stuck fuel assembly. This force may be caused at any angle between horizontal and vertical.

Note: For the APR1400, the operating basis earthquake (OBE) ground motion is defined as one-third the SSE ground motion design response spectra. Therefore, in accordance with 10 CFR Part 50, Appendix S, an OBE design analysis is not required and load combinations involving E have been removed.

Table 3-2 Rack Size and Weight

Rack Modules(*)		Array Size	Weight, kgf (lbf)
NFSR		7 x 8	
SFSR	A1-1, A1-2, A1-3 & A1-4	8 x 8	
	A2-1 & A2-2	6 x 8	
	B1 B2-1, B2-2, B2-3 B3, B4 B5-1, B5-2, B5-3, B5-4, B5-5, B5-6 B6-1, B6-2, B6-3 B7, B8 B9, B10	8 x 8	
	C1, C2, C3 & C4	8 x 7	

TS

(*) Refer to Figure 2-1 and Figure 2-4.

Table 3-3 Data for Fuel Assembly

Parameter		Data (*)
Weight of Fuel Assembly, kN (lbf)		
Grid width of Fuel Assembly, mm (in)		
Max. Fuel Rod Length between Spacer Grid, mm (in)		
Mass of Fuel Rod, kg/m (lbm/in)		
Outer Diameter of Fuel Rod, mm (in)		
Inner Diameter of Fuel Rod, mm (in)		
Clad Thickness, mm (in)		
Area Moment of Inertia of Fuel Rod Clad, mm^4 (in^4)		
Young's Modulus of Fuel Rod Clad, MPa (psi) at 93.3 °C (200°F)		
Yield Strength of Fuel Rod Clad, MPa (psi) at 93.3 °C (200 °F)		
One-sided Grid Stiffness, kN/m (lbf/in) at 93.3 °C (200 °F)		
One-sided Grid Crushing Strength, kN (lbf) at 93.3 °C (200 °F)	BOL	
	EOL	
Fuel Assembly Flexural Rigidity (EI), m^2-kN (in^2-lbf) at 93.3 °C (200 °F)		
Total Grid Number, ea		

TS

(*) All of the dimensions are nominal values.

Table 3-4 Material Properties

Part	Material	Young's Modulus (E) MPa (psi)	Yield Strength (S_y) MPa (psi)	Ultimate Strength (S_u) MPa (psi)
Rack	SA-240 Type 304L	189,605 (27.5E+06)	147.5 (21,400)	455.7 (66,100)
Support Pedestal (Upper Part)	SA-240 Type 304L	189,605 (27.5E+06)	147.5 (21,400)	455.7 (66,100)
Pedestal Bolt Part	SA-564 Grade 630 (Hardened at 1100 ^{o}F)	191,674 (27.8E+06)	732.9 (106,300)	965.3 (140,000)
Stud Bolt (for NFSR)	SA-564 Grade 630 (Hardened at 1100 ^{o}F)	191,674 (27.8E+06)	732.9 (106,300)	965.3 (140,000)

Table 3-5 List of Simulations

Rack	Run No.	Time History	COF(*)	Rack-to-Floor Stiffness	Rack-to-Rack Stiffness	Fuel-to-Rack Stiffness	Fuel Assembly Elastic Modulus x Moment-of-Inertia (EI)	Rack Elastic Modulus x Moment-of-Inertia (EI)	Time Step (sec.)	Loading
NFSR	1	1	N/A	N/A	N/A	Nominal	BOL	Nominal	2×10^{-4}	Full
	2	2								
	3	3								
	4	4								
	5	5								
SFSR	6	1	0.2	Nominal	Nominal					
	7	2								
	8	3								
	9	4								
	10	5								
	11	1	0.5							
	12	2								
	13	3								
	14	4								
	15	5								
	16	1	0.8							
	17	2								
	18	3								
	19	4								
	20	5								
Sensitivity Runs										
NFSR	21	Note 1	N/A	N/A	N/A	Nominal	BOL	20%	2×10^{-4}	Full
	22							-20%		
SFSR	23	Note 2	0.8	Nominal	Nominal	Nominal	BOL	20%	2×10^{-4}	Full
	24							-20%		
	25	Note 3	0.8	20%	Nominal	Nominal	BOL	Nominal	2×10^{-4}	Full
	26			-20%						
	27	Note 4	0.5	Nominal	20%	Nominal	BOL	Nominal	2×10^{-4}	Full
	28				-20%					
	29	Note 5	0.8	Nominal	Nominal	20%	BOL	Nominal	2×10^{-4}	Full
	30					-20%				
	31	Note 6	0.8	Nominal	Nominal	20%	BOL	Nominal	2×10^{-4}	Full
	32					-20%				
	33	Note 6	0.8	Nominal	Nominal	Nominal	EOL	Nominal	2×10^{-4}	Full
	34	Note 4	0.5	Nominal	Nominal	Nominal	BOL	Nominal	2×10^{-4}	Empty
	35									Mixed
	36	Note 7	0.8	Nominal	Nominal	Nominal	BOL	Nominal	1×10^{-4}	Full

Notes on following page.

Notes:

1. Run No. 5: Apply sensitivity to the NFSR run from runs 1 through 5 that yielded the maximum horizontal (E-W or N-S) force on a pedestal.
2. Run No. 17: Apply sensitivity to the SFSR run from runs 6 through 20 that yielded the maximum horizontal (E-W or N-S) force on a pedestal.
3. Run No. 17: Apply sensitivity to the SFSR run from runs 6 through 20 that yielded the maximum vertical pedestal force.
4. Run No. 12: Apply sensitivity to the SFSR run from runs 6 through 20 that yielded the maximum rack-to-rack impact force.
5. Run No. 18: Apply sensitivity to the SFSR run from runs 6 through 20 that yielded the maximum total fuel impact force.
6. Run No. 19: Apply sensitivity to the SFSR run from runs 6 through 20 that yielded the maximum fuel grid impact force.
7. Run No. 17: Apply sensitivity to the SFSR run from runs 6 through 20 that yielded the maximum horizontal (E-W or N-S) and vertical force on a pedestal.

(*) : Coefficient of Friction

Table 3-6 Displacement of Racks for All Simulations

Rack	Run Number	Top of Rack (in)		Reduction in Gap between Adjacent Racks (in)*				Displacement of Pedestal Relative to Pool Floor (in)		Coefficient of Friction
				Region I		Region II				
		E-W	N-S	E-W	N-S	E-W	N-S	E-W	N-S	
NFSR	1	0.288	0.452	-	-	-	-	-	-	N/A
	2	0.317	0.582	-	-	-	-	-	-	
	3	0.325	0.475	-	-	-	-	-	-	
	4	0.306	0.490	-	-	-	-	-	-	
	5	0.290	0.528	-	-	-	-	-	-	
SFSR	6	0.149	0.203	0.119	0.185	0.174	0.279	3.171	2.696	0.2
	7	0.159	0.231	0.119	0.208	0.193	0.182	1.565	2.775	
	8	0.138	0.188	0.127	0.224	0.152	0.210	1.906	2.054	
	9	0.125	0.181	0.106	0.166	0.147	0.158	1.944	1.804	
	10	0.140	0.201	0.112	0.232	0.210	0.157	4.108	2.261	
	11	0.206	0.269	0.202	0.278	0.181	0.179	2.032	1.591	0.5
	12	0.219	0.240	0.180	0.232	0.179	0.206	1.463	1.209	
	13	0.226	0.267	0.139	0.292	0.159	0.205	1.248	1.161	
	14	0.218	0.270	0.197	0.285	0.144	0.186	1.652	1.026	
	15	0.225	0.251	0.129	0.258	0.171	0.159	2.334	1.487	
	16	0.278	0.334	0.233	0.365	0.182	0.254	1.957	1.171	0.8
	17	0.285	0.314	0.199	0.307	0.196	0.208	1.157	1.213	
	18	0.268	0.367	0.162	0.361	0.197	0.227	0.837	0.860	
	19	0.276	0.331	0.162	0.309	0.195	0.224	1.380	1.187	
	20	0.329	0.318	0.176	0.369	0.196	0.182	1.130	1.207	
Sensitivity Runs										
NFSR	21	0.274	0.434	-	-	-	-	-	-	N/A
	22	0.369	0.631	-	-	-	-	-	-	
SFSR	23	0.239	0.250	0.156	0.257	0.161	0.139	1.056	0.941	0.8
	24	0.358	0.392	0.188	0.335	0.210	0.270	1.159	1.266	
	25	0.277	0.293	0.189	0.274	0.215	0.243	1.206	1.247	0.8
	26	0.279	0.336	0.190	0.289	0.175	0.183	1.150	1.252	
	27	0.220	0.233	0.131	0.243	0.134	0.191	1.305	1.073	0.5
	28	0.217	0.256	0.183	0.283	0.186	0.172	1.373	1.246	
	29	0.249	0.336	0.203	0.327	0.149	0.243	1.080	0.889	0.8
	30	0.280	0.338	0.167	0.328	0.186	0.220	0.835	0.845	
	31	0.269	0.331	0.169	0.344	0.196	0.271	1.323	0.965	0.8
	32	0.260	0.323	0.194	0.391	0.178	0.270	1.324	1.004	
	33	0.288	0.331	0.157	0.339	0.176	0.213	1.573	0.982	0.8
	34	0.106	0.090	0.078	0.092	0.094	0.068	0.569	0.514	0.5
	35	0.165	0.170	0.155	0.185	0.166	0.123	1.085	1.162	
	36	0.294	0.306	0.189	0.357	0.166	0.183	1.125	1.241	0.8

* Maximum displacements of less than 2.36 in (60 mm) (Region I) and 1.18 in (30 mm) (Region II) indicate no contact occurs.

Table 3-7 Maximum Pedestal Loads of Each Simulation(1)

Rack	Run No.	Load on Single Pedestal (lbf)				Coefficient of Friction
		Horizontal(2)			Vertical	
		E-W	N-S	Combined(3)		
NFSR	1	174,000	151,000	230,384	68,050	N/A
	2	148,700	129,000	196,857	69,810	
	3	162,300	142,100	215,717	61,330	
	4	183,300	160,400	243,571	72,540	
	5	197,300	172,300	261,944	58,000	
SFSR (Region I)	6	33,000	32,800	46,528	170,000	0.2
	7	29,700	27,400	40,409	156,000	
	8	27,100	32,800	42,547	174,000	
	9	30,400	25,600	39,743	154,000	
	10	22,900	26,500	35,024	133,000	
	11	63,200	78,200	100,546	168,000	0.5
	12	47,000	77,100	90,296	157,000	
	13	67,400	80,000	104,608	182,000	
	14	67,100	63,900	92,659	154,000	
	15	66,200	56,700	87,163	134,000	
	16	105,000	122,000	160,963	169,000	0.8
	17	72,900	120,000	140,408	154,000	
	18	108,000	102,000	148,553	159,000	
	19	88,100	90,600	126,372	154,000	
	20	79,100	94,800	123,466	135,000	
SFSR (Region II)	6	26,400	31,000	40,718	156,000	0.2
	7	29,500	27,600	40,398	157,000	
	8	18,400	24,800	30,880	124,000	
	9	34,700	29,600	45,610	178,000	
	10	18,800	21,700	28,711	111,000	
	11	63,400	77,300	99,974	155,000	0.5
	12	70,800	68,100	98,236	157,000	
	13	48,100	67,600	82,966	136,000	
	14	58,100	72,700	93,064	164,000	
	15	47,700	55,000	72,803	110,000	

SFSR (Region II)	16	102,000	120,000	157,493	173,000	0.8
	17	121,000	137,000	182,784	191,000	
	18	70,300	95,300	118,424	129,000	
	19	94,300	94,900	133,785	168,000	
	20	78,000	72,700	106,627	109,000	
Sensitivity Runs						
NFSR	21	172,900	151,100	229,621	58,000	N/A
	22	164,400	143,600	218,285	58,000	N/A
SFSR (Region I)	23	107,000	117,000	158,550	158,000	0.8
	24	104,000	109,000	150,655	152,000	0.8
	25	84,300	111,000	139,383	145,000	0.8
	26	91,700	136,000	164,027	183,000	0.8
	27	59,200	67,600	89,858	144,000	0.5
	28	52,700	67,900	85,952	150,000	0.5
	29	104,000	97,500	142,556	139,000	0.8
	30	103,000	93,100	138,840	161,000	0.8
	31	101,000	95,000	138,658	157,000	0.8
	32	109,000	101,000	148,600	155,000	0.8
	33	92,600	90,200	129,270	156,000	0.8
	34	20,600	20,600	29,133	41,400	0.5
	35	52,700	57,700	78,145	151,000	0.5
	36	85,100	121,000	147,929	163,000	0.8
SFSR (Region II)	23	111,000	102,000	150,748	158,000	0.8
	24	121,000	118,000	169,012	159,000	0.8
	25	123,000	131,000	179,694	174,000	0.8
	26	119,000	118,000	167,586	173,000	0.8
	27	76,000	71,400	104,278	157,000	0.5
	28	78,200	83,800	114,620	174,000	0.5
	29	74,700	97,100	122,509	130,000	0.8
	30	81,700	95,500	125,679	133,000	0.8
	31	102,000	98,700	141,936	188,000	0.8
	32	93,300	95,300	133,368	182,000	0.8
	33	101,000	87,400	133,566	166,000	0.8
	34	13,500	13,500	19,092	27,500	0.5
	35	75,600	77,500	108,266	159,000	0.5
	36	108,000	116,000	158,493	157,000	0.8

Notes:
(1) Reported values are maximum for a run at any time during the transient for any rack of that type (e.g., Region II SFSR).
(2) Although the horizontal loads are for the same rack, the maximum vertical load listed for a run may be from a different rack.
(3) Because combined horizontal loads are SRSS of maximum horizontal E-W & N-S loads at any time during the transient and it is very unlikely for horizontal loads in both directions to peak simultaneously, the combined horizontal load has considerable but unquantified conservatism.

Table 3-8 Maximum Impact Loads of Each Simulation(1)

Rack	Run No.	Rack-to-Rack Baseplate Impact Load (lbf)	Fuel-to-Cell Wall Impact Load per Cell (lbf)			Combined Fuel Grid(2) Impact Load (lbf)	Coefficient of Friction
			Horizontal		Vertical		
			E-W	N-S			
NFSR	1	-	6,173	10,948	5,879	2,219	N/A
	2	-	6,255	13,789	3,966	3,011	
	3	-	7,879	9,320	3,189	3,177	
	4	-	14,166	14,154	4,139	2,957	
	5	-	5,179	10,609	5,311	2,550	
SFSR (Region I)	6	215,000	17,969	13,656	9,063	3,405	0.2
	7	210,000	17,031	18,906	11,406	3,300	
	8	231,000	18,563	16,167	10,516	3,311	
	9	158,000	19,219	15,563	8,292	3,268	
	10	161,000	19,375	14,781	6,229	3,216	
	11	241,000	17,344	15,938	8,922	3,215	0.5
	12	320,000	17,969	15,781	9,578	3,112	
	13	215,000	21,563	15,125	12,516	3,168	
	14	193,000	19,063	15,229	8,292	3,416	
	15	205,000	17,969	16,875	6,203	3,737	
	16	226,000	18,125	17,031	9,188	3,279	0.8
	17	197,000	17,396	17,344	9,234	3,258	
	18	271,000	18,125	15,938	7,625	3,244	
	19	227,000	18,281	15,625	7,344	3,052	
	20	157,000	18,281	15,484	6,047	3,220	
SFSR (Region II)	6	157,000	19,844	16,719	7,375	3,397	0.2
	7	144,000	20,313	15,781	7,891	3,495	
	8	176,000	20,469	17,188	6,911	3,421	
	9	123,000	20,313	16,875	10,286	3,204	
	10	189,000	18,281	16,875	5,625	3,090	
	11	180,000	18,906	15,781	9,781	3,247	0.5
	12	184,000	19,844	17,500	7,203	3,452	
	13	192,000	20,313	18,281	7,446	3,222	
	14	162,000	18,750	17,500	9,946	3,351	
	15	174,000	19,063	17,054	5,161	3,538	

SFSR (Region II)	16	193,000	22,031	16,094	11,688	3,543	0.8
	17	245,000	19,286	17,500	7,734	3,353	
	18	213,000	24,063	17,656	6,109	3,196	
	19	182,000	19,375	17,344	10,304	3,807	
	20	191,000	18,906	19,844	6,188	3,250	
Sensitivity Runs							
NFSR	21	-	5,784	9,971	5,311	2,764	N/A
	22	-	6,589	14,361	5,311	2,741	
SFSR (Region I)	23	239000	19,375	16,250	8,125	3,154	0.8
	24	188000	15,667	16,563	9,719	3,154	
	25	167000	19,500	15,417	7,516	3,252	0.8
	26	245000	18,125	15,438	7,979	3,846	
	27	328000	20,938	15,547	9,141	3,459	0.5
	28	290000	15,729	16,094	9,563	3,364	
	29	188000	20,156	18,750	6,938	3,734	0.8
	30	217000	16,875	13,984	9,344	3,472	
	31	206000	18,438	21,250	8,167	3,322	0.8
	32	203000	16,719	15,688	10,604	3,011	
	33	295000	16,563	13,422	8,396	2,986	0.8
	34	123000	-	-	-	-	0.5
	35	244,000	16,958	14,458	7,844	3,140	0.5
	36	198000	17,188	14,313	9,203	3,349	0.8
SFSR (Region II)	23	147,000	19,688	17,500	6,359	3,445	0.8
	24	240,000	19,063	17,031	10,109	3,445	
	25	239,000	22,344	16,089	6,828	3,764	0.8
	26	223,000	17,344	17,214	9,391	3,278	
	27	205,000	17,813	17,031	6,813	3,664	0.5
	28	142,000	18,438	15,781	7,984	3,243	
	29	163,000	21,406	16,563	7,411	3,712	0.8
	30	184,000	19,844	16,563	6,484	3,352	
	31	170,000	22,969	18,438	11,875	3,522	0.8
	32	222,000	22,031	15,375	10,304	2,975	
	33	248,000	19,375	15,938	9,750	3,089	0.8
	34	68,800	-	-	-	-	0.5
	35	147,000	19,156	18,281	7,172	3,197	0.5
	36	224000	19,844	17,500	6,859	3,257	0.8

Notes:

(1) Reported values are maximum for a run for any rack of that type (e.g., Region II SFSR). Although the horizontal loads are for the same rack, the maximum loads listed in other columns for a run may be from different racks.

(2) Combined fuel grid impact loads are calculated by SRSS of horizontal (E-W and N-S) fuel impact loads for the most highly loaded grid. Since horizontal loads calculated at five vertical nodes are not uniform, and a different number of grids shares the load, the SRSS of the fuel-to-fuel impact loads does not yield the combined fuel grid impact load for a run.

Table 3-9 Maximum Stress Factors on Racks

Service Level	Rack	Pedestal Stress Factors			Cell Wall Stress Factors			COF
		FACT1	FACT2	FACT3	FACT1	FACT2	FACT3	
A	NFSRs	0.060	0.044	-	0.030	0.032	-	N/A
	SFSRs (Region I)	0.032	0.024	-	$\frac{0.034}{0.779^{(2)}} = 0.044$	0.037	-	N/A
	SFSRs (Region II)	0.034	0.026	-	$\frac{0.042}{0.779^{(2)}} = 0.054$	0.045	-	N/A
D	NFSRs	0.556	0.627	0.452	0.059	0.064	0.036	N/A
	SFSRs (Region I)	0.147	0.125	0.128	$\frac{0.181}{0.779^{(2)}} = 0.235$	0.194	0.045	0.8
	SFSRs (Region II)	0.168	0.140	0.155	$\frac{0.376}{0.779^{(2)}} = 0.483$	0.401	0.097	0.8

Notes:
(1) Dimensionless stress factors, FACT1, FACT2, and FACT3, are described in Section 3.2.3.
(2) Stress correction factor considering slenderness ratio (from Appendix F.3 through F.5 of Reference 17)
(3) Since the width-thickness ratio of NFSR in not greater than 51.4, no additional adjustment for the stress is necessary.

Table 3-10 Overturning Evaluation of Racks

Run No.	Rack No.	Relative Displacement	Angle of Rotation	Allowable Rotation	Safety Factor (1.5 required)
24	B5-4	10 mm (0.392 in)	0.12°	18.5°	154

Table 3-11 Stress Evaluation for Fuel Assembly

Location	Category	Calculated Value	Allowable Limit	Safety Factor (-)
Fuel spacer grid	Buckling Load	17.1 kN (3,846 lbf)	24.8 kN (5,567 lbf)	1.45
Fuel rod cladding	Bending Stress	65.2 MPa (9,449 psi)	540.3 MPa (78,365 psi)	8.3
	Yield Strain	0.0007 in/in	0.0058 in/in	8.3

Table 3-12 Stress Evaluation for Fuel Racks

Region	Type	Calculated Stress, MPa (psi)	Allowable Stress, MPa (psi)	Safety Factor (-)
Rack Cell-to-Baseplate	Weld	154.3 (22,379)	246.1 (35,694)	1.59
	Base Metal Shear	109.1 (15,824)	118.0(2) (17,120)	1.08
Baseplate-to-Pedestal(1)	Weld	133.5 (19,363)	246.1 (35,694)	1.84
	Base Metal Shear	94.4 (13,690)	118.0(2) (17,120)	1.25
Cell-to-Cell	Weld	66.4 (9,630)	246.1 (35,694)	3.71
	Base Metal Shear	46.9 (6,808)	118.0(2) (17,120)	2.51

Notes:
(1) Stresses on weld of the baseplate-to-support pedestal of the rack are conservatively evaluated by applying the maximum support loads acting on the NFSRs to the weld of the support pedestal of the SFSRs, as described in Appendix G.2 of Reference 17.
(2) The allowable stress is calculated using 304 material yield strength.

Table 3-13 Maximum Stresses on SFSR Pedestal Thread

Region	Type	Calculated Stress MPa (psi)	Allowable Stress MPa (psi)
Pedestal Thread	Shear	31.5 (4,565)	106.2 (15,408)

Table 3-14 Maximum Stresses on NFSR Stud Bolt

Load Condition	Stress Category	Calculated Stress	Allowable Stress
Level D	Tensile, MPa (ksi)	f_t = 143.5 (20.8)	F_{tb} = 675.7 (98)
	Shear, MPa (ksi)	f_v = 287.8 (41.7)	F_{vb} = 405.4 (58.8)
	Combined Stress Factor	0.55	1.0

Table 3-15 Local Structural Integrity Evaluation of Rack

Region	Rack	Calculated Value	Allowable Value	Safety Factor (-)
Cell Wall Impact	NFSR	14.1 kN (3,177 lbf)	273.2 kN (61,410 lbf)	19.4
	SFSR	17.1 kN (3,846 lbf)	47.4 kN (10,660 lbf)	2.8
Cell Wall Buckling	SFSR	85 MPa (12,401 psi)	103.2 MPa (14,964 psi)	1.2
Secondary Stress by Temperature Effects		117.1 MPa (16,981 psi)	191.4 MPa (27,762 psi)	1.6
Punching Shear Capacity due to Vertical Pedestal Load		849.6 kN (191,000 lbf)	2,427 kN (545,611 lbf)	2.9
Punching Shear Stress due to FA Impact Load in Vertical Direction		5.4 MPa (782 psi)	106.2 MPa (15,408 psi)	19.7

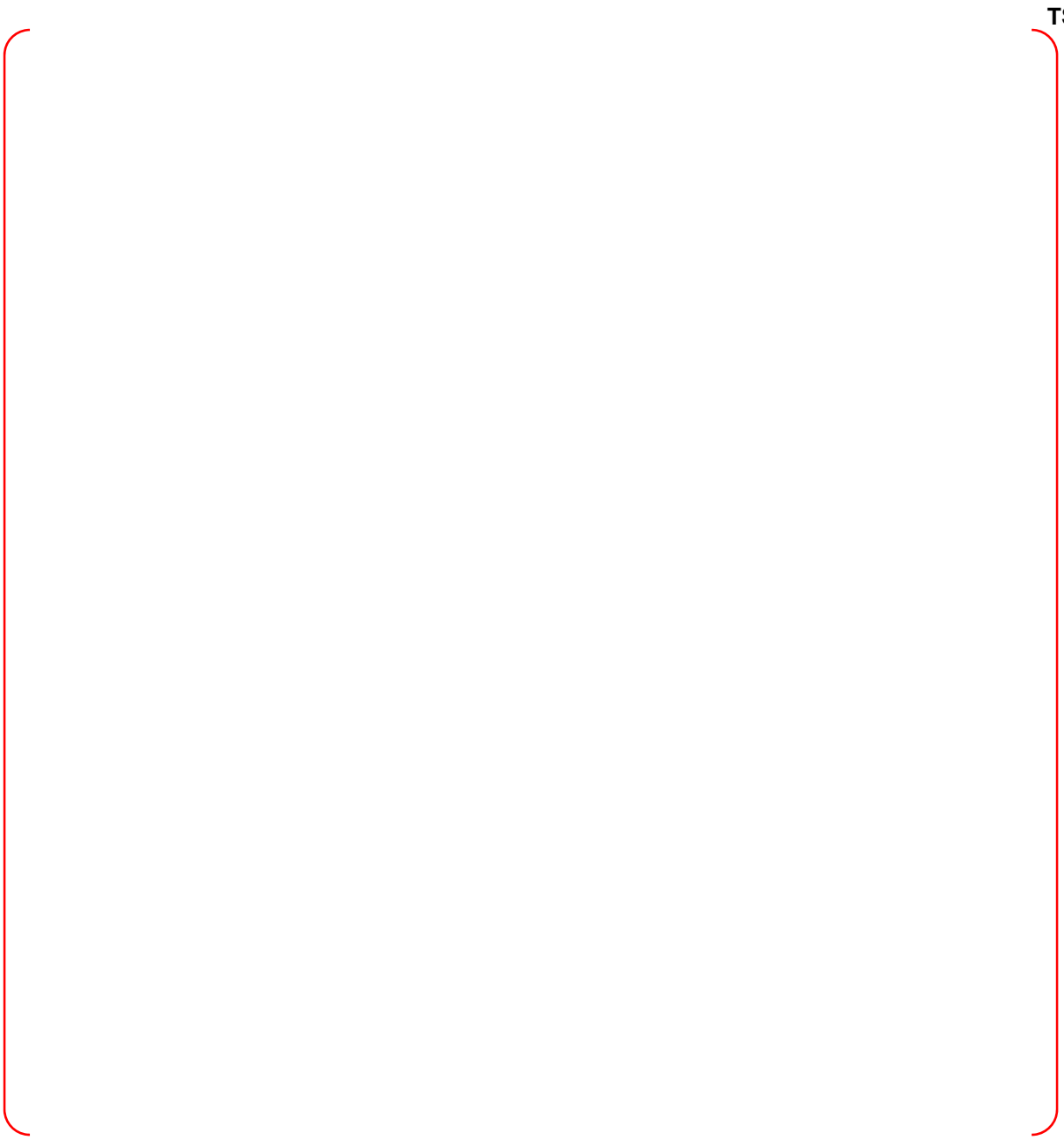

Figure 3-1 Dynamic Analysis Model of NFSR

TS

Figure 3-2 Dynamic Analysis Model of SFSR

TS

Figure 3-3 Dynamic Analysis Model for Whole Pool Multi-Rack

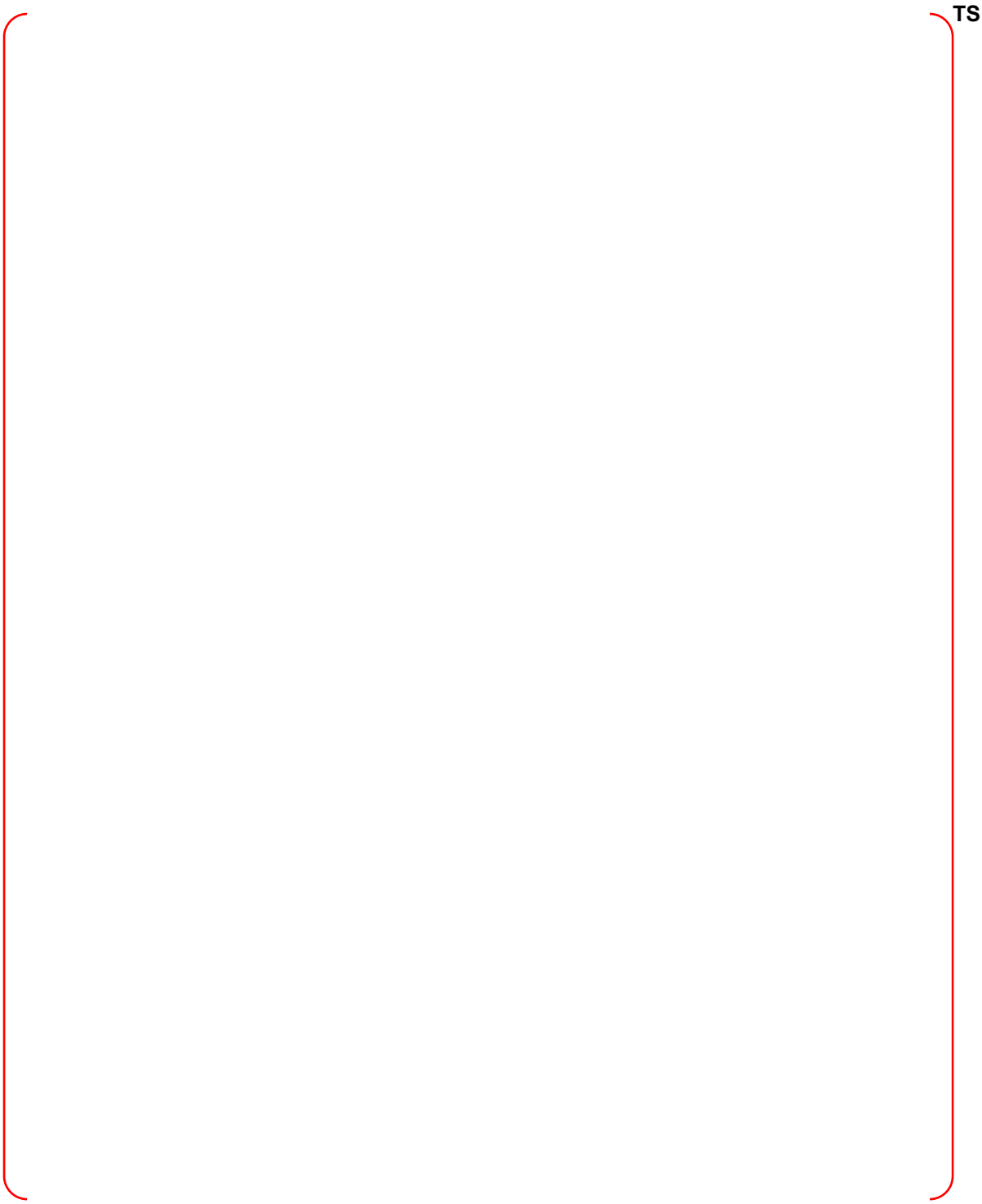

Figure 3-4 Mixed Loading Configuration

TS

Figure 3-5 NFSR East-West Acceleration Time Histories

TS

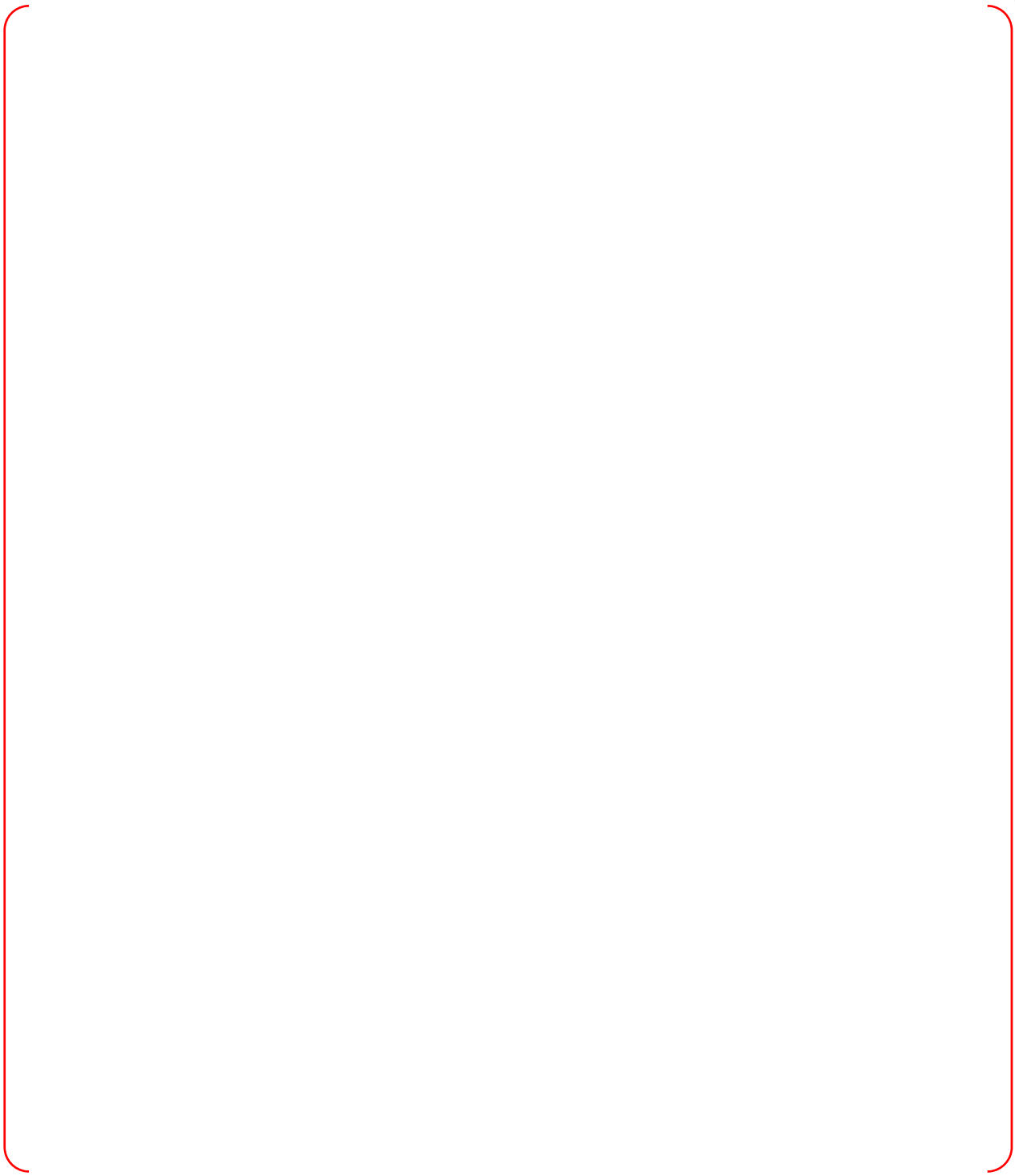

Figure 3-6 NFSR North-South Acceleration Time Histories

TS

Figure 3-7 NFSR Vertical Acceleration Time Histories

TS

Figure 3-8 SFSR East-West Acceleration Time Histories

TS

Figure 3-9 SFSR North-South Acceleration Time Histories

TS

Figure 3-10 SFSR Vertical Acceleration Time Histories

TS

Figure 3-11 NFSR East-West Average Generated Response Spectra

TS

Figure 3-12 NFSR North-South Average Generated Response Spectra

TS

Figure 3-13 NFSR Vertical Average Generated Response Spectra

TS

Figure 3-14 SFSR East-West Average Generated Response Spectra

TS

Figure 3-15 SFSR North-South Average Generated Response Spectra

TS

Figure 3-16 SFSR Vertical Average Generated Response Spectra

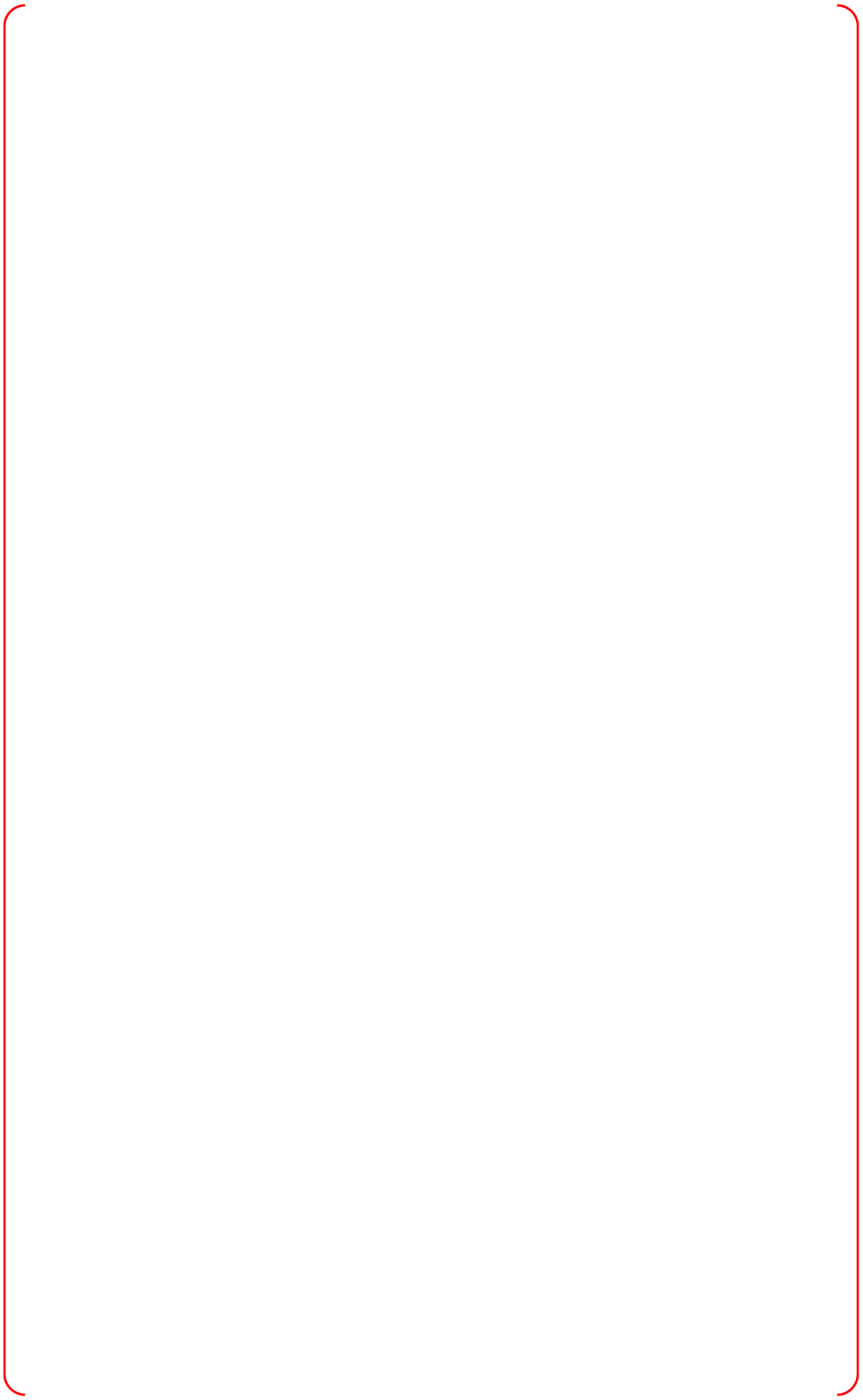

Figure 3-17 Average PSD for NFSR (SSE)

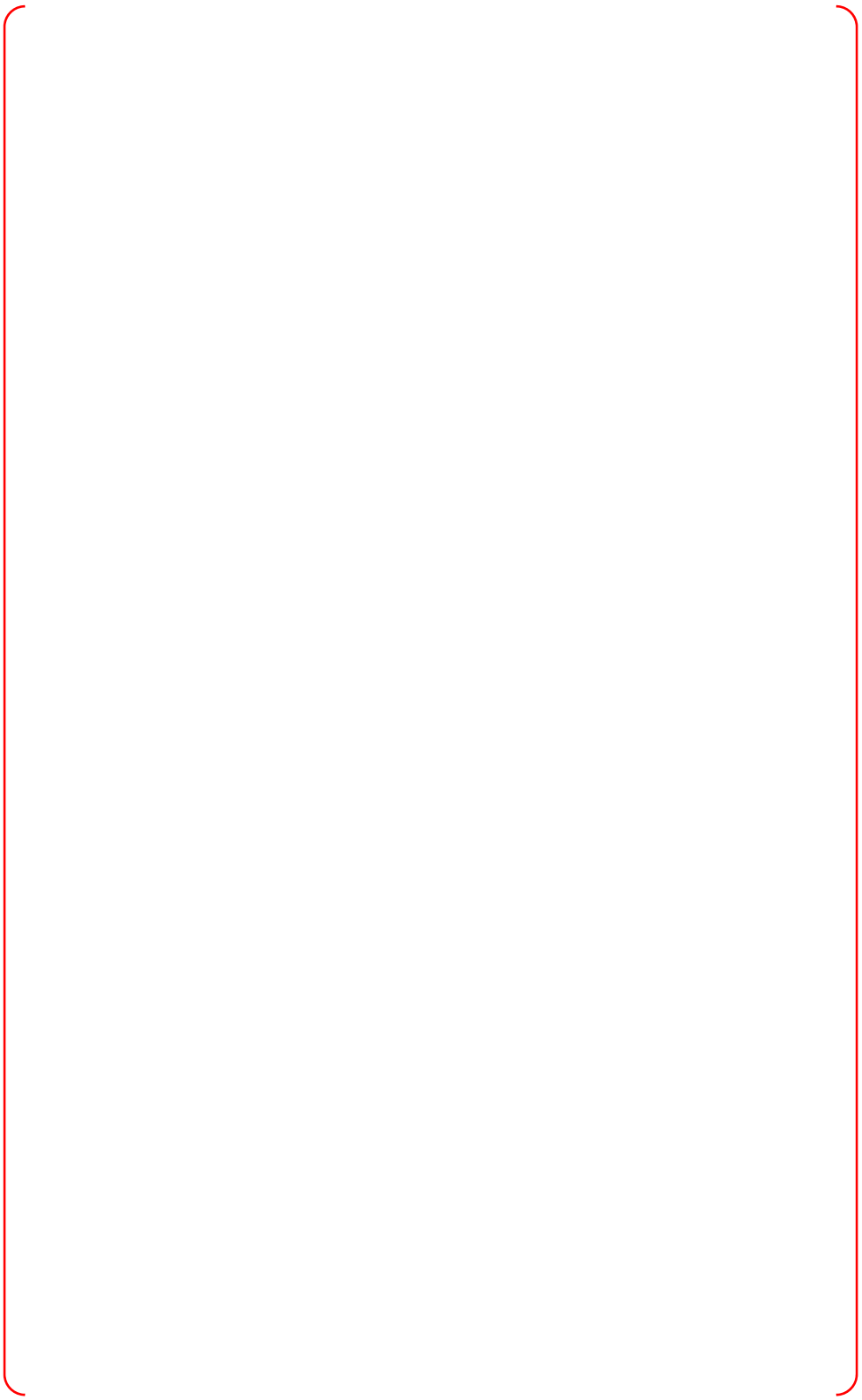

Figure 3-18 Average PSD for SFSR (SSE)

TS

Figure 3-19 SFSR Weld Stress Diagram

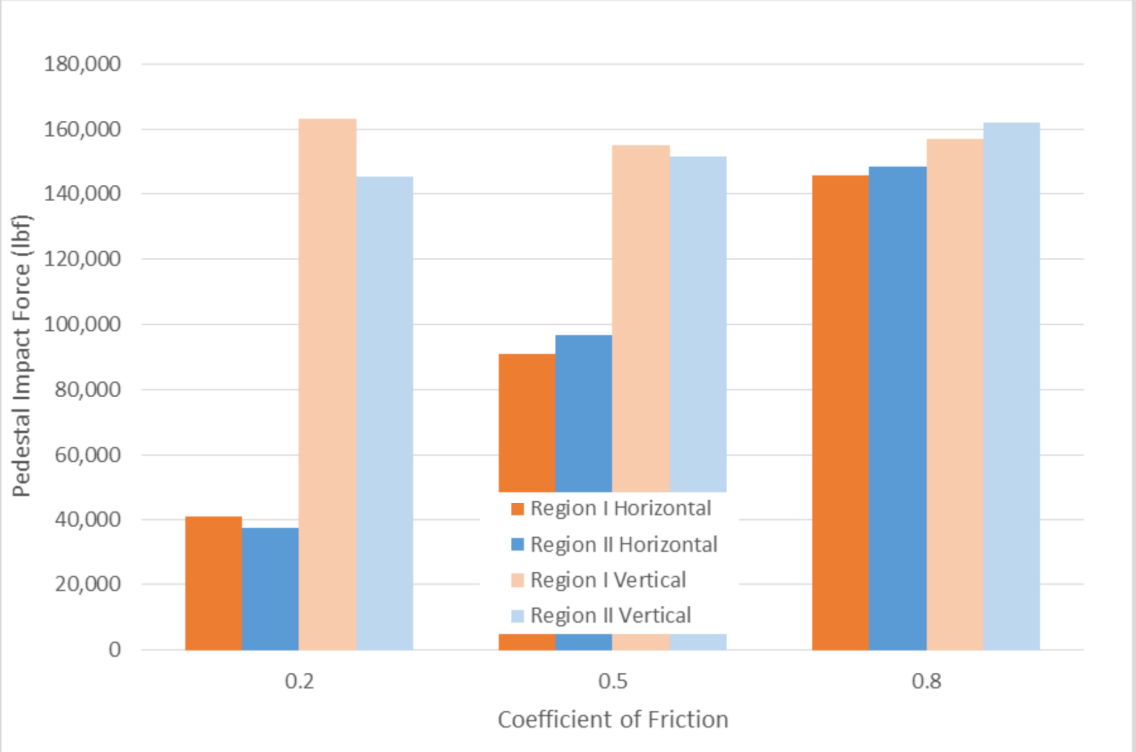

Figure 3-20 SFSR Loads for Varying Coefficients of Friction

Figure 3-21 Displacement of Top of SFSRs

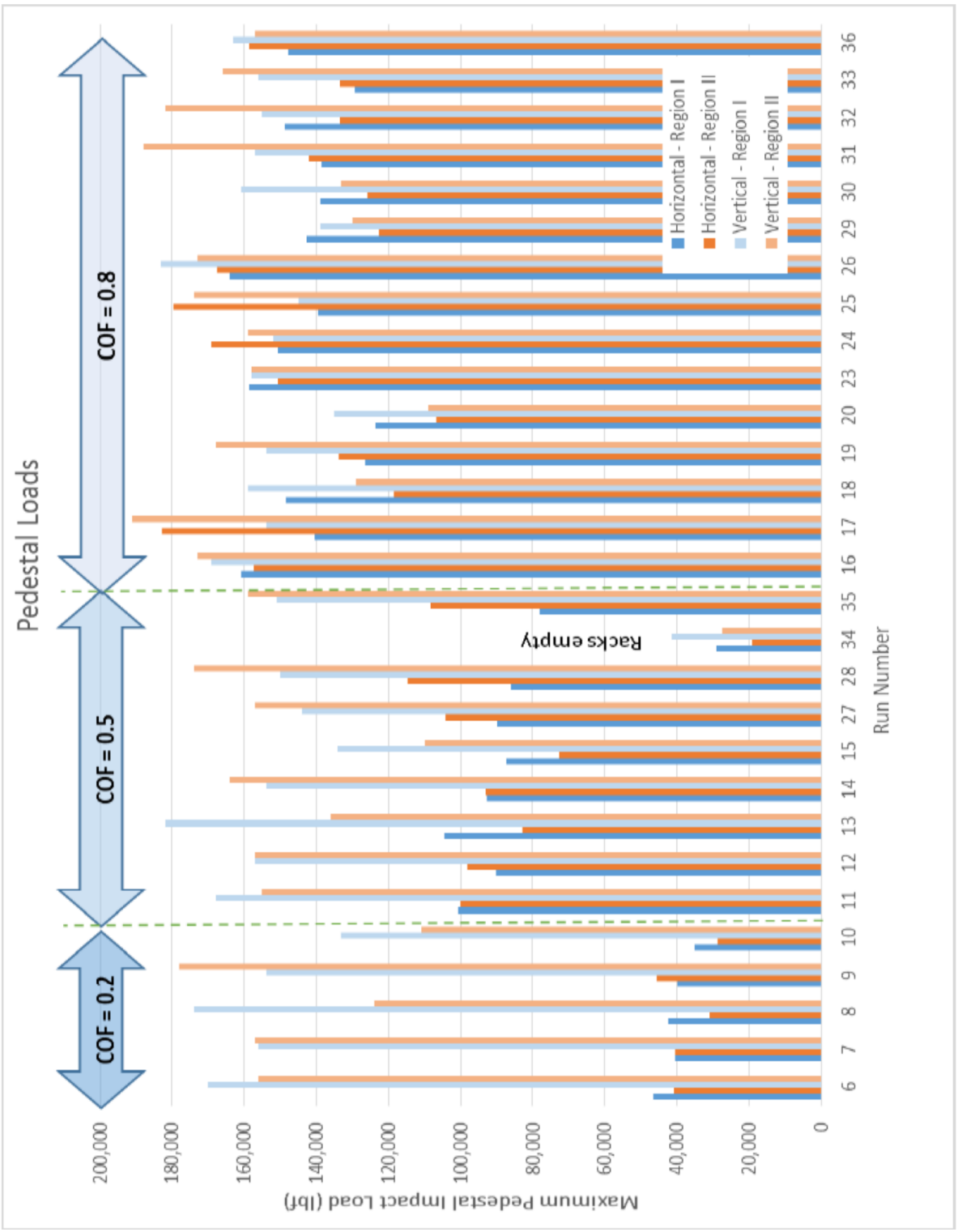

Figure 3-22 SFSR Horizontal (SRSS) and Vertical Pedestal Loads

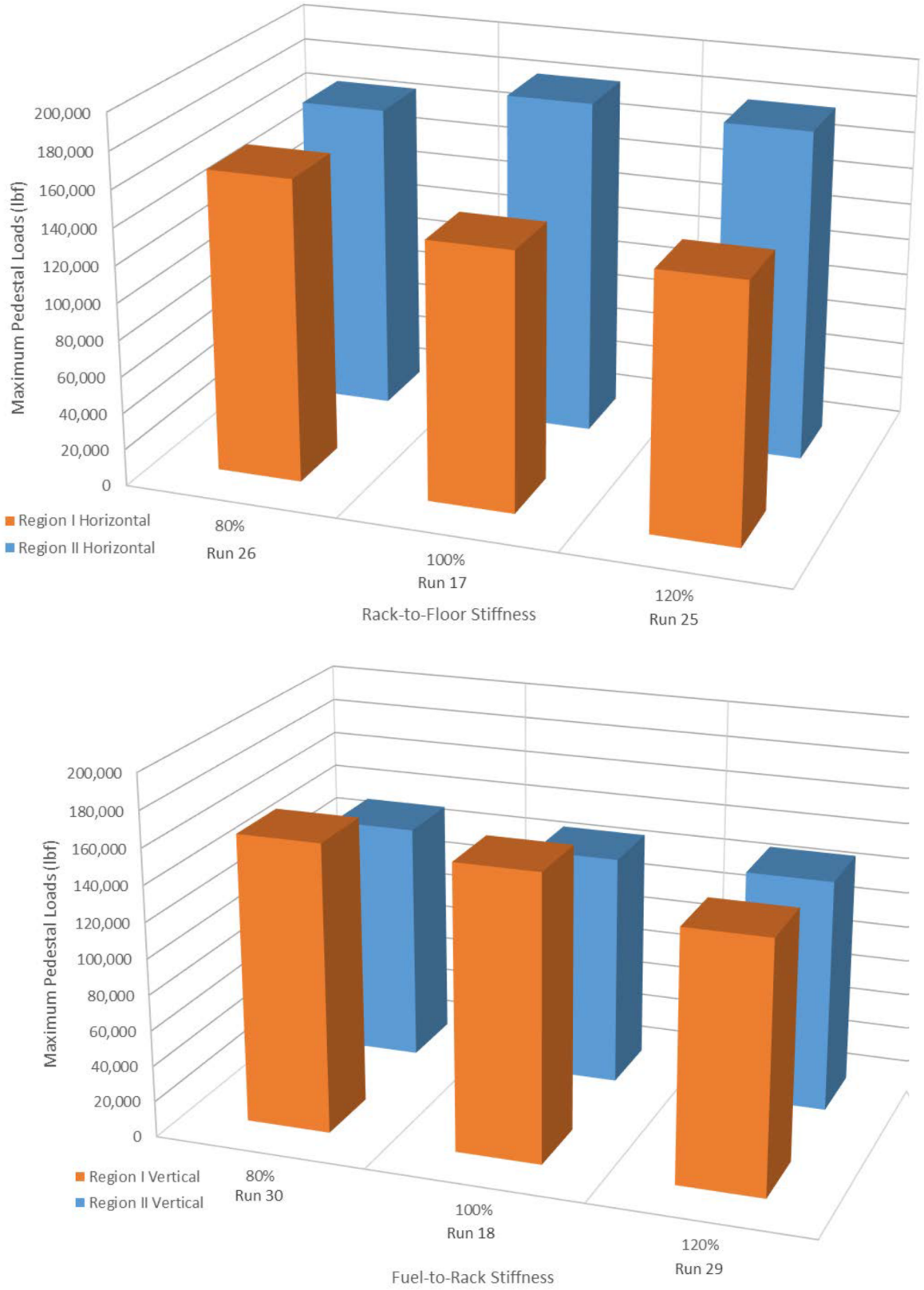

Figure 3-23 Effect of Sensitivities on SFSR Horizontal (SRSS) & Vertical Pedestal Loads

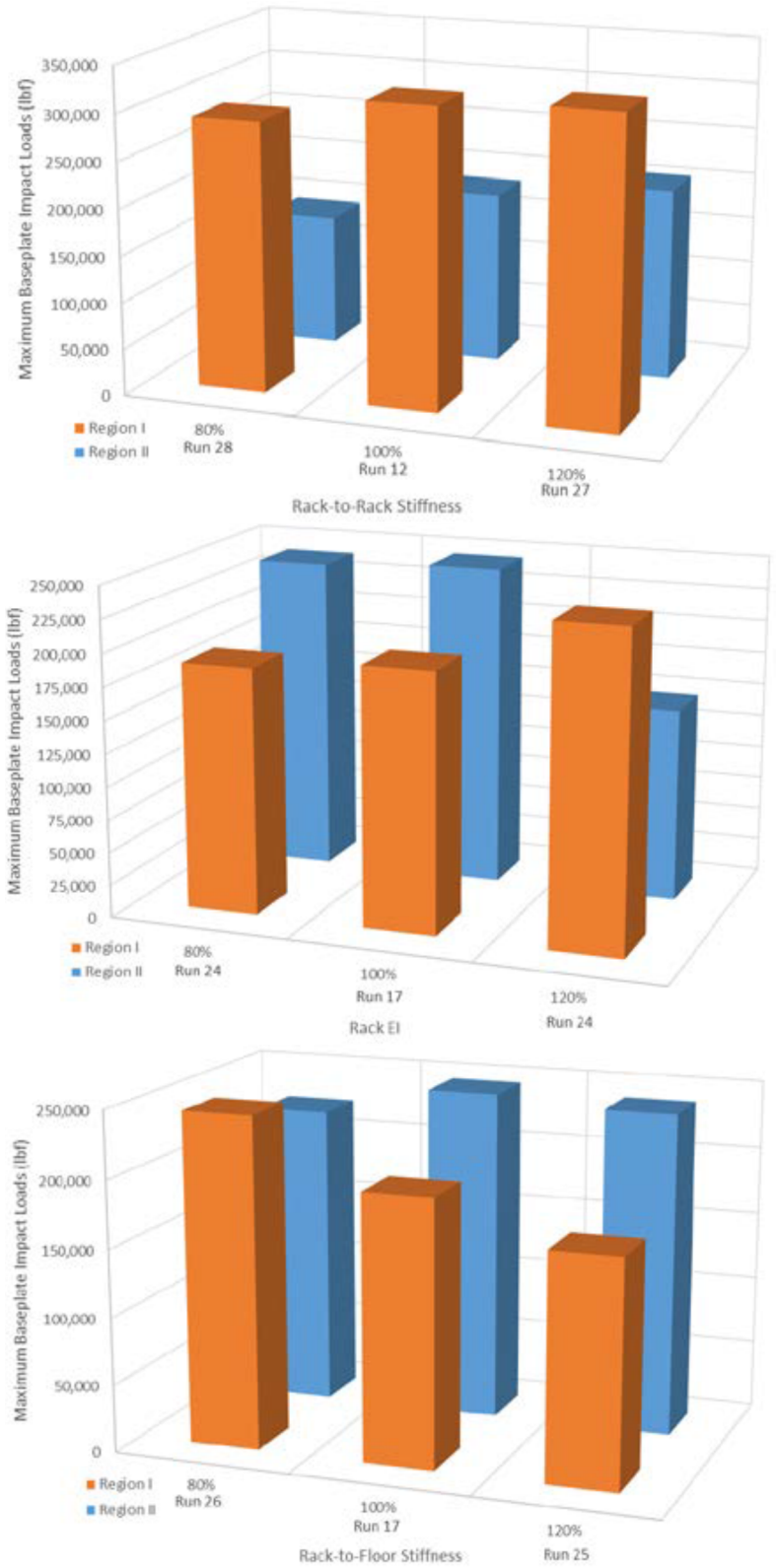

Figure 3-24 Effect of Sensitivities on Baseplate Impact Loads

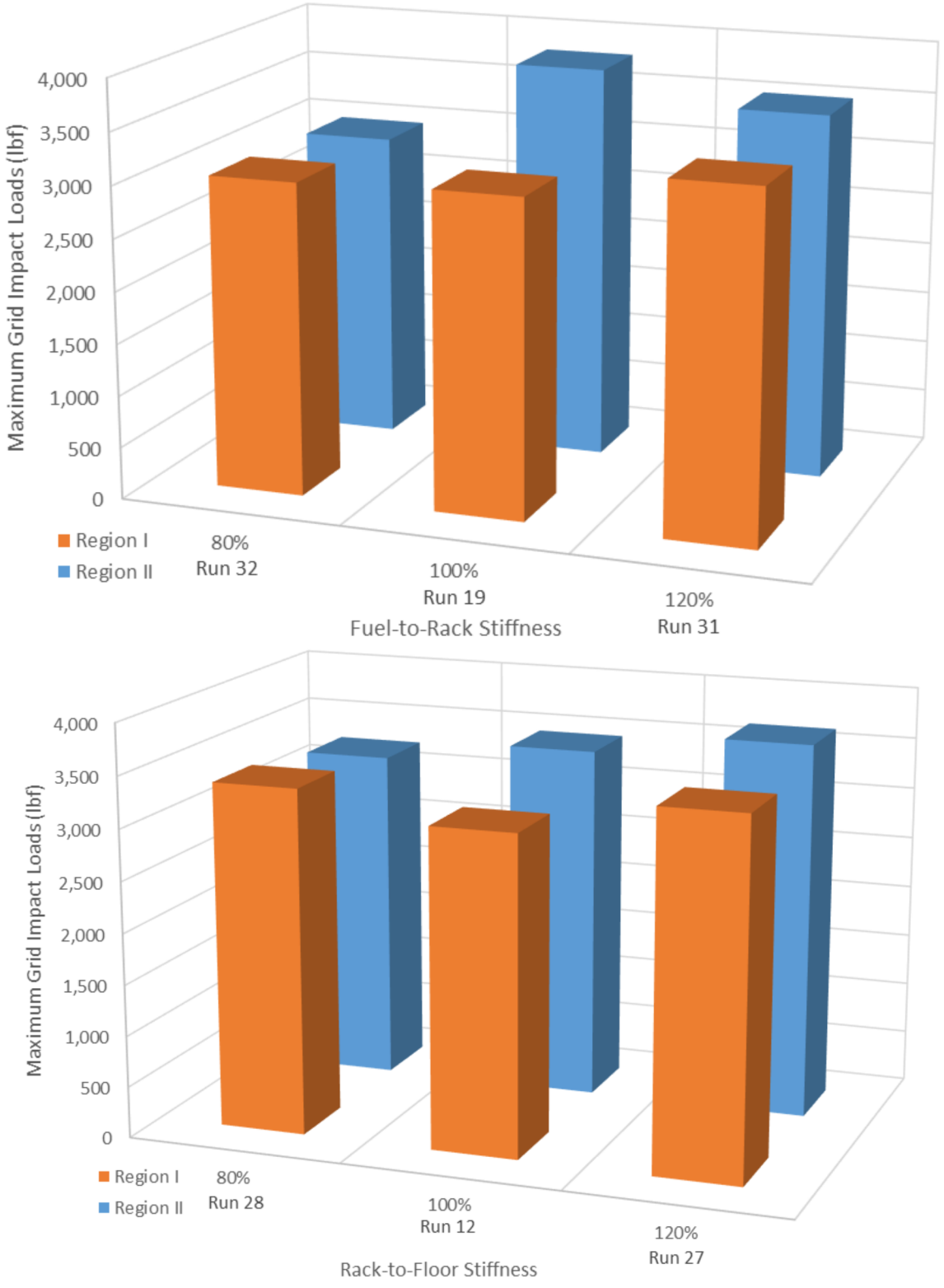

Figure 3-25 Effect of Sensitivities on Grid Impact Loads

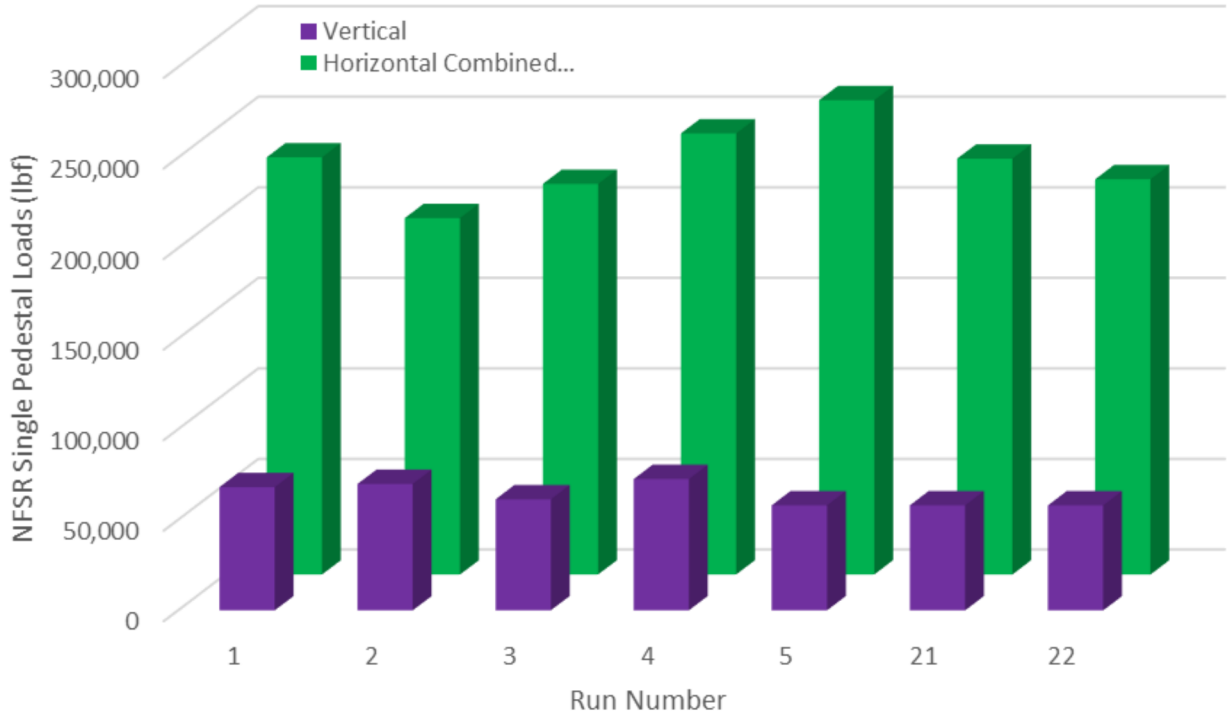

Figure 3-26 Maximum NFSR Single Pedestal Loads for Base and Sensitivity Runs

4 MECHANICAL ACCIDENTS ANALYSIS

This chapter presents the structural integrity evaluation for new and spent fuel storage racks for dropped and stuck fuel assembly scenarios. Only the effect of the accident scenarios on the racks is considered. The postulated fuel handling accident including a drop of fuel assemblies is addressed in the APR1400 Design Control Document, Section 15.7.4.

The accident analyses demonstrate that the APR1400 fuel racks meet the acceptance criteria specified in Appendix D of SRP 3.8.4 (Reference 1).

4.1 Description of Mechanical Accidents

The NRC SRP 3.8.4, Appendix D (Reference 1) identifies load combinations for SFSR that are to be evaluated in accordance with ASME Code, Section III, Division 1, Subsection NF. Specifically, a stuck fuel assembly analysis should meet Class 3 Level B service limits, while a dropped fuel assembly analysis should demonstrate that the functional capability of the fuel rack is maintained. A subset of accident scenarios is applied to the NFSR due to their different design and environment (e.g., not underwater, no neutron absorber plates). The pedestal of NFSR is supported by the overlapped intermediate plate and embedment plate on concrete slab as shown in Figure **2**-**3**. The following scenarios have been evaluated:

(1) Straight Shallow Drop (Scenario 1)

In the so-called "straight shallow drop" accident, the fuel assembly and handling tool (total mass = 1,100 kg (2,425 lbm)) are dropped from a height of 0.61 m (2 ft) [or the transport container handling tool (= 214.55 kg (473 lbm)) drops from a height of 5.0 m (196.8 in)] above the top of the SFSR and impacts on a top edge of the rack. The dropping mass is assumed to impact the top edge of the rack. Potential for damage to a neutron absorber plate is evaluated. A schematic of the straight shallow drop is shown as Figure 4-1. The shallow drop accident for the NFSR is not relevant since there is no neutron absorber to damage.

(2) Straight Deep Drop Away from a Pedestal (Scenario 2)

For assessing the impact of a drop on baseplate deformation, drops as far away from the support provided by a pedestal are considered at two locations (a central cell and a peripheral cell at the midpoint of a side) that maximize the distance to the points of support. A fuel assembly along with the handling tool (total mass = 1,100 kg (2,425 lbm)) is dropped from a fuel bottom height of 0.61 m (2 ft) above the racks. The falling assembly is assumed to enter an unoccupied storage cell away from a pedestal (as shown in Figure 4-2) and impact the rack baseplate. This scenario is also evaluated for the NFSR, and analysis for this scenario is the same as done for the SFSR, except speed at impact is higher because the drop does not have the viscous drag associated with falling through water.

(3) Straight Deep Drop Over a Pedestal (Scenario 3)

In this case, the fuel assembly enters a corner storage cell which is above a pedestal (as shown in Figure 4-3). This is most limiting for evaluating the concentrated loading on the concrete underlying the baseplate on which the pedestal rests.

(4) Stuck Fuel Assembly (Scenario 4)

In this scenario, it is assumed that a fuel assembly becomes stuck while being lifted out of an SFSR cell resulting in the lifting force of the crane being applied against the SFSR structure. The fuel hoists are provided with load-measuring devices and interlocks to interrupt hoisting if the load increases above the overload setpoint, as identified in DCD Section 9.1.4.5. A tensile force of 22.2 kN (5,000 lbf) on the

SFSR (limited by the motor stall torque or load-limiting device of the crane used to load fuel into the racks) represents the maximum uplift force of a stuck fuel assembly.

4.2 Acceptance Criteria

For mechanical accidents above, the acceptance criteria to ensure damage of the racks is limited as described below:

(1) Straight Shallow Drop (Scenario 1)

For the postulated shallow drop event, the crushed rack walls must not extend down into the "poison zone" that shadows the entire length of the active fuel. This will ensure that the configuration analyzed in the criticality evaluation remains valid. The distance measured from the top of the rack to the upper boundary of the "poison zone" is 610 mm (24.0 in). The depth of damage to the impacted cell walls must be demonstrated to remain limited to the portion of the cell above the top of the "poison zone", which is the elevation of the top of the neutron absorber. This will ensure that the configuration analyzed in the criticality evaluation remains valid. The distance measured from the top of the rack to the upper boundary of the "poison zone" is 0.61 m (2 ft).

(2) Straight Deep Drop (Scenario 2; Away from the pedestal)

The dropping mass impacts the rack baseplate. The acceptance criteria are that the baseplate is not pierced and that the deformed baseplate of the rack must not impact the concrete floor (NFSRs) or pool liner (SFSRs). The normal separation between the underside of the NFSR baseplate and the pit floor is 185 mm (7.28 in) and between the underside of the SFSR baseplate and pool liner is 160 mm (6.30 in).

(3) Straight Deep Drop (Scenario 3; Over a pedestal)

For the postulated deep drop event (over a pedestal), the compressive stress on the concrete floor underneath the embedment plates shall not exceed the maximum allowable stress of 16.4 MPa (2,375 psi) as specified on the paragraph 5.3.4.4 of design specification (Reference 22).

(4) Stuck Fuel Assembly (Scenario 4)

The stuck fuel assembly is evaluated to Level B service limits to ensure the integrity of the rack is unaffected.

4.3 Analysis Method

The finite element method is used for the impact analysis of the postulated drop accidents. ANSYS LS-DYNA, a commercial computer code that has been independently validated by Doosan (Reference 30), is used to numerically simulate the impact events. For uplift force, a classical strength of materials calculation is used to determine the amount of area needed to support the forces.

4.3.1 Assumptions

- Scenario masses and heights are constrained as follows:
    - Fuel assembly plus handling tool (1,100 kg (2,425 lbm)) drops from a maximum initial height of 0.61 m (2 ft) above the top of the rack in accordance with paragraph 5.3.4.4.2 of the rack design specification (Reference 22) for all drop scenarios.
    - Transport container handling tool (214.55 kg (473 lbm)) drops from a maximum initial height of 5.0 m (196.8 in) above the top of the rack for shallow drop scenario rack in accordance with paragraph 5.3.4.4.2 of the rack design specification (Reference 22).

  - A tensile force of 22.2 kN (5,000 lbf) on the SFSR (limited by the motor stall torque or load-limiting device of the crane used to load fuel into the racks) represents the maximum uplift force of a stuck fuel assembly.
  - In addition, interlocks are installed so that movement of the refueling machine is not possible when the hoist is withdrawing or inserting a fuel assembly. The movement of bridge and trolley is allowed when the fuel assembly has reached the up-limit.
  - The fuel hoists are provided with load-measuring devices and interlocks to interrupt hoisting if the load increases above the overload setpoint and to interrupt lowering if the load decreases below the underload setpoint.
  - Heavy loads, as described in DCD Subsection 9.1.4.2.1, are prevented from traveling over the NFSRs by the use of mechanical and electrical interlocks on the cask handling hoist.

- The spent fuel rack is in a stationary status before the impact. The only postulated means by which the racks could move is a seismic event. Mechanical accidents, however, are not postulated to occur concurrently with a seismic event.
- The fuel assemblies on rack are fully loaded.
- The trajectory of the dropped objects is vertical which minimizes the fluid drag. This assumption increases the impact velocity and results in higher energy impacts.
- In the initial impact velocity calculations, the dropped fuel assembly is treated as a solid rectangular bar. In reality, the fuel assembly is not a solid bar; the lower nozzle block of the fuel assembly may have numerous small flow holes, which allow water to pass between the fuel rods. Although these flow holes reduce the form drag of the lower nozzle, they introduce significant energy loss at the entrance of each flow hole and significant internal flow resistance at the grid spacers and on the fuel rod surfaces. Thus, a solid rectangular bar is considered to reasonably represent the real behavior of the fuel assembly.
- The ultimate load that can be sustained by a cell wall is based on the load carrying capacity of thin plate sections.
- The stainless steels used to fabricate the new and spent fuel rack are considered to be bilinear elastoplastic materials with a stress-strain curve to that shown in the following sketch.

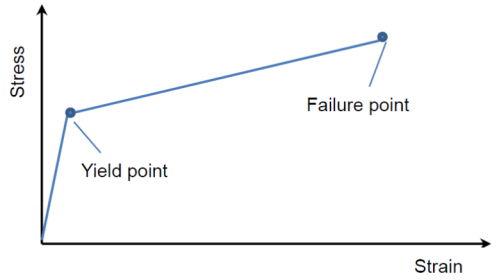

- The fuel assembly is assumed to hit a periphery cell wall in the shallow drop event. This is a conservative assumption, since the periphery cell wall has less support from adjacent cells than an interior cell and, therefore, is more vulnerable in a shallow drop accident.
- The concrete steel reinforcement, which is designed to take the tension load, is conservatively neglected in the SFP slab concrete model.
- The energy absorbed through failure of connecting welds is ignored in the analysis.
- Impact damping is conservatively neglected in the finite element analysis.

4.3.2 Calculation of Impact Velocity

The objective of the analysis is to calculate the final velocity of the dropping object. A dropping object is modeled as a single lumped mass under the influence of gravity in a drag inducing medium. The effects of buoyant mass, gravity, and fluid drag are accounted for in the model. The drag force is based on the exposed frontal area of the fuel assembly. The governing equation to calculate the impact velocity for a body of mass subject to gravity and drag effects is

TS

For a given drop height, impact velocities for shallow drops are identical for both SFSR regions. However, some of the Region II periphery cells, which are formed by welding a panel plate to three adjacent box cells, are structurally weaker. Therefore, a shallow drop over a Region II rack periphery panel plate governs.

For deep drops over a pedestal, impact velocities are the same for both regions. For deep drops away from a pedestal, different drag conditions cause the impact velocity for Region I SFSRs to be greater than that of Region II.

Since a drop into a NFSR is through air, rather than water, it has a higher impact velocity.

4.3.3 Finite Element Model

All drops were analyzed by developing a finite element model in ANSYS LS-DYNA. The impactor (e.g., the fuel assembly and its handling tool) is conservatively modeled as a rigid solid with no energy absorption capacity except for drop scenario 3. The detailed configurations of the impact target (i.e., the rack) are modeled in all analyzed events. The deep drop analysis model considers the effects of all of the stored fuel assemblies in the rack by modifying the density of the baseplate to simulate the loading effects of the other fuel assemblies. In most cases, the model of the rack did not include any the structure underneath the rack, but for the deep drop over a pedestal, the effect of the impact on concrete underneath the pedestal baseplate was evaluated. Figure 4-4 through Figure 4-16 show the finite element models and results for individual scenarios, which are discussed in the following sections. ANSYS LS-DYNA Elements, SHELL163 (explicit thin structural shell) and SOLID164 (explicit 3-D structural solid), are used to mesh the cell walls, baseplate and rack feet. SHELL163 is a 4-node element with both bending and membrane capabilities. Both in-plane and normal loads are permitted. The element has 12 degrees of freedom at each node: translations, accelerations, and velocities in the nodal x, y, and z directions and rotations about the nodal x, y, and z-axes. SOLID164 is used for the 3-D modeling of solid structures. The element is defined by eight nodes having the degrees of freedom at each node: translations, velocities, and accelerations in the nodal x, y, and z directions. The bottom of the modeled rack feet is fixed in the finite element model because the NFSRs are bolted and horizontal motion is not relevant to a SFSR or NFSR straight vertical drop.

4.3.4 Methodology for Straight Shallow Drop Accident onto a SFSR

The straight shallow drop accident analysis determines the extent of the damage to the rack structure due to the impact of the dropping object. The impact velocity of the dropping mass is calculated first to determine the bounding kinetic energy that will be used to evaluate the postulated shallow drop accident. In analyzing the shallow drop, the rack model consists of 25 cells as shown in Figure 4-4. Modeling only 25 of 56 or 64 SFSR cells has negligible effect since damage is locally limited to the top of cell walls at the point of impact.

4.3.5 Methodology for Straight Deep Drop Accident (Away from Pedestal)

When a dropping object impacts the baseplate of a rack, the deformation of the baseplate and the potential for impact on the pool liner is evaluated. In analyzing the deep drop scenario 1 (away from the pedestal), the NFSR model consists of 56 cells as shown in Figure 4-5. Figure 4-7 shows the 16 cell model used for the SFSR. The deep drop analysis model considers the effects of all of the stored fuel assemblies in the rack by modifying the density of the baseplate to simulate the dynamic effects of the other fuel assemblies.

4.3.6 Methodology for Straight Deep Drop Accident (Over a Pedestal of SFSR)

The model was developed mainly for capturing the structural responses of the rack pedestal, the SFP embedment plate and the underlying concrete slab as shown in the Figure 4-9. The impactor (i.e., the

fuel assembly and its handling tool) model consists of two parts: a bottom end nozzle with instrument tube and an elastic beam representing the fuel rods. The mass and cross-sectional area properties of the elastic beam are based on the entire array of fuel rods (cladding material only). The other mass properties including handling tool are distributed on a model of the bottom end nozzle with instrument tube. Therefore, the impactor model has the same mass as an actual fuel assembly and handling tool. Using the impact velocity described in Section 4.3.2 above ensures that the impact energy will be representative of an actual drop accident. Bi-linear material properties have been assigned to the bottom end nozzle with instrument tube. The fuel cladding is modeled using beam elements with elastic material properties for conservatism. ANSYS LS-DYNA Elements, BEAM161 (explicit 3-D beam) and SOLID164 (explicit 3-D structural solid), are used to mesh the fuel assembly. ANSYS LS-DYNA Element SOLID164 is used to mesh the base plate, rack feet, embedment plate and SFP slab. The slab model is fixed at the bottom surface with the peripheral boundary surface nodes restrained laterally. The deep drop analysis model considers the effects of all of the stored fuel assemblies in the rack by modifying the density of the baseplate to simulate the dynamic effects of the other fuel assemblies.

4.3.7 Methodology for Stuck Fuel Accident

This analysis evaluates the ability of the rack walls to withstand the uplift force due to a stuck fuel assembly. There are a number of ways that a fuel assembly can become stuck in a cell, and most involve contact with more than one cell wall (i.e., wedging). Assuming that the uplift force is imposed on a single cell wall is conservative. A classical strength of materials equation is used to determine the amount of area needed to support the uplift force on a stuck fuel assembly.

(1) Vertical uplift force at top of cell

The critical location for load application is to have this load applied near the top of the rack along or against a single cell wall. If the vertical uplift load is resisted only by shear stress and the allowable in shear is the Level B limit. The depth (h_{sf}) of the cell that can support the applied load is obtained from the classical strength of materials equation to determine the amount of area needed to support the forces. If the damage depth of the cell is above the active fuel area, the vertical uplift force is not a safety concern.

$$h_{sf} = \frac{F_{Uplift}}{2 \cdot \tau_y \cdot t_{cell}}$$

Where,

F_{Uplift} : Uplift force applied to the rack,

τ_y : Allowable in shear of cell wall for Level B limit (=1.33 x 0.4 x S_y), and

t_{cell} : Cell wall thickness.

(2) Vertical uplift along length of cell

The cell wall stress (σ) due to vertical uplift force along length of cell is determined as follows:

$$\sigma = \frac{F_{Uplift}}{D_{cell} \cdot t_{cell}}$$

Where,

D_{cell} : Cell Inside dimension

If the calculated stress is below the Level B limit (1.33 x 0.6 x S_y) of rack cell, the damage of the cell will not occur.

4.4 Computer Codes

The explicit, dynamic finite element code LS-DYNA is used for the drop accident analyses. LS-DYNA was previously used for the South Texas Project 3&4 analysis of drops into/onto fuel storage racks. In the STP 3&4 Safety Evaluation Report (Reference 31), the NRC states:

> "LS-DYNA is a nonlinear, explicit, three–dimensional, finite element code used to numerically simulate dynamic impact events. It has been independently subjected to QA validation by Holtec. This analytical methodology is widely used in the industry and has been applied by Holtec to drop analyses for numerous wet storage projects approved by the NRC. Based on the above information, the staff considers the use of the LS-DYNA program acceptable for the FEA of the postulated fuel drop accidents."

Therefore, LS-DYNA analysis for APR1400 equivalent fuel assembly drop events is considered to be consistent with prior NRC reviews and approval. Reference 30 documents verification of proper code installation.

4.5 Results of Analyses

The postulated drop accidents analyses are performed based on the impact energy and configuration of each drop scenario. The impact velocities for mechanical accident scenarios 1, 2 and 3 are summarized in Table 4-1. The following results are determined based on the methodologies, which are discussed on section 4.3, and the detailed calculations are described in the mechanical accident analysis report (Reference 32).

(1) Straight Shallow Drop (Scenario 1)

In the straight shallow drop of either a fuel assembly along with the handling tool or a transport container handling tool, it is demonstrated that the permanent damage to any fuel storage cell is limited to the maximum depth of 220 mm (8.66 in) below the top of the rack. This is less than the distance from the top of the rack to the beginning of the active fuel region, 0.61 m (2 ft). Therefore, there will be no effect on the configuration and subcriticality of the fuel in the adjacent cells due to this accident.

(2) Straight Deep Drop (Scenario 2)

During a straight deep drop accident away from the pedestal locations, the baseplates of the new and the spent fuel storage racks do not experience gross failure (puncture). The baseplates of the new and the spent fuel storage racks are calculated to deform 75.9 mm (2.99 in) and 69.1 mm (2.72 in), respectively. These values are less than the minimum distances between the baseplate and the underlying surface, which are 185 mm (7.28 in) and 160 mm (6.30 in) for the new and the spent fuel storage racks, respectively. Therefore, a dropped fuel assembly along with the handling tool will not cause the NFSR baseplate to contact the pit floor or the SFSR baseplate to contact the pool liner.

(3) Straight Deep Drop (Scenario 3)

In the straight deep drop accident over a pedestal, the resulting impact transmits a load of 471.6 kN (1.06E+05 lbf) to the concrete pool slab through the embedment plate under the pedestal of racks. The peak compressive stress due to this impact load on concrete pool slab is calculated as 11.6 MPa (1,688 psi), which is less than allowable stress limit of 16.4 MPa (2,375 psi). Therefore, the compressive stress on concrete due to dropping mass is less than the allowable stress limit.

(4) Stuck Fuel Assembly (Scenario 4)

The fuel racks are adequate to withstand the uplift force of 22.2 kN (5,000 lbf) due to a stuck fuel assembly because the neutron absorbing poison plate is not damaged and structural integrity of the rack is maintained. Two cases are considered:

(a) For vertical uplift when a fuel assembly was nearly free of the top of a SFSR, the effect is concentrated at the top of the rack structure along a single cell wall. If the vertical uplift force is resisted only by shear stress, the allowable shear stress level be limit is:

$$\tau_y = 1.33 * 0.4 * S_y = 1.33 * 0.4 * 21{,}400\ psi = 11{,}385\ psi$$

The depth of the cell structure h_{sf} that can support the load is obtained from

$$h_{sf} = \frac{F_e}{2 * \tau_y * t_{cell}} = \frac{5000\ lbf}{2 * 11{,}385\ psi * 0.098\ in} = 2.24\ in$$

Where,

t_{cell} = cell wall thickness of 0.098 in

The top of the neutron absorbing plate is at about 24.0 inches below the top of the cell wall. Since the damaged area is above the location of the neutron absorber and is limited to a small section of one cell wall, margin to criticality and structural integrity are not affected.

(b) For vertical uplift when a fuel assembly is fully seated, the force is assumed to be resisted by a single cell wall, which is 0.098 in thick and 8.66 in wide. If the stress is uniformly distributed across that cross section, it is equal to

$$\sigma = \frac{F_e}{D_{cell} * t_{cell}} = \frac{5000\ lbf}{8.66\ in * 0.098\ in} = 5892\ psi$$

The calculated stress is less than allowable tensile stress (1.33 x 0.6 x S_y = 17,077 psi), which means that damage to the cell wall will not occur.

The results of the evaluation for the cell wall tensile stress, cell to cell weld shear stress, and the base metal shear stress for stuck fuel assembly accident scenario are summarized in Table 4-2.

The forces caused by uplift of a stuck fuel assembly does not cause damage that affects the margin to criticality or structural integrity.

Table 4-1 Impact Evaluation Data

Rack	Cases	Drop Weight(*), kN (lbf)	Drop Height, m (in)	Impact Velocity, m/sec (in/sec)
NFSR	Straight Deep Drop (Away from Pedestal)	10.8 (2,425)	5.18 (203.9)	10.1 (396.8)
SFSR	Straight Shallow Drop	10.8 (2,425)	0.61 (24.0)	3.14 (123.6)
		2.1 (473)	4.98 (196.0)	7.15 (281.3)
	Straight Deep Drop (Away from Pedestal)	10.8 (2,425)	5.2 (204.7)	8.22 (323.5)
	Straight Deep Drop (Over a Pedestal)	10.8 (2,425)	5.2 (204.7)	7.36 (154.9)

(*) Drop Weight = Fuel assembly along with the handling tool (2,425 lbf) or transport container handling tool (473 lbf)

Table 4-2 Stress Evaluation for Stuck Fuel Assembly

Region	Stress Category	Calculated Stress MPa (psi)	Allowable Stress(1) MPa (psi)
Cell Wall	Tensile	40.6 (5,892)	117.7 (17,077)
Cell-to-Cell Weld	Shear	8.9 (1,294)	136.7 (19,830)
Base Metal	Shear	8.9 (1,294)	78.5 (11,385)

Note:

(1) Per Appendix D of SRP 3.8.4, the allowable stresses for Level B service condition were applied to the stuck fuel assembly load.

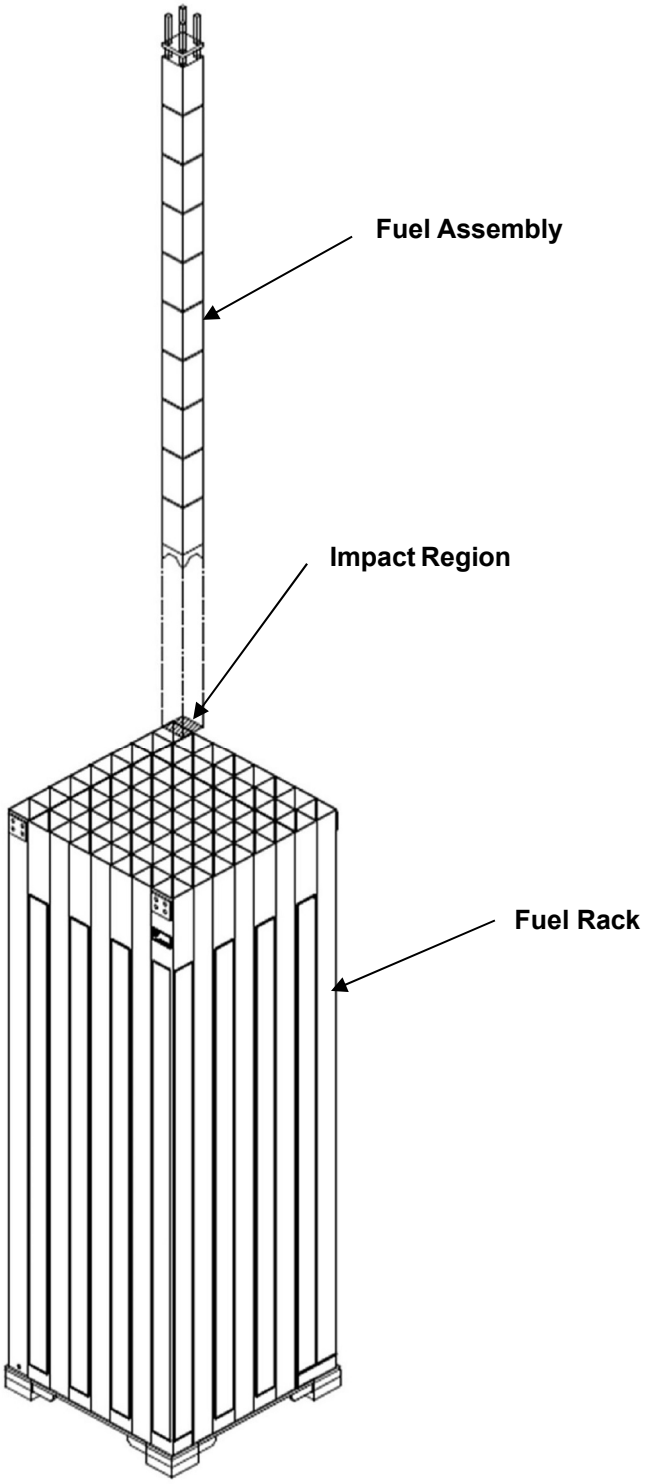

Figure 4-1 Schematic of the Straight Shallow Drop

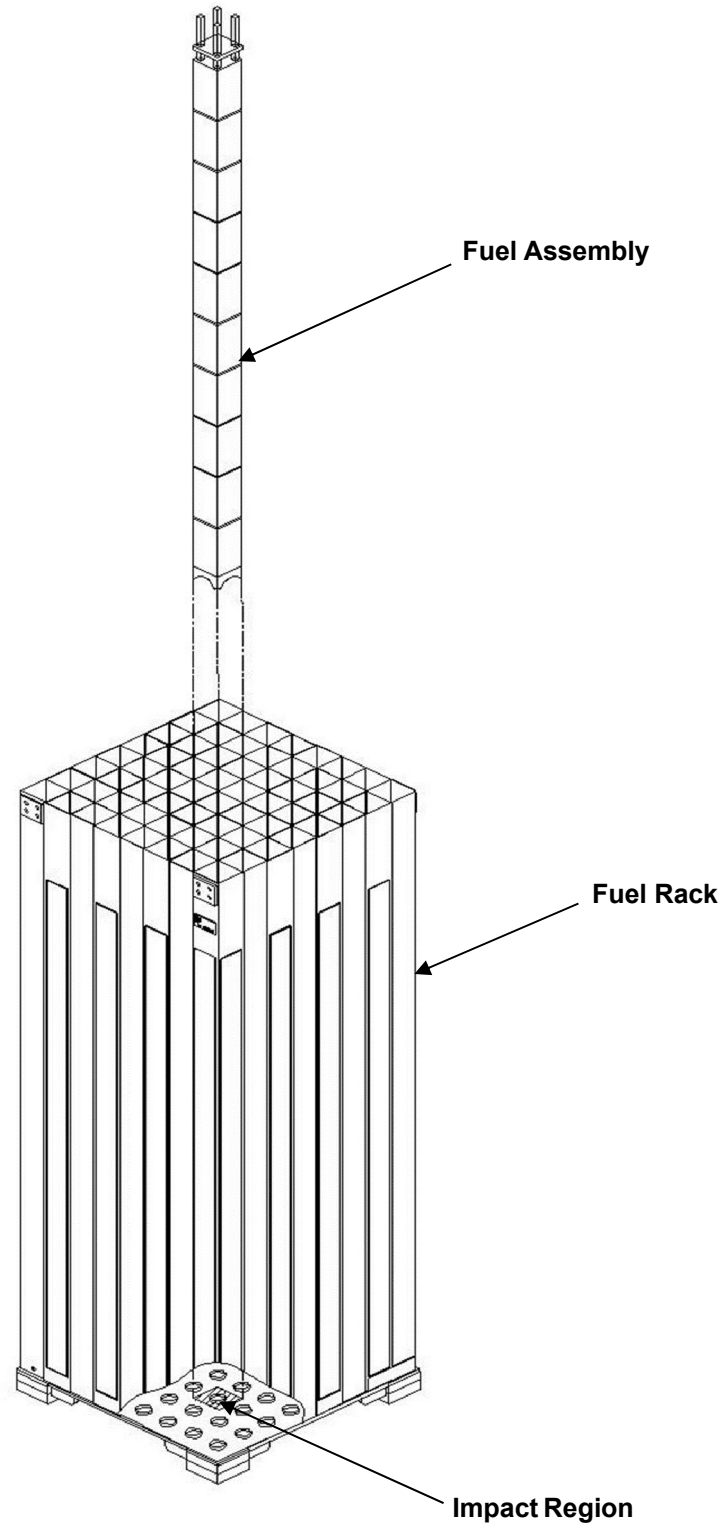

Figure 4-2 Schematic of the Deep Drop Away from a Pedestal (Scenario 2)

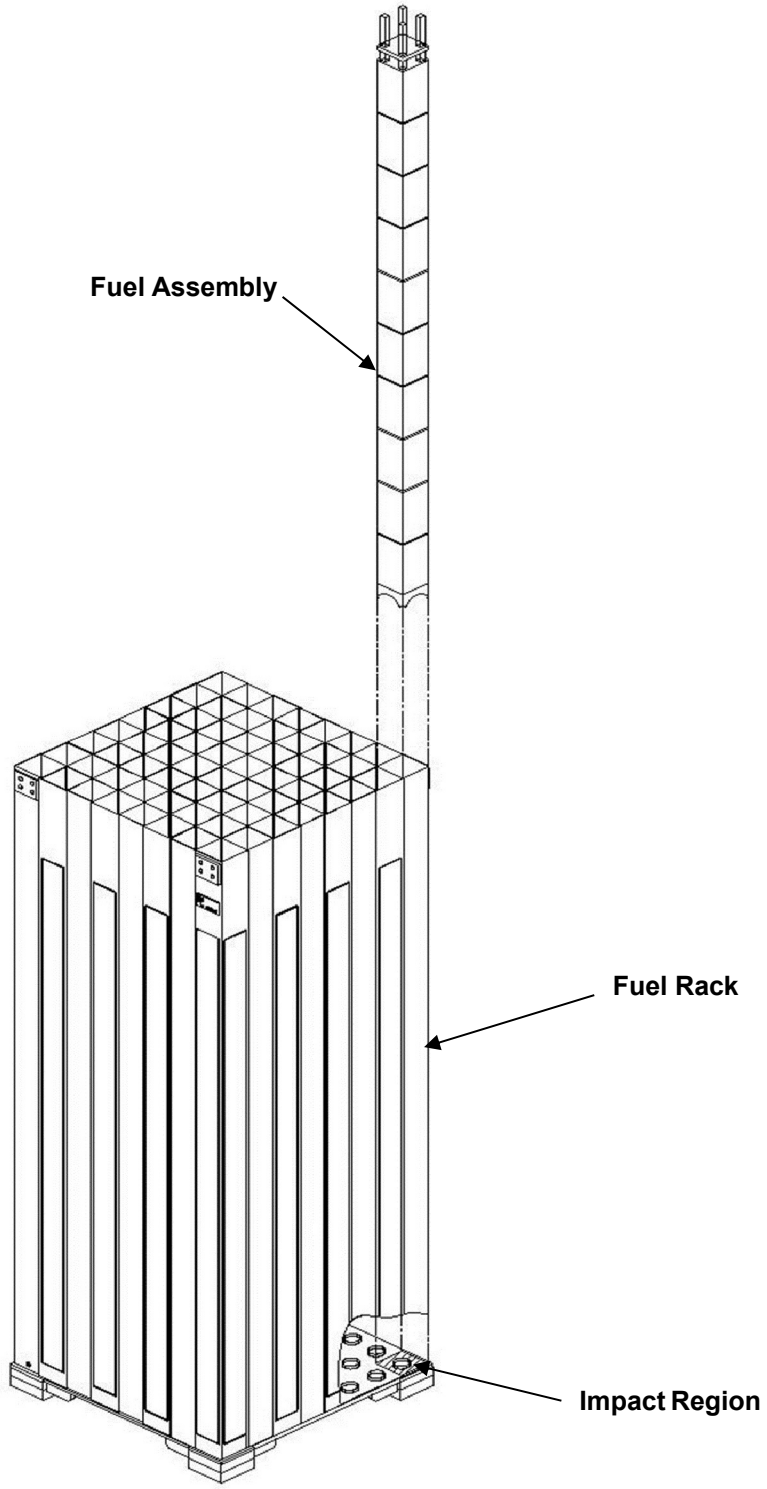

Figure 4-3 Schematic of the Deep Drop Over a Pedestal (Scenario 3)

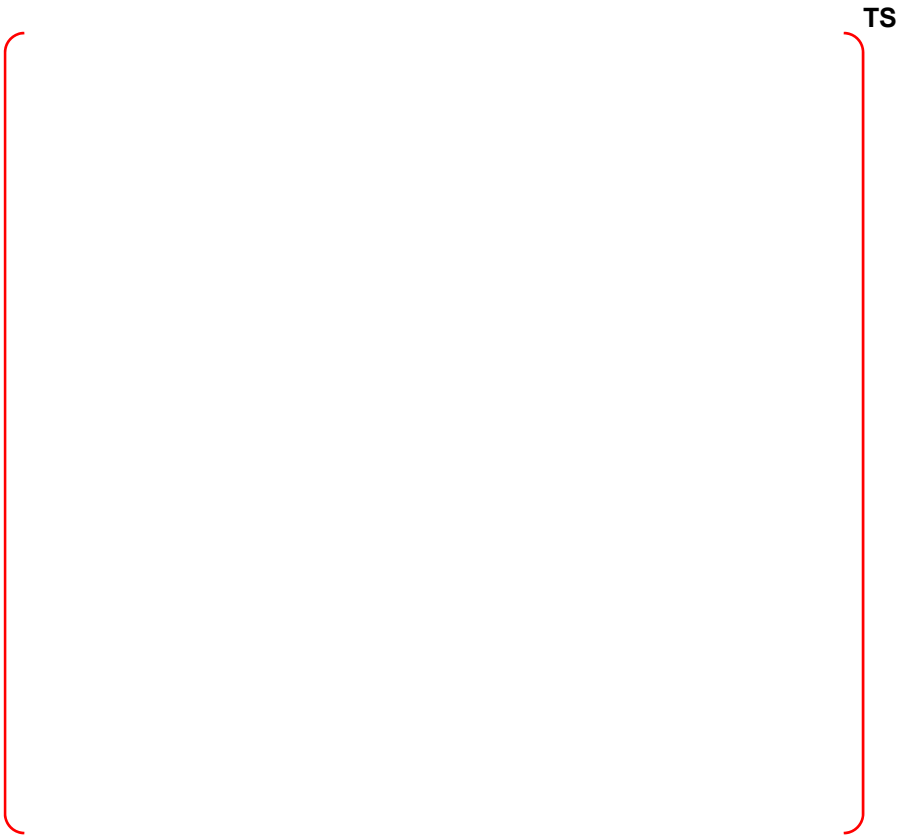

Figure 4-4 Finite Element Model – Shallow Drop

TS

Figure 4-5 NFSR Model – Deep Drop Away from Pedestal (Scenario 2)

TS

Figure 4-6 NFSR Impact Location-1 (left) and Location-2 (right) on Baseplate

TS

Figure 4-7 SFSR Model – Deep Drop Away from Pedestal (Scenario 2)

TS

Figure 4-8 SFSR Impact Location on Baseplate

TS

Figure 4-9 SFSR Model – Deep Drop Over a Pedestal (Scenario 3)

TS

Figure 4-10 Plastic Strain of the SFSR Cell Wall – Shallow Drop

TS

Figure 4-11 Plastic Strain of Baseplate - NFSR Drop Location 1

TS

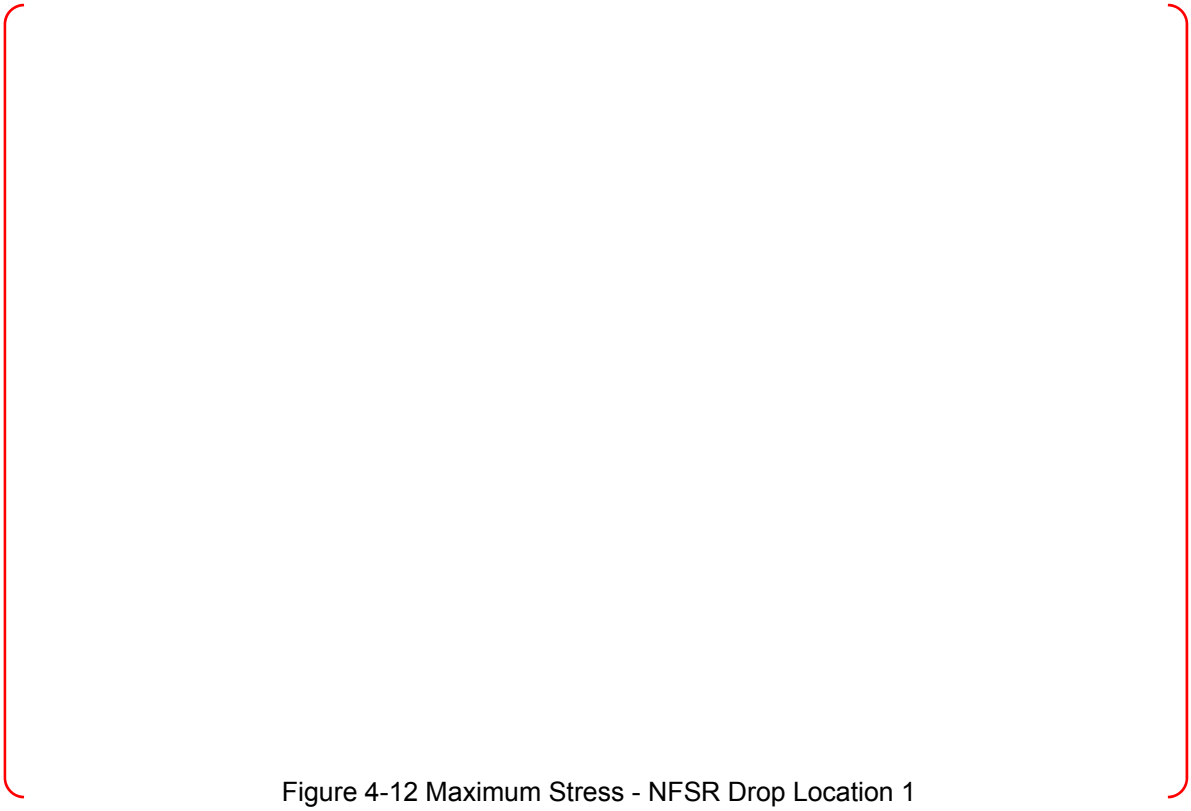

Figure 4-12 Maximum Stress - NFSR Drop Location 1

TS

Figure 4-13 NFSR Peripheral Deep Drop – Baseplate Plastic Strain

TS

Figure 4-14 NFSR Peripheral Deep Drop – Baseplate Maximum Stress

TS

Figure 4-15 Plastic Strain of Baseplate – SFSR Deep Drop Away from Pedestal

TS

Figure 4-16 Maximum Stress – SFSR Deep Drop Away from Pedestal

5 CONCLUSIONS

SRP Section 3.8.4 Appendix D specifies acceptance criteria for SFSRs. Also, as identified in DCD Section 3.8.4.1.3, the SFSRs are designed to meet the following criteria:

- Protect the stored fuel against a physical damage
- Maintain the stored fuel in a subcritical configuration
- Maintain the capability to load and unload fuel assemblies
- Maintain the stored fuel in a coolable geometry

The design of the new and spent fuel storage racks of the APR1400 design is acceptable because the results of conservatively performed structural and seismic analyses and mechanical accident analyses meet all requirements. The results are summarized as follows:

(1) The racks do not impact the pool/pit walls or adjacent racks above the baseplate.

(2) The overturning of rack module under seismic events does not occur.

(3) The SFSRs do experience rack-to-rack impact during SSE events at the baseplate because they are installed in contacts with adjacent baseplate of other racks. However, the calculated impact loads are lesser than the capacity limit of the baseplate.

(4) All rack cell wall and pedestal stress factors are below the allowable stress factor limit.

(5) All weld stresses are below the allowable stress limits.

(6) The fuel spacer grid does not buckle and the bending stress induced in the fuel rod cladding is well below the yield strength of the fuel rod clad. Therefore, the structural integrity of the spent fuel assembly is maintained.

(7) The NFSRs and the SFSRs under the postulated mechanical accident possess acceptable margins of safety.

(8) A stuck fuel assembly does not cause damage that affects the integrity of neutron absorber plates.

Therefore, it is demonstrated that the design of the NFSRs and the SFSRs of the APR1400 design meets the structural integrity requirements for Level A and Level D conditions which are specified on NRC SRP 3.8.4, appendix D (Reference 1).

6 REFERENCES

1. U.S. Nuclear Regulatory Commission, NUREG-0800, Standard Review Plan, Section 3.8.4, “Other Seismic Category I Structures,” Rev. 4, September 2013.

2. US NRC, “Seismic Design Classification,” Regulatory Guide 1.29, Rev. 4, March 2007.

3. American Nuclear Standards Institute, “Design Requirements for New Fuel Storage Facilities at Light Water Reactor Plants, ANSI/ANS-57.3-1983;W1993 (W=Withdrawn).

4. American Society of Mechanical Engineers, ASME Boiler and Pressure Vessel Code, Section III, Division 1, “Rules for Construction of Nuclear Facility Components,” 2007 Edition with the 2008 Addenda.

5. Doosan, Outline Drawing, N13027-224CD-1000, “New Fuel Storage Pit Layout,” Rev. 2, November 2016 (Doosan Proprietary).

6. Doosan, Outline Drawing, N13027-224CD-2000, “Spent Fuel Pool Layout,” Rev. 2, November 2016 (Doosan Proprietary).

7. MPR, “Seismic Time-History Verification for Spent Fuel Storage Racks (SFSR),” 0938-0006-CALC-008, Rev. 1, December 2016.

8. MPR, “Seismic Time-History Verification for New Fuel Storage Racks (NFSR),” 0938-0006-CALC-009, Rev. 1, December 2016.

9. U.S. Nuclear Regulatory Commission, NUREG-0800, Standard Review Plan, Section 3.7.1, “Seismic Design Parameters,” Rev. 3, March 2007.

10. Borsoi L. and Ricard A., "A Simple Accelerogram Correction Method to Prevent Unrealistic Displacement Drift," 8th SMIRT, Vol .K(a), Paper K2/7, Brussels, 1985.

11. J. Nie, J. Xu, and C. Costantino, Brookhaven National Laboratory, “P-CARES: Probabilistic Computer Analysis for Rapid Evaluation of Structures, “ NUREG/CR-6922 / BNL-NUREG-77338-2006, November 2006.

12. Brookhaven National Laboratory, “Seismic Analysis of Large-Scale Piping Systems for the JNES-NUPEC Ultimate Strength Piping Test Program,” NUREG/CR-6983 BNL-NUREG-81548-2008.

13. MPR, “Acceleration Time History Correction,” 0938-0009-CALC-002, Rev. 1, December 2016.

14. Rabinowicz, E., “Friction Coefficients of Water Lubricated Stainless Steels for a Spent Fuel Rack Facility,” MIT, Report for Boston Edison Company, 1976.

15. S. Singh, et. Al., “Structural Evaluation of Onsite Spent Fuel Storage: Recent Developments,” Proceedings of the Third Symposium, Orlando, Florida, December 1990, North Carolina State University, Raleigh, NC 27695, pp V/4-1 through V/4-18.

16. Fritz, R.J., “The Effects of Liquids on the Dynamic Motions of Immersed Solids,” Journal of Engineering for Industry, Trans. of ASME, February 1972, pp 167-172.

17. Doosan, “Structural and Seismic Analysis Report for New and Spent Fuel Storage Racks,” N14014-224CN-0001, Rev.2, December 2016 (Doosan Proprietary).

18. Computer code, ANSYS Version 15.07; Installed on DELL PowerEdge M620, Verification Document No. DAVM1507HPC, Rev.0, April 2015 (Doosan Proprietary).

19. American Society of Mechanical Engineers, ASME Boiler and Pressure Vessel Code, Section II, “Materials,” 2007 Edition with the 2008 Addenda.

20. U.S. Nuclear Regulatory Commission, NUREG-0800, Standard Review Plan, Section 3.8.5, “Foundations,” Rev. 4, September 2013.

21. U.S. Atomic Energy Commission, “Nuclear Reactors and Earthquakes,” TID-7024, August 1963.

22. KEPCO Engineering & Construction Co. Inc., KEPCO E&C Job No. 11E47, 1-423-N462-003, Rev. 2, "Design Specification for Fuel Storage Rack," October 2016.

23. KEPCO Nuclear Fuel Company, Memo No. MFD/HS-160001M, APR1400 NRC DC PLUS7 FA Material Properties and Bottom Nozzle Dimension, November 2016.

24. U.S. Nuclear Regulatory Commission, Regulatory Guide 1.61, “Damping Values for Seismic Design of Nuclear Power Plants,” Rev. 1, March 2007.

25. MPR, “APR1400 Fuel Rack Dynamic Analysis Benchmarking,” 0938-0006-RPT-001, Rev. 0, October 2016 (Doosan Proprietary).

26. U.S. Nuclear Regulatory Commission, NUREG-0800, Standard Review Plan, Section 3.8.1, “Concrete Containment” Rev. 3, May 2010.

27. KEPCO E&C, Memo No. MES/HS-160011M, APR1400 NRC DC (II) SFP Concrete Slab Parameter’s & Detail Drawing of SFP Embedment Plate, November 08, 2016.

28. Warren C Young, Roark's Formulas for Stress & Strain, 6th Edition.

29. Doosan, “Thermal-Hydraulic Analysis for Spent Fuel Racks,” APR1400-H-N-NR-14013-P/NP, Rev. 0, December 2016.

30. Computer Code, ANSYS LS-DYNA Version 15.07: Installed on DELL PowerEdge M620 (or DELL PowerEdge M630, HP PROLIANT BL460C G8 & HP PROLIANT BL460C G9), In-Use Test Report Document No. DAVM1507LS_IUT-HPC, Rev. 0., Feb. 2016 (Doosan Proprietary).

31. US NRC, “Final Safety Evaluation Report for South Texas Project Units 3 & 4,” [Chapter 9] September 2015.

32. Doosan, “Accident Analysis Report for New and Spent Fuel Storage Racks," N14014-224CN-0002, Rev.2, December 2016 (Doosan Proprietary).

APPENDIX A

Cross-reference of NRC RAIs to Information in Report that Addresses Questions

The body of this report provides information responsive to NRC Requests for Additional Information (RAIs) questions pertaining to the APR1400 fuel storage racks. As requested by NRC reviewers in an August 9. 2016, public (closed) meeting, the report provides a complete description of the analyses and acceptability of the new fuel storage racks (NFSRs) and spent fuel storage racks. The approach provides a more readily understood and complete description of rack design acceptability with less duplication than would a series of individual RAI responses.

To ensure this report is responsive to RAI questions pertaining to fuel storage racks and to allow readers to readily find the relevant information, the following table is included to provide a response traceability matrix.

- Each relevant Section 9.1.2 RAI question number is listed in the leftmost column.
- The text of each question is included in its entirety in the second column. Note that some of these questions were developed over a year ago and may be obviated by changes in analytical approach. For example, use of the ANSYS finite element analysis program makes moot questions pertaining to the prior calculational method for drop accidents. The matrix will still direct readers to the most relevant discussion associated with the current methodology.
- The third column indicates if other APR1400 documentation is affected.
    - Where Design Control Document (DCD) revisions are appropriate (i.e., “Yes” entry), the mark-up of the existing DCD Section 9.1.2 is provided.
    - None of the RAI questions nor information included in this report affects the probabilistic risk assessment; hence all entries are “No.”
- The rightmost column directs the reader to where in the body of the report the discussion addresses the RAI question. In some cases, more than one report section is relevant; in which case multiple locations are identified where the first entry is usually the most pertinent, although all cross-references may need to be used to provide a complete response. If a question has separately labeled subquestions (e.g., 36a, 36b), each one has a cross-reference.

As this report pertains to the NFSR and SFSR design but not to the buildings, the New Fuel Storage Pit, the Spent Fuel Pool (or its liner or active systems), a number of RAI questions are outside its scope and not discussed herein. Only RAI questions within this scope are listed. Questions not included in the table are addressed through the usual process of issuing individual RAI responses. Those question responses are submitted for NRC consideration through the customary process of individual answers.

Number	Question	Impacts	See Section
09.01.02-			
11	The 10 CFR Part 50, Appendix A, General Design Criteria (GDC) 1, 2, 4, 5, 63, and 10CFR 52.80 (a) provide the regulatory requirements for the design of the new and spent fuel storage facilities. Standard Review Plan (SRP) Sections 9.1.2 and 3.8.4, Appendix D describes specific SRP acceptance criteria for the review of the fuel racks that are acceptable to meet the relevant requirements of the Commission's regulations identified above. In DCD Tier 2, Section 9.1.2.2.3, “New and Spent Fuel Storage Rack Design”, the applicant stated that “The dynamic and stress analyses are performed as described in report APR1400-H-N-NR-14012- P & NP”. In the report APR1400-H-N-NR-14012-P, Rev.0, Section 3.4.7.4 (3), the applicant stated that “The thermal stress is classified as secondary stress on the ASME Code Section III, Division 1. Therefore, it is independently evaluated without combining with primary stress of other load condition.” The staff notes that the thermal stress may not be combined with the primary stress; however, the thermal expansion will reduce the gaps between the fuel assembly and the cell as well as between racks. The gap reduction increases the possibility for impact between the fuel assembly and the cell as well as between racks. The applicant in Subsection 3.7.1.3, “Impact Loads” stated that “the baseplate the fuel storage rack for the APR1400 design is installed almost in contact with the adjacent baseplate”. The thermal expansion of the rack potentially imposes load at the base of the pedestal. In accordance with SRP 3.8.4 Appendix D I(4), the applicant is requested to quantify thermally imposed loads at the base of the pedestal and discuss how these thermal load effects have been considered in the analysis and design of the new and spent fuel storage racks.	DCD **No** PRA **No** Technical Specifications **No** Technical/Topical/ Environmental Reports **Yes**	**3.7.3.5(3)**
12	The 10 CFR Part 50, Appendix A, General Design Criteria (GDC) 1, 2, 4, 5, 63, and 10CFR 52.80 (a) provide the regulatory requirements for the design of the new and spent fuel storage facilities. Standard Review Plan (SRP) Sections 9.1.2 and 3.8.4, Appendix D describes specific SRP acceptance criteria for the review of the fuel racks that are acceptable to meet the relevant requirements of the Commission's regulations identified above. The SRP 3.8.4 Appendix D I.3 ‘Seismic and Impact loads’ requires that “For freestanding spent fuel pool racks, which are potentially subject to sliding, uplift, and Impact between racks and with the pool walls, time-varying seismic excitation along three orthogonal directions (2 horizontal and vertical) should be imposed simultaneously”. The staff did not find sufficient information regarding the input seismic time histories considered for the nonlinear seismic evaluation of the new and the spent fuel racks. In accordance with SRP 3.8.4 Appendix D I.3, the applicant is requested to provide the following information so that the staff can perform its safety evaluation of the seismic and impact loads. a. Design target response spectra at the locations of new and spent fuel storage that were used to generate the synthetic time histories. Please describe the basis for selecting the target response spectra.	DCD **No** PRA **No** Technical Specifications **No** Technical/Topical/ Environmental Reports **Yes**	**3.1.1** **3.1.1**

	b. Seeds of earthquake ground motions used to generate the synthetic time histories. c. The record length and the time increment of the synthetic time histories. d. Coefficient of correlation to verify the statistical independence of the generated artificial time histories from given target response spectra. e. Provide a comparison of PSD (Power Spectral Density) of original (target) with PSD developed from synthetic time histories. f. Clarify and confirm that the seismic excitation time histories along three orthogonal directions (2 horizontal and vertical) in the nonlinear seismic analysis are applied simultaneously. g. Discuss the validation and verification procedure used for the computer codes ATIGEN and STCOR referenced in Table 3-5 of the report APR1400-H-N-NR-14012, Rev.0. The applicant is also requested to provide reference to operating or new nuclear power plants that have been licensed using ATIGEN and STCOR computer codes.		**3.1.1** **3.1.1.1** **3.1.1.1** **3.1.1.1** **3.1.1** **Reference to codes removed**
13	The 10 CFR Part 50, Appendix A, General Design Criteria (GDC) 1, 2, 4, 5, 63, and 10CFR 52.80 (a) provide the regulatory requirements for the design of the new and spent fuel storage facilities. Standard Review Plan (SRP) Sections 9.1.2 and 3.8.4, Appendix D describes specific SRP acceptance criteria for the review of the fuel racks that are acceptable to meet the relevant requirements of the Commission's regulations identified above. The SRP 3.8.4 Appendix D section I (3), “Seismic and Impact Loads” requires that “Because of gaps between fuel assemblies and the walls of the guide tubes, additional loads will be generated by the impact of fuel assemblies during a postulated seismic excitation. Additional loads resulting from this impact effect may be determined by estimating the kinetic energy of the fuel assembly. The maximum velocity of the fuel assembly may be estimated to be the spectral velocity associated with the natural frequency of the submerged fuel assembly. Loads thus generated should be considered for local as well as overall effects on the walls of the rack, the supporting framework. It should be demonstrated that the consequent loads on the fuel assembly do not lead to damage of the fuel.” In order for the staff to perform its safety evaluation of the racks for impact loads, the applicant in accordance with SRP 3.8.4 Appendix D I.3, is requested to provide the details of how the additional loads due to the impact of fuel assemblies during a postulated seismic excitation are computed and how these loads are considered in the analysis and design of the walls of the rack and supporting framework and demonstrating the structural integrity of the fuel.	DCD **No** PRA **No** Technical Specifications **No** Technical/Topical/ Environmental Reports **Yes**	**3.1.2.2** **3.1.2.4(1)** **3.2** **3.7.1.3(1)** **3.7.2** **3.7.3.5**
14	The 10 CFR Part 50, Appendix A, General Design Criteria (GDC) 1, 2, 4, 5, 63, and 10CFR 52.80 (a) provide the regulatory requirements for the design of the new and spent fuel storage facilities. Standard Review Plan (SRP) Sections 9.1.2 and 3.8.4, Appendix D describes specific SRP acceptance criteria for the review of the fuel racks that	DCD **No** PRA **No**	3.7.1.2

	are acceptable to meet the relevant requirements of the Commission's regulations identified above. In DCD Tier 2, Section 9.1.2.2.3, “New and Spent Fuel Storage Rack Design”, the applicant stated that “The dynamic and stress analyses are performed as described in report APR1400-H-N-NR-14012- P & NP”. In the report APR1400-H-N-NR-14012-P, Rev.0, Table 3-9 “Maximum Loads on single Pedestal”, the staff noted that for the spent fuel storage rack, generally the force on the pedestal in the north-south direction is much less (about 50%) than that in the east-west direction. The staff did not find sufficient details and description of the underlying analyses in the report and is not able to confirm large variation in forces in the two horizontal directions. In order for the staff to perform its safety evaluation of the racks, the applicant is requested to provide the basis and justification for such large difference in pedestal forces in the two horizontal directions.	Technical Specifications **No** Technical/Topical/ Environmental Reports **No**	
15	The 10 CFR Part 50, Appendix A, General Design Criteria (GDC) 1, 2, 4, 5, 63, and 10CFR 52.80 (a) provide the regulatory requirements for the design of the new and spent fuel storage facilities. Standard Review Plan (SRP) Sections 9.1.2 and 3.8.4, Appendix D describes specific SRP acceptance criteria for the review of the fuel racks that are acceptable to meet the relevant requirements of the Commission's regulations identified above. In DCD Tier 2, Section 9.1.2.1(f), the applicant committed to meet the requirements of SRP 3.8.4 Appendix D for the new and spent fuel storage racks rack design. The SRP 3.8.4 Appendix D, Section I (5) requires that “For nonlinear seismic analysis of the racks, multiple time histories analysis should be performed in accordance with the criteria for nonlinear analysis described in SRP 3.7.1, unless otherwise justified”. The DCD Tier 2 Section 9.1.2.2.3 makes reference to a technical report APR1400-H-N-NR- 14012-P, Rev.0, for the dynamic and stress analysis of the racks. In Subsection 3.1.1 of the technical report, the applicant stated that “An accurate evaluation of nonlinear response requires a 3-D time-history analysis to establish the proper response during a seismic loading. Therefore, the initial step in a 3-D time-history analysis is to develop time-history seismic loadings for three orthogonal directions that comply with the guidelines of the NRC SRP 3.7.1.” The SRP Section 3.7.1 acceptance criteria for the nonlinear seismic analysis states that “For nonlinear structural analysis problems, multiple sets of ground motion time histories should be used to represent the design ground motion. Each set of ground motion time histories can be selected from real recorded or artificial time histories. The amplitude of these ground motions may be scaled but the phasing of Fourier components should be maintained. The adequacy of this set of ground motions, including duration estimates, is reviewed on a case-by- case basis.” The SRP Section 3.7.1, option 2 delineates the requirements for multiple sets of time histories. It states, ““For nonlinear structural analyses, the number of time histories should be greater than four and the technical basis for the appropriate number of time histories are reviewed on a case-by-case basis. This review also includes the adequacy of the	DCD **No** PRA **No** Technical Specifications **No** Technical/Topical/ Environmental Reports **Yes**	**3.1.1** **3.1.1.1** **3.7.5**

	characteristics of the multiple time histories." Based on the review of the DCD Tier 2 Section 9.1.2 and the referenced technical report APR1400-H-N-NR-14012-P, Rev.0, it is not clear to the staff whether the applicant met the acceptance criteria for nonlinear seismic analyses in SRP 3.8.4 Appendix D and in SRP 3.7.1 as stated above. In order for the staff to perform its safety evaluation of the seismic input to the racks, the applicant in accordance with SRP 3.8.4 Appendix D and SRP Section 3.7.1 is requested to clarify and confirm that it used at least the five sets (greater than the required four) of time histories for the nonlinear structural analyses of the new and spent fuel storage racks and provide the technical basis and justification for selecting the number of time history sets used in the nonlinear seismic analyses. The applicant is requested to identify any proposed changes to and provide a mark-up of Subsections in the DCD Tier 2 and the report APR1400-H-N-NR-14012-P, Rev.0, as appropriate.		
16	The 10 CFR Part 50, Appendix A, General Design Criteria (GDC) 1, 2, 4, 5, 63, and 10 CFR 52.80 (a) provide the regulatory requirements for the design of the new and spent fuel storage facilities. Standard Review Plan (SRP) Sections 9.1.2 and 3.8.4, Appendix D describes specific SRP acceptance criteria for the review of the fuel racks that are acceptable to meet the relevant requirements of the Commission's regulations identified above. In DCD Tier 2, Section 9.1.2.2.3, "New and Spent Fuel Storage Rack Design", the applicant stated that "The dynamic and stress analyses are performed as described in report APR1400-H-N-NR-14012-P & NP". In the report APR1400-H-N-NR-14012-P, Rev.0, Section 3.6, "Dynamic Simulations", it is stated that "The storage rack configurations at the full loading are considered in the dynamic simulations." This sentence implies that assuming every rack with the full loading in the seismic or impact analyses results in a conservative design. It is not apparent to the staff that assuming the full loading for every rack is conservative. For example, consider the following scenario: Assume a fully loaded rack subjected to an earthquake does not slide; now consider two racks with one rack empty; and the other rack fully loaded. During the same earthquake, the lighter rack slides because its friction force at the base is now less than if it were fully loaded. The fully loaded one by itself would not slide; however, it may slide due to the impact from the lighter rack; thus, the whole system (the lighter rack and the fully loaded rack) slides. Based on the above example, the applicant is requested to provide a technical rationale and the results of any study performed to demonstrate that the assumption of all fully loaded racks will always result in a conservative design. Otherwise, the applicant is requested to consider appropriate loading patterns in the analyses. The loading patterns considered should include the case of all racks completely empty to demonstrate that the racks and liner of the spent fuel pool would not be damaged due to the impact.	DCD **No** PRA **No** Technical Specifications **No** Technical/Topical/ Environmental Reports **Yes**	**3.7.4.5** **Table 3-5** **Figure 3-4** **3.1.2.1(2)** **3.6**
17	The 10 CFR Part 50, Appendix A, General Design Criteria (GDC) 1, 2, 4, 5, 63, and 10CFR 52.80 (a) provide the regulatory requirements for the design of the new and spent fuel storage facilities. Standard Review Plan (SRP)	DCD **No** PRA	3.7.3.5(4)

	Sections 9.1.2 and 3.8.4, Appendix D describes specific SRP acceptance criteria for the review of the fuel racks that are acceptable to meet the relevant requirements of the Commission's regulations identified above. In DCD Tier 2, Section 9.1.2.2.3, “New and Spent Fuel Storage Rack Design”, the applicant stated that “The dynamic and stress analyses are performed as described in report APR1400-H-N-NR-14012- P & NP”. In the report APR1400-H-N-NR-14012-P, Rev.0, Subsection 3.1.2.2 “Details for Rack and Fuel Assembly” it is stated that “A vertical movement of fuel assembly is assumed to be the same as the vertical movement of the storage rack”. The applicant’s assumption implies that that there is no fuel rattling in the vertical direction because the vertical displacement of the fuel is the same as the vertical displacement of the rack. However, there is a potential for the fuel assembly to separate from the baseplate during vertical ground motion depending on the vertical frequencies, phasing, and relative maximum vertical input acceleration of the fuel assembly and the storage rack. In order for the staff to perform its safety evaluation of the fuel and the rack assembly for the vertical seismic input motion, the applicant in accordance with SRP 3.8.4 Appendix D I.3 is requested to provide a technical basis to justify the assumption that the vertical movement of fuel assembly and the storage rack is the same. The applicant is requested to provide the information for the fundamental frequency of the fuel assembly and the storage rack in the vertical direction; and the design response spectrum for the vertical motion at the new and the spent fuel rack locations. The applicant is also requested to show that the fundamental frequency of the fuel assembly and the fuel rack in the vertical direction is above the frequency where the spectral acceleration returns to the ZPA and that the ZPA is less than 1.0g.	**No** Technical Specifications **No** Technical/Topical/ Environmental Reports **Yes**	
18	The 10 CFR Part 50, Appendix A, General Design Criteria (GDC) 1, 2, 4, 5, 63, and 10CFR 52.80 (a) provide the regulatory requirements for the design of the new and spent fuel storage facilities. Standard Review Plan (SRP) Sections 9.1.2 and 3.8.4, Appendix D describes specific SRP acceptance criteria for the review of the fuel racks that are acceptable to meet the relevant requirements of the Commission's regulations identified above. In DCD Tier 2, Section 9.1.2.2.3, “New and Spent Fuel Storage Rack Design”, the applicant stated that “The dynamic and stress analyses are performed as described in report APR1400-H-N-NR-14012- P & NP”. In the report APR1400-H-N-NR-14012-P, Rev.0, Subsection 3.4.3 “Structural Damping”, Rayleigh damping is used to specify mass (M) and stiffness (K) proportional damping (C)”. The applicant stated that the constant multiplier to the mass and stiffness matrix are calculated in the range of the lowest and highest frequencies of interest in the dynamic analysis. In accordance with SRP 3.8.4 Appendix D I.5, the applicant is requested to provide (1) the numerical value of the range of the lowest and the highest frequency considered (2) natural frequencies of new and spent fuel storage racks identifying primary horizontal, vertical and rocking frequencies of vibration, and (3) the technical basis why the range of the lowest and highest frequencies specified in the	DCD **No** PRA **No** Technical Specifications **No** Technical/Topical/ Environmental Reports **Yes**	3.4.3 3.1.2.7

	analysis will provide conservative results.		
20	The 10 CFR Part 50, Appendix A, General Design Criteria (GDC) 1, 2, 4, 5, 63, and 10CFR 52.80 (a) provide the regulatory requirements for the design of the new and spent fuel storage facilities. Standard Review Plan (SRP) Sections 9.1.2 and 3.8.4, Appendix D describes specific SRP acceptance criteria for the review of the fuel racks that are acceptable to meet the relevant requirements of the Commission's regulations identified above. The SRP 3.8.4 Appendix D section I.5, 'Design and analysis Procedure" requires that "Details of the mathematical model, including a description of how the important parameters are obtained, should be provided"." The seismic response of the freestanding fuel storage rack modules is highly nonlinear and involves a complex combination of motions (sliding, rocking, and twisting).The staff did not find sufficient information of the mathematical model and its parameters considered for the seismic evaluation of the new and the spent fuel racks. In accordance with SRP 3.8.4 Appendix D section I.5, the applicant is requested to provide the following information so that the staff can perform its safety evaluation of the seismic analysis. a. In Subsection 3.3 (3), it is stated that "Each concentrated mass has a degree of freedom in horizontal direction". The applicant is requested to clarify if the same mass is considered effective in both the horizontal directions. Also, the applicant is requested to provide the technical basis for not including the rack and the fuel lumped masses associated with the rocking and twisting degrees of freedom to simulate sliding, rocking and twisting of the free standing racks. b. In Figures 3-1 and 3-3 (APR1400-H-N-NR-14012, Rev.0), dynamic analysis model of new fuel and spent fuel storage racks respectively, rack equivalent element and fuel assembly equivalent element are shown. Please describe the methodology for determining the rack and fuel assembly equivalent element properties including the acceptance criteria for dynamic equivalency. Provide a comparison of natural frequencies and significant modes of vibrations of the equivalent rack-fuel assembly with the actual rack-fuel assembly. c. In Figure 3-4 (APR1400-H-N-NR-14012-P, Rev.0), schematic of spring elements used for SFSR are shown. The applicant is requested to provide the spring values and explain how the different spring stiffness values are determined. Since the impact forces are affected by the impact spring stiffness , the applicant is also requested to explain how is the sensitivity of the impact forces and rack responses to variation in these spring constants is considered in the nonlinear seismic analyses. Provide the results of any sensitivity analysis performed. d. Provide the integration time step used in performing the nonlinear time history analyses for SSE. Please explain the sensitivity of the numerical results to the integration time step used in the nonlinear seismic analyses. Provide the results of any sensitivity analysis performed.	DCD **No** PRA **No** Technical Specifications **No** Technical/Topical/ Environmental Reports **Yes**	3.1.2 3.3 3.1.2.2 3.1.2.2 3.1.2.4 3.7.4 3.7.4.6 Table 3-6 3.1.3(3)

	e. The applicant is also requested to explain the methods used to incorporate gaps between the racks, fuel bundles and the guide tubes and how the sensitivity of variation in gaps is considered in the nonlinear seismic analyses. Provide the results of any sensitivity analysis performed. f. The applicant is requested to discuss how the effect of the installation tolerances for the nominal gap are considered in the seismic analysis and design of the NFSR and SFSR and provide the results of any sensitivity analysis performed. The applicant is requested to identify any proposed changes to and provide a mark-up of Subsections in the DCD Tier 2 and the report APR1400-H-N-NR-14012, Rev.0, as appropriate.		3.1.2.1(5) 3.1.2.1(5) 3.7.1.3(2)
21	The 10 CFR Part 50, Appendix A, General Design Criteria (GDC) 1, 2, 4, 5, 63, and 10CFR 52.80 (a) provide the regulatory requirements for the design of the new and spent fuel storage facilities. Standard Review Plan (SRP) Sections 9.1.2 and 3.8.4, Appendix D describes specific SRP acceptance criteria for the review of the fuel racks that are acceptable to meet the relevant requirements of the Commission's regulations identified above. In DCD Tier 2, Section 9.1.2.2.3, “New and Spent Fuel Storage Rack Design”, the applicant stated that “The dynamic and stress analyses are performed as described in report APR1400-H-N-NR-14012-P & NP”. In the report APR1400-H-N-NR-14012-P, Rev.0, Section 3.1.2.3 “Hydrodynamic Mass”, the staff notes that the Applicant did not describe the hydrodynamic mass under the baseplate of each rack. The SRP 3.8.4 Appendix D section I.5, ‘Design and analysis Procedure” requires that the effect of effective mass from submergence in water should be quantified. In accordance with SRP 3.8.4 Appendix D section I.5, the Applicant is requested to (1) clarify whether the hydrodynamic mass under the rack baseplate of each rack has been considered in all nonlinear seismic analyses and (2) provide the methodology for calculating this hydrodynamic mass. If the hydrodynamic mass under the base plate of each rack is not considered in the nonlinear dynamic analyses, the applicant is requested to provide the technical basis and justification to show that ignoring the hydrodynamic mass under the baseplate of each rack is conservative. The second part of Subsection 3.1.2.3 states “(2) Hydrodynamic masses between Rack-to- Rack and Rack-to-Pool Wall are calculated based on height of rack, density of fluid and gap of adjacent racks, assuming that the fluid is filled between two objects.” The applicant is requested to provide a technical reference to any recognized method for this calculation. Also, describe how changes in the gap during seismic response affect the gap-dependent hydrodynamic mass and the subsequent seismic response due to the revised hydrodynamic mass. This could potentially be significant for low coefficient of friction cases where more sliding is expected.	DCD **No** PRA **No** Technical Specifications **No** Technical/Topical/ Environmental Reports **Yes**	3.1.2.3(3) 3.1.2.3(3)
22	The 10 CFR Part 50, Appendix A, General Design Criteria (GDC) 1, 2, 4, 5, 63, and 10CFR 52.80 (a) provide the regulatory requirements for the design of the new and spent fuel storage facilities. Standard Review Plan (SRP) Sections 9.1.2 and 3.8.4, Appendix D describes specific SRP acceptance criteria for the review of the fuel racks that are acceptable to meet the relevant requirements of the	DCD **No** PRA **No** Technical	3.7.3.5(3)

	Commission's regulations identified above. In DCD Tier 2, Section 9.1.2.2.3, "New and Spent Fuel Storage Rack Design", the applicant stated that "The dynamic and stress analyses are performed as described in report APR1400-H-N-NR-14012- P & NP". In the report APR1400-H-N-NR-14012-P, Rev.0, Subsection 3.7.3.4 (3) "Secondary Stress by Temperature Effects", it is stated that "a conservative estimate of the weld stresses along the length of an isolated hot cell is obtained by considering a beam strip uniformly heated by 65° F and restrained from growth along one long edge. The Applicant further stated that temperature rise envelops the difference between the maximum local spent fuel pool water temperature (155°F) inside a storage cell and the bulk pool temperature (121°F)) based on the thermal-hydraulic analysis of the spent fuel pool". The Applicant is requested to provide appropriate references and the methodology to calculate the maximum local spent fuel pool water temperature inside a storage cell and the bulk pool temperature.	Specifications **No** Technical/Topical/ Environmental Reports **Yes**	
23	The 10 CFR Part 50, Appendix A, General Design Criteria (GDC) 1, 2, 4, 5, 63, and 10CFR 52.80 (a) provide the regulatory requirements for the design of the new and spent fuel storage facilities. Standard Review Plan (SRP) Sections 9.1.2 and 3.8.4, Appendix D describes specific SRP acceptance criteria for the review of the fuel racks that are acceptable to meet the relevant requirements of the Commission's regulations identified above. In DCD Tier 2, Section 9.1.2.2.3, "New and Spent Fuel Storage Rack Design", the applicant stated that "The dynamic and stress analyses are performed as described in report APR1400-H-N-NR-14012- P & NP". In the report APR1400-H-N-NR-14012-P, Rev.0, Section 4.1 "Description of Mechanical Accident", the applicant considered a drop of fuel assembly in an interior cell away from the support pedestal for one of the 'Straight Deep Drops' scenario. The applicant is requested to provide specific location(s) of the drop on the rack base plate that were considered to maximize the deformation of the rack base plate and whether it also considered a deep drop into a cell along the perimeter and half way between the supports. It is not clear from the description whether the rack baseplate evaluation due to fuel impact assumed that other fuel assemblies are in place when a fuel assembly drops through an empty cell. A full load of fuel assemblies may introduce progressive deformation of the baseplate after a fuel assembly impacts the rack baseplate. The maximum downward deformation of the baseplate may be significant enough to initiate a progressive deformation. Therefore, the applicant is also requested to provide (1) the technical basis and justification for not considering all other fuel assemblies in place when a fuel assembly drops through an empty cell and (2) the design basis for the rack baseplate including the basis for determining the most critical locations of the fuel assembly drop. The applicant is requested to identify any proposed changes to and provide a mark-up of Subsections in the DCD Tier 2 and the report APR1400-H-N-NR-14012-P, Rev.0, as appropriate.	DCD **No** PRA **No** Technical Specifications **No** Technical/Topical/ Environmental Reports **Yes**	4.3.1 4.3.3 4.1(2)
24	<u>Background</u> RAI 09.01.02-18 (Reference 1) requested that the applicant explain special preparation of surfaces in the	DCD **No**	2.3.2 2.3.5

	spent fuel pit to ensure that (1) corrosion products and fission products do not accumulate, (2) surfaces can easily be decontaminated, and (3) fuel assemblies will not be damaged. In the applicant's response (Reference 2), information was supplied about the SFP liner material and surfaces. In addition, the New and Spent Fuel racks were assured to be free of burrs, sharp corners, edges, and weld beads or splatter which could damage fuel assembly surfaces. Both of these explanations partially answer the original request, and satisfy provisions of the acceptance criteria (ANSI/ANS-57.2). However, the applicant does not address the surface finish of the racks themselves, which must have a minimum smoothness (ANSI/ANS-57.2, paragraph 6.4.2.11). Requested Information State the acceptable surface finish requirements for storage rack materials which must come into contact with fuel assemblies. <u>References</u> 1. "Request for Additional Information No. 248-2178 Revision 1, SRP Section: 09.01.02 – New and Spent Fuel Storage, Application Section: DCD Tier 2, Section 9.1.2" dated December 18, 2008. (ADAMS Accession No. ML090620646) 2. Letter from Yoshiki Ogata, MHI, to NRC dated March 30, 2009; Docket No. 52-021 MHI Ref: UAP-HF-09128; Subject: MHI's Response to US-APWR DCD RAI No. 248-2178 Revision 1 (ADAMS Accession No. ML090910646	PRA **No** Technical Specifications **No** Technical/Topical/ Environmental Reports **Yes**	
25	The 10 CFR Part 50, Appendix A, General Design Criteria (GDC) 1, 2, 4, 5, 63, and 10CFR 52.80 (a) provide the regulatory requirements for the design of the new and spent fuel storage facilities. Standard Review Plan (SRP) Sections 9.1.2 and 3.8.4, Appendix D describes specific SRP acceptance criteria for the review of the fuel racks that are acceptable to meet the relevant requirements of the Commission's regulations identified above. In DCD Tier 2, Section 9.1.2.2.3, "New and Spent Fuel Storage Rack Design", the applicant stated that "The dynamic and stress analyses are performed as described in report APR1400-H-N-NR-14012- P & NP". In the report APR1400-H-N-NR-14012-P, Rev.0, Section 4.5 "Results of Analyses", the applicant provided the results of fuel assembly drop analyses but did not provide the structural assessment of the dropped fuel assemblies due to impact with the rack and the rack baseplate. The staff notes that the applicant in Subsection 3.7.2 of the report provided structural evaluation of the fuel for the lateral impact loads on the fuel assembly due to fuel-to-cell wall impact. The applicant is requested to provide the results of its structural evaluation of the fuel assembly from the mechanical drop accident scenarios described in Section 4.1 of the report. The applicant is requested to identify any proposed changes to and provide a mark-up of Subsections in the DCD Tier 2 and the report APR1400-H-N-NR-14012-P, Rev.0, as appropriate.	DCD **No** PRA **No** Technical Specifications **No** Technical/Topical/ Environmental Reports **Yes**	4.

26	The 10 CFR Part 50, Appendix A, General Design Criteria (GDC) 1, 2, 4, 5, 63, and 10CFR 52.80 (a) provide the regulatory requirements for the design of the new and spent fuel storage facilities. Standard Review Plan (SRP) Sections 9.1.2 and 3.8.4, Appendix D describes specific SRP acceptance criteria for the review of the fuel racks that are acceptable to meet the relevant requirements of the Commission's regulations identified above. In DCD Tier 2, Section 9.1.2.2.3, “New and Spent Fuel Storage Rack Design”, the applicant stated that “The dynamic and stress analyses are performed as described in report APR1400-H-N-NR-14012- P & NP”. The staff noted that APR1400-H-N-NR-14012-P, Rev.0 did not consider seismic-induced sloshing effects in the nonlinear seismic analyses of the rack structure. The SRP 3.8.4 Appendix D, Section I.5 requires that the effect of sloshing water be quantified. In accordance with SRP 3.8.4 Appendix D, Section I.5, the applicant is requested to quantify the effect of sloshing water or provide the technical basis and justification for not considering the seismic sloshing effect on the dynamic response of the spent fuel racks. The applicant is requested to identify any proposed changes to and provide a mark-up of Subsections in the DCD Tier 2 and the report APR1400-H-N-NR-14012-P, Rev.0, as appropriate.	DCD **No** PRA **No** Technical Specifications **No** Technical/Topical/ Environmental Reports **Yes**	3.3(2)
28	The 10 CFR Part 50, Appendix A, General Design Criteria (GDC) 1, 2, 4, 5, 63, and 10CFR 52.80 (a) provide the regulatory requirements for the design of the new and spent fuel storage facilities. Standard Review Plan (SRP) Sections 9.1.2 and 3.8.4, Appendix D describes specific SRP acceptance criteria for the review of the fuel racks that are acceptable to meet the relevant requirements of the Commission's regulations identified above. In DCD Tier 2, Section 9.1.2.2.3, “New and Spent Fuel Storage Rack Design”, the applicant stated that “The dynamic and stress analyses are performed as described in report APR1400-H-N-NR-14012- P & NP”. In the technical report APR1400-H-N-NR-14012-P, Rev 0, Subsection 3.7.3.3, “Stresses on Welds”, the applicant evaluated stresses in cell-to-baseplate and baseplate-to-pedestal welds but did not calculate the base metal shear stress. The safety factor (ratio of allowable to actual shear stress) for the base metal may be lower than that for the weld. This reduction is noted in safety factors in Table 3-13 “Stress Evaluation for Fuel Racks. The staff notes that the safety factor for the cell-to cell weld stress is 5.42 that is reduced to 3.68 for the base metal shear. The applicant is requested to provide the base metal shear stress and corresponding safety factor for the cell-to-baseplate and baseplate-to-pedestal weld connections so the staff can make safety conclusions related to the rack welded connections	DCD **No** PRA **No** Technical Specifications **No** Technical/Topical/ Environmental Reports **Yes**	3.7.3.3
29	The 10 CFR Part 50, Appendix A, General Design Criteria (GDC) 1, 2, 4, 5, 63, and 10CFR 52.80 (a) provide the regulatory requirements for the design of the new and spent fuel storage facilities. Standard Review Plan (SRP) Sections 9.1.2 and 3.8.4, Appendix D describes specific SRP acceptance criteria for the review of the fuel racks that are acceptable to meet the relevant requirements of the Commission's regulations identified above. In DCD Tier 2, Section 9.1.2.2.3, “New and Spent Fuel Storage Rack Design”, the applicant stated that “The dynamic and stress	DCD **No** PRA **No** Technical Specifications **No**	3.7.3.3

	analyses are performed as described in report APR1400-H-N-NR-14012- P & NP". In the technical report APR1400-H-N-NR-14012-P, Rev 0, Subsection 3.7.3.3, "Stresses on Welds", the applicant evaluated stresses in cell-to-cell welds. An underlying assumption in the modeling of the rack as a single beam using the overall bending stiffness of the entire rack is that the cell-to-cell welds are intact and can carry the internal forces necessary to validate this assumption. This is not addressed in the report. The applicant is requested to provide a quantitative evaluation demonstrating that this loading in conjunction with the other loadings discussed in the report does not create an overstress condition in the cell-to-cell welds.	Technical/Topical/ Environmental Reports **Yes**	
30	The 10 CFR Part 50, Appendix A, General Design Criteria (GDC) 1, 2, 4, 5, 63, and 10CFR 52.80 (a) provide the regulatory requirements for the design of the new and spent fuel storage facilities. Standard Review Plan (SRP) Sections 9.1.2 and 3.8.4, Appendix D describes specific SRP acceptance criteria for the review of the fuel racks that are acceptable to meet the relevant requirements of the Commission's regulations identified above. SRP 3.8.4 Appendix D I (5) states that" Details of the mathematical model, including a description of how the important parameters are obtained, should be provided". In DCD Tier 2, Section 9.1.2.2.3, "New and Spent Fuel Storage Rack Design", the applicant stated that "The dynamic and stress analyses are performed as described in report APR1400-H-NNR-14012-P & NP". In the technical report APR1400-H-N-NR-14012-P, Rev 0, Subsection 3.1.2.2, "Details of Rack and Fuel Assembly" the staff finds that the information of the rack and fuel assembly mathematical model and the computer program used for the nonlinear seismic analysis is insufficient. The applicant is requested to provide the following additional information so that the staff can perform its safety evaluation of the seismic analysis of the rack and fuel assembly. a. The applicant stated that "There are three nodes for rack cells and fuel assemblies". The applicant did not provide any technical basis to show that the three node model of the fuel assembly adequately represents the dynamic characteristics of the fuel assembly. The applicant is requested to provide the fuel frequencies of the three lumped mass fuel model along with a comparison with frequency of the fuel assuming the fuel assembly as a simply supported beam, and with any physical test measurements of a PWR fuel assembly. b. The applicant stated that "All the fuel assemblies in each storage rack module are modeled as one beam of which the mass equals the sum of the masses of all the fuel assemblies in a rack". The applicant is requested to discuss and provide the details of how the stiffness properties of the beam that represents all the fuel assemblies in a rack are calculated to capture the dynamic characteristics of the free standing racks under seismic loading. The applicant is also requested to provide the assumptions and computational details of the contact stiffness between the fuel and the rack's cell wall that is used to predict the maximum fuel-to-cell impact loads.	DCD **No** PRA **No** Technical Specifications **No** Technical/Topical/ Environmental Reports **Yes**	3.1.2.4 3.5 3.1.2.2 3.1.2.7 3.1.2.4 3.1.2.7

	c. The applicant used ANSYS, Version 10 finite element program for the nonlinear dynamic analysis. The applicant is requested to provide reference to operating or new nuclear power plants free standing fuel racks that have been licensed using ANSYS Version 10 [Note: analysis has been reperformed using Version 15]. The applicant is also requested to provide the details of benchmarking, validation and verification of ANSYS commuter program for the specific application to the nonlinear seismic analysis of the free standing submerged fuel rack structures that includes nonlinear springs. The applicant is requested to identify any proposed changes to and provide a mark-up of Subsections in the DCD Tier 2 and the report APR1400-H-N-NR-14012-P, Rev.0, as appropriate.		3.5.1 3.5.1
31	The 10 CFR Part 50, Appendix A, General Design Criteria (GDC) 1, 2, 4, 5, 63, and 10CFR 52.80 (a) provide the regulatory requirements for the design of the new and spent fuel storage facilities. Standard Review Plan (SRP) Sections 9.1.2 and 3.8.4, Appendix D describes specific SRP acceptance criteria for the review of the fuel racks that are acceptable to meet the relevant requirements of the Commission's regulations identified above. In DCD Tier 2, Section 9.1.2.2.3, “New and Spent Fuel Storage Rack Design”, the applicant stated that “The dynamic and stress analyses are performed as described in report APR1400-H-N-NR-14012-P & NP”. In the technical report APR1400-H-N-NR-14012-P, Rev 0, Subsection 3.7.1.3, “Impact Loads”, for the case of rack-to-rack impacts, states that “The prominent baseplate of the fuel storage rack for the APR1400 design is installed almost in contact with the adjacent baseplate. According to the analysis result, the impact occurs not between the pool wall and the upper part of the rack, but between the baseplate of racks. SRP 3.8.4 Appendix D I(5) states that ” Details of the mathematical model, including a description of how the important parameters are obtained, should be provided” .In order for the staff to conclude that the applicant has adequately evaluated the rack-to-rack impact effects using a reasonable estimate of the impact spring rate, the applicant is requested to provide in accordance with the SRP 3.8.4 Appendix D I(5) the technical basis for calculating the impact spring constant for the rack-to-rack and rack baseplate-to-rack baseplate impact analysis in order to maximize the impact force. The applicant is also requested to address how the sensitivity of the impact force to the impact spring constant was considered in the analysis and design. The applicant is requested to identify any proposed changes to and provide a mark-up of Subsections in the DCD Tier 2 and the report APR1400-H-N-NR-14012-P, Rev.0, as appropriate.	DCD **No** PRA **No** Technical Specifications **No** Technical/Topical/ Environmental Reports **Yes**	3.7.1.3 3.7.4.3
32	The 10 CFR Part 50, Appendix A, General Design Criteria (GDC) 1, 2, 4, 5, 63, and 10CFR 52.80 (a) provide the regulatory requirements for the design of the new and spent fuel storage facilities. Standard Review Plan (SRP) Sections 9.1.2 and 3.8.4, Appendix D describes specific SRP acceptance criteria for the review of the fuel racks that are acceptable to meet the relevant requirements of the	DCD **No** PRA **No** Technical	2.2

	Commission's regulations identified above. In DCD Tier 2, Section 9.1.2.2.3, “New and Spent Fuel Storage Rack Design”, the applicant stated that “The dynamic and stress analyses are performed as described in report APR1400-H-N-NR-14012- P & NP”. In the technical report APR1400-H-N-NR-14012-P, Rev 0, Subsection 3.1.2.1 (2) **“**General Considerations” the applicant included the pedestal-to-bearing pad interface in the dynamic model of the rack for the impact loads. However, the staff did not find any acceptance criteria for the bearing pad. In order for the staff to perform its safety evaluation of the rack supports, the applicant in accordance with SRP 3.8.4 Appendix D I (3), is requested to provide a sketch showing the bearing pad dimensions and a layout of bearing pad with respect to the rack pedestal and the pool floor and acceptance criteria for the bearing pads including the maximum calculated and allowable bearing stress. The applicant is requested to identify any proposed changes to and provide a mark-up of Subsections in the DCD Tier 2 and the report APR1400-HN-NR-14012-P, Rev.0, as appropriate.	Specifications **No** Technical/Topical/ Environmental Reports **Yes**	
33	The 10 CFR Part 50, Appendix A, General Design Criteria (GDC) 1, 2, 4, 5, 63, and 10CFR 52.80 (a) provide the regulatory requirements for the design of the new and spent fuel storage facilities. Standard Review Plan (SRP) Sections 9.1.2 and 3.8.4, Appendix D describes specific SRP acceptance criteria for the review of the fuel racks that are acceptable to meet the relevant requirements of the Commission's regulations identified above. In DCD Tier 2, Section 9.1.2.2.3, “New and Spent Fuel Storage Rack Design”, the applicant stated that “The dynamic and stress analyses are performed as described in report APR1400-H-N-NR-14012- P & NP”. In the technical report APR1400-H-N-NR-14012-P, Rev 0, Section 4, “MECHANICAL ACCIDENTS ANALYSIS”, Subsection 4.3, “Analysis Method”, states that “This calculation covers the new fuel storage racks in NFP and the spent fuel storage racks of Region I and Region II in SFP. Region I racks are structurally stronger than Region II racks. To conservatively estimate the damage of the racks due to the postulated drop accidents, the calculation is performed for Region II racks. Since the new fuel storage rack is held down by firmly attached to the embedment plates of NFP using a stud bolt and is supported by additional intermediate plate, and has no “poison zone”, the drop accident evaluation is performed only for the case of drop (away from pedestal) on baseplate of the fuel rack”. The applicant is requested to provide the technical basis for concluding that the spent fuel storage racks of Region I are structurally stronger than the Region II racks and also provide a technical justification that the dynamic response and the design safety factors for the Region II racks will bound the Region I racks and the design stress limits for region I racks will not be exceeded under the required load combinations in the Table 3-1. The applicant is requested to identify any proposed changes to and provide a mark-up of Subsections in the DCD Tier 2 and the report APR1400-H-N-NR-14012-P, Rev.0, as appropriate.	DCD **No** PRA **No** Technical Specifications **No** Technical/Topical/ Environmental Reports **Yes**	4.3.2
34	The 10 CFR Part 50, Appendix A, General Design Criteria (GDC) 1, 2, 4, 5, 63, and 10CFR 52.80 (a) provide the regulatory requirements for the design of the new and spent fuel storage facilities. Standard Review Plan (SRP)	DCD **Yes** PRA	3.2.2.1 3.2.2.2 3.7.1 Table 3-9

	Sections 9.1.2 and 3.8.4, Appendix D describes specific SRP acceptance criteria for the review of the fuel racks that are acceptable to meet the relevant requirements of the Commission's regulations identified above. In DCD Tier 2, Section 9.1.2.2.3, “New and Spent Fuel Storage Rack Design”, the applicant stated that “The dynamic and stress analyses are performed as described in report APR1400-H-N-NR-14012- P & NP”. In the technical report APR1400-H-N-NR-14012-P, Rev 0, Subsections 3.2.2.1 and 3.2.2.2, the applicant provided the acceptance criteria for normal and upset conditions, Service Level A and Service Level B respectively, but did not discuss or provide the evaluation results for the normal and upset conditions. In accordance with SRP 3.8.4 Appendix D I (6), the applicant is requested to provide its evaluation results for the normal and upset conditions. The applicant is requested to identify any proposed changes to and provide a mark-up of Subsections in the DCD Tier 2 and the report APR1400-H-N-NR-14012- P, Rev.0, as appropriate.	**No** Technical Specifications **No** Technical/Topical/ Environmental Reports **Yes**	4.5
35	The 10 CFR Part 50, Appendix A, General Design Criteria (GDC) 1, 2, 4, 5, 63, and 10CFR 52.80 (a) provide the regulatory requirements for the design of the new and spent fuel storage facilities. Standard Review Plan (SRP) Sections 9.1.2 and 3.8.4, Appendix D describes specific SRP acceptance criteria for the review of the fuel racks that are acceptable to meet the relevant requirements of the Commission's regulations identified above. In DCD Tier 2, Section 9.1.2.2.3, “New and Spent Fuel Storage Rack Design”, the applicant stated that “The dynamic and stress analyses are performed as described in report APR1400-H-N-NR-14012- P & NP”. In the technical report APR1400-H-N-NR-14012-P, Rev 0, Subsection 3.2.2.2, “Upset Conditions (Level B)”, the Service Level B acceptance criteria states that “allowable stress of Level A is used for Level B for conservatism”. The staff notes that in Section 4.3.5, “Methodology for Stuck Fuel Accident”, the applicant did not use the allowable stress of Level A but instead increased the Service Level A allowable in shear to Service Level B allowable. In accordance with SRP 3.8.4 Appendix D I (6), the applicant is requested to clarify the apparent inconsistency in the implementation of its Service Level B acceptance criteria for the stuck fuel assembly scenario. The applicant is also requested to provide the results of its evaluation and safety factors for the cell wall tensile stress, cell to cell weld shear stress, and the base metal shear stress for this accident scenario. The applicant is requested to identify any proposed changes to and provide a mark-up of Subsections in the DCD Tier 2 and the report APR1400-H-N-NR-14012-P, Rev.0, as appropriate.	DCD **No** PRA **No** Technical Specifications **No** Technical/Topical/ Environmental Reports **Yes**	4.2(4) 4.5(4) Table 4-2
36 (except e)	The 10 CFR Part 50, Appendix A, General Design Criteria (GDC) 1, 2, 4, 5, 63, and 10CFR 52.80 (a) provide the regulatory requirements for the design of the new and spent fuel storage facilities. Standard Review Plan (SRP) Sections 9.1.2 and 3.8.4, Appendix D describes specific SRP acceptance criteria for the review of the fuel racks that are acceptable to meet the relevant requirements of the Commission's regulations identified above. In DCD Tier 2, Section 9.1.2.2.3, “New and Spent Fuel Storage Rack Design”, the applicant stated that “The dynamic and stress analyses are performed as described in report APR1400-H-N-NR-14012- P & NP”. In the technical report APR1400-	DCD **No** PRA **No** Technical Specifications **No** Technical/Topical/ Environmental	**See below**

	H-N-NR-14012-P, Rev 0, Subsection 3.7.1.1, “Displacements of Rack”, it is stated that “Actually, impact on rack-to-rack occurs at baseplate of the SFSRs because the installed racks are in contact with each other. The maximum impact loads generated at the NFSRs and the SFSRs are summarized in Table 3-10.” In Subsection 3.7.1.3 (2), “Impact Loads”, it is stated that “The prominent baseplate of the fuel storage rack for the APR1400 design is installed almost in contact with the adjacent baseplate.” In accordance with SRP 3.8.4 Appendix D I (3, 5), the applicant is requested to provide the following information so that the staff can perform its safety evaluation of the seismic analysis of new and spent fuel storage racks (NFSR and SFSR). a. For NFSR and SFSR, provide the baseplate dimensions and layout and plan view clearly showing gap or no gap between the adjacent baseplates; the gaps between the baseplates and the spent fuel pool walls; and the rack-to-rack gaps at midheight and at the top of the racks. Identify the elevation of the gaps shown in Figure 2-4. b. Discuss how the effect of adjacent baseplates that are in contact is modeled in the nonlinear dynamic models. c. The pool multi-rack dynamic analysis model in Figure 3-2 shows gaps between the adjacent base plates of all 29 racks. Describe how the contact between the baseplates is modeled in the whole pool multi-rack model. If the racks are installed such that their baseplates are in contact, provide the technical basis why the whole pool multi-rack model, with gaps, shown in Figure 3-2, predicts conservative dynamic responses for the racks and SFP walls. d. Discuss how the thermal load effects are considered for the installed racks that are in contact (no gap) with each other at the baseplate. Also discuss the effect on the design forces at the pedestal due to the thermal expansion of the installed racks.	Reports **Yes**	 Figure 2-1 Figure 2-5 Figure 2-6 3.1.2.1 3.1.2.2 3.1.2.1 3.1.2.2 3.7.1.1 3.2.2 3.7.3.5(3)
37	The 10 CFR Part 50, Appendix A, General Design Criteria (GDC) 1, 2, 4, 5, 63, and 10CFR 52.80 (a) provide the regulatory requirements for the design of the new and spent fuel storage facilities. Standard Review Plan (SRP) Sections 9.1.2 and 3.8.4, Appendix D describes specific SRP acceptance criteria for the review of the fuel racks that are acceptable to meet the relevant requirements of the Commission's regulations identified above. In DCD Tier 2, Section 9.1.2.2.3, “New and Spent Fuel Storage Rack Design”, the applicant stated that “The dynamic and stress analyses are performed as described in report APR1400-H-N-NR-14012- P & NP”. In the technical report APR1400-H-N-NR-14012-P, Rev 0, Table 3-9, “Maximum Loads on single Pedestal”, the applicant provided the pedestal forces for the new and spent fuel racks. In accordance with SRP 3.8.4 Appendix D I (5), the applicant is requested to provide the details how the pedestal forces were converted to the bending moment and shear force at the bottom baseplate-to-pedestal interface. The applicant is requested to identify any proposed changes to and provide a mark-up of Subsections in the DCD Tier 2 and the report APR1400-H-	DCD **No** PRA **No** Technical Specifications **No** Technical/Topical/ Environmental Reports **Yes**	3.7.1.2 3.7.2.2 3.7.3.1 3.2.2.1 3.7.1.2 3.2.2.3(3) 3.2.3

	N-NR-14012-P, Rev.0, as appropriate.		
38	The 10 CFR Part 50, Appendix A, General Design Criteria (GDC) 1, 2, 4, 5, 63, and 10CFR 52.80 (a) provide the regulatory requirements for the design of the new and spent fuel storage facilities. Standard Review Plan (SRP) Sections 9.1.2 and 3.8.4, Appendix D describes specific SRP acceptance criteria for the review of the fuel racks that are acceptable to meet the relevant requirements of the Commission's regulations identified above. In DCD Tier 2, Section 9.1.2.2.3, “New and Spent Fuel Storage Rack Design”, the applicant stated that “The dynamic and stress analyses are performed as described in report APR1400-H-N-NR-14012- P & NP”. In the technical report APR1400-H-N-NR-14012-P, Rev 0, Subsection 3.7.3.3 (3) “Cell-to-Cell Weld” provides a general description of the forces considered in the evaluation of cell-to-cell welds but did not provide any descriptions of how the stresses in the weld were calculated. In accordance with SRP 3.8.4 Appendix D I (3, 4, 5, 6), the applicant is requested to provide details of how the stresses in the cell-to-cell welds were determined, including a free-body diagram explaining how the loads were transferred and used to evaluate the cell-to-cell welds. The applicant is requested to identify any proposed changes to and provide a mark-up of Subsections in the DCD Tier 2 and the report APR1400-H-N-NR-14012-P, Rev.0, as appropriate.	DCD **No** PRA **No** Technical Specifications **No** Technical/Topical/ Environmental Reports **Yes**	3.7.3.3 Figure 3-19
39	The 10 CFR Part 50, Appendix A, General Design Criteria (GDC) 1, 2, 4, 5, 63, and 10CFR 52.80 (a) provide the regulatory requirements for the design of the new and spent fuel storage facilities. Standard Review Plan (SRP) Sections 9.1.2 and 3.8.4, Appendix D describes specific SRP acceptance criteria for the review of the fuel racks that are acceptable to meet the relevant requirements of the Commission's regulations identified above. In DCD Tier 2, Section 9.1.2.2.3, “New and Spent Fuel Storage Rack Design”, the applicant stated that “The dynamic and stress analyses are performed as described in report APR1400-H-N-NR-14012- P & NP”. In the technical report APR1400-H-N-NR-14012-P, Rev 0, Subsection 3.7.3.3(2) “Baseplate-to-Pedestal Weld”, it is stated that “The weld between baseplate and support pedestal is checked using finite element analysis to determine that the maximum stress is 124.1 MPa (17,992 psi) under a Level D condition”. In accordance with SRP 3.8.4 Appendix D I (3, 4, 5, 6), the applicant is requested to provide details of the finite element analysis performed, including the finite element computer program, the computer model, and the loads considered in the weld stress analysis. The applicant is requested to identify any proposed changes to and provide a mark-up of Subsections in the DCD Tier 2 and the report APR1400- H-N-NR-14012-P, Rev.0, as appropriate.	DCD **No** PRA **No** Technical Specifications **No** Technical/Topical/ Environmental Reports **Yes**	3.7.3.3(2)
40	The 10 CFR Part 50, Appendix A, General Design Criteria (GDC) 1, 2, 4, 5, 63, and 10CFR 52.80 (a) provide the regulatory requirements for the design of the new and spent fuel storage facilities. Standard Review Plan (SRP) Sections 9.1.2 and 3.8.4, Appendix D describes specific SRP acceptance criteria for the review of the fuel racks that are acceptable to meet the relevant requirements of the Commission's regulations identified above. In DCD Tier 2,	DCD **No** PRA **No** Technical Specifications	3.2.2.3 3.7.3.5(2)

	Section 9.1.2.2.3, “New and Spent Fuel Storage Rack Design”, the applicant stated that “The dynamic and stress analyses are performed as described in report APR1400-H-N-NR-14012- P & NP”. In the technical report APR1400-H-N-NR-14012-P, Rev 0, the applicant in Subsection 3.2.2.3 “Faulted (Abnormal) Conditions (Level D)”, specified the allowable compressive stress as two-thirds of the critical buckling stress for the stress limit criteria for combined axial compression + bending loads,. However, in subsection 3.7.3.4(2), “Local Stress Evaluation”, the applicant calculated the critical buckling stress of 12,731 psi but did not reduce it to two-thirds to obtain allowable compressive stress for the rack cell wall. In accordance with SRP 3.8.4 Appendix D I (3), the applicant is requested to provide the technical justification for using the calculated critical buckling stress as the limit under Service Level D condition, instead of the two-thirds of the critical buckling stress as stated in the Level D stress limit criteria. Also, in the calculation of critical buckling stress, BETA (value of coefficient) = 4.0 is used. The applicant is requested to explain what boundary conditions are assumed on the long edges of the simplified cell wall buckling model, and provide the technical basis for this designation. The applicant is requested to identify any proposed changes to and provide a mark-up of Subsections in the DCD Tier 2 and the report APR1400- H-N-NR-14012-P, Rev.0, as appropriate.	**No** Technical/Topical/ Environmental Reports **Yes**	
41	The 10 CFR Part 50, Appendix A, General Design Criteria (GDC) 1, 2, 4, 5, 63, and 10CFR 52.80 (a) provide the regulatory requirements for the design of the new and spent fuel storage facilities. Standard Review Plan (SRP) Sections 9.1.2 and 3.8.4, Appendix D describes specific SRP acceptance criteria for the review of the fuel racks that are acceptable to meet the relevant requirements of the Commission's regulations identified above. In DCD Tier 2, Section 9.1.2.2.3, “New and Spent Fuel Storage Rack Design”, the applicant stated that “The dynamic and stress analyses are performed as described in report APR1400-H-N-NR-14012- P & NP”. In accordance with SRP 3.8.4 Appendix D I (3, 4, 5, 6), the applicant is requested to provide the following additional information in the technical report. (a) In the technical report APR1400-H-N-NR-14012-P, Rev 0, Subsection 3.7.2, “Fuel structural Evaluation”, the applicant did not discuss the location of the impact on the fuel where the maximum impact force occurs. The applicant is requested to provide the impact load for both the top and at the mid height of the fuel assembly. The staff notes in Subsection 3.1.2.2**,** “Details for Rack and Fuel Assembly**”,** that “The mass of the upper, the central and the lower nodes is 1/4, 1/2 and 1/4 of the total mass, respectively”. Since only 25 percent of the mass is assumed at the ends of the fuel assembly, there is a potential for a higher g-load on the fuel assembly at the top compared to that at the mid height if the impact load at the top of the fuel assembly is more than half the impact load calculated at the mid height. The applicant is requested to provide a technical justification for not determining the g-load on the fuel assembly at the top and at the mid-height and then using the maximum of the g-load in subsequent	DCD **No** PRA **No** Technical Specifications **No** Technical/Topical/ Environmental Reports **Yes**	3.7.1.3(1) 3.7.2.1 3.1.2.2(1)

	fuel assembly structural integrity evaluations. (b) The staff in reviewing Table 3-10, “Impact Loads on Rack”, notes that the impact load on the fuel assembly in the East-West and North-South directions is 25000 lbf and 18,594 lbf respectively. In subsection 3.7.2,”Fuel structural Evaluation”, the applicant considered only the 25000 lbf load in evaluation the fuel assembly. The applicant is requested to provide the technical basis for not combining the impact load on the fuel assembly in the north-south and east-west directions simultaneously to obtain the total lateral impact load for use in evaluating the structural integrity of the fuel assembly. (c) The applicant is also requested to provide the general criteria used for combining the seismic responses in the design and analysis of the fuel assembly, rack structure, welded connections, and the rack supports of NFSR and SFSR due to the SSE excitation along the three orthogonal directions (2 horizontal and vertical) imposed simultaneously. The applicant is requested to identify any proposed changes to and provide a mark-up of Subsections in the DCD Tier 2 and the report APR1400-H-N-NR-14012-P, Rev.0, as appropriate.		3.7.1.3 3.7.2 Table 3-8 Table 3-11 3.1.2.1 3.7
42	The 10 CFR Part 50, Appendix A, General Design Criteria (GDC) 1, 2, 4, 5, 63, and 10CFR 52.80 provide the regulatory requirements for the design of the new and spent fuel storage facilities. Standard Review Plan (SRP) Sections 9.1.2 and 3.8.4, Appendix D describes specific SRP acceptance criteria for the review of the fuel racks that are acceptable to meet the relevant requirements of the Commission's regulations identified above. In DCD Tier 2, Section 9.1.2.2.3, “New and Spent Fuel Storage Rack Design”, the applicant stated that “The dynamic and stress analyses are performed as described in report APR1400-H-N-NR-14012- P & NP”. In the technical report APR1400-H-N-NR-14012-P, Rev 0, Table 3-11, “Stress Evaluation for Fuel Assembly”, the applicant provides allowable limit for fuel grid spacer and fuel rod cladding. The staff did not find the basis for the bending stress calculation in the fuel rod cladding reported in the Table 3-11. In order for the staff to perform its safety evaluation of the fuel assembly, the applicant in accordance with SRP 3.8.4 Appendix D I (6) is requested to provide the technical basis for calculating the bending stress and the acceptance criteria used for the evaluation the fuel cladding. The applicant is also requested to provide the stress/strain evaluation of fuel cladding and an evaluation of the fuel channel. The applicant is requested to identify any proposed changes to and provide a mark-up of Subsections in the DCD Tier 2 and the report APR1400-H-N-NR-14012-P, Rev.0, as appropriate.	DCD **No** PRA **No** Technical Specifications **No** Technical/Topical/ Environmental Reports **Yes**	3.7.2.2 Table 3-11
43	The 10 CFR Part 50, Appendix A, General Design Criteria (GDC) 1, 2, 4, 5, 63, and 10CFR 52.80 provide the regulatory requirements for the design of the new and spent fuel storage facilities. Standard Review Plan (SRP) Sections 9.1.2 and 3.8.4, Appendix D describes specific SRP acceptance criteria for the review of the fuel racks that are acceptable to meet the relevant requirements of the	DCD **No** PRA **No** Technical	3.7.3.5(4)

	Commission's regulations identified above. In DCD Tier 2, Section 9.1.2.2.3, “New and Spent Fuel Storage Rack Design”, the applicant stated that “The dynamic and stress analyses are performed as described in report APR1400-H-N-NR-14012- P & NP”. In the technical report APR1400-H-N-NR-14012-P, Rev 0, Subsection 3.7.3, “Rack structural evaluation”, the staff did not find the punching shear evaluation of the baseplate against the rack pedestal impact loads. The credible failure mode for the rack baseplate is a punching shear failure due to the concentrated load transmitted by a support pedestal under SSE conditions and impact load on the rack baseplate due to an accidental drop of a fuel assembly. In order for the staff to perform its safety evaluation of the rack supports, the applicant in accordance with SRP 3.8.4 Appendix D I (3) is requested to demonstrate that the capacity of the baseplate against the punching is larger than the calculated rack pedestal impact load. The applicant is requested to identify any proposed changes to and provide a mark-up of Subsections in the DCD Tier 2 and the report APR1400-H-N-NR-14012-P, Rev.0, as appropriate.	Specifications **No** Technical/Topical/ Environmental Reports **Yes**	
44	The 10 CFR Part 50, Appendix A, General Design Criteria (GDC) 1, 2, 4, 5, 63, and 10CFR 52.80 (a) provide the regulatory requirements for the design of the new and spent fuel storage facilities. Standard Review Plan (SRP) Sections 9.1.2 and 3.8.4, Appendix D describes specific SRP acceptance criteria for the review of the fuel racks that are acceptable to meet the relevant requirements of the Commission's regulations identified above. SRP Section 3.8.4, “Other Seismic Category I Structures,” Appendix D (7) in parts requires that the applicant should describe materials, quality control procedures, and any special construction techniques. In DCD Tier 2, Section 9.1.2, the staff did not find the governing quality control requirements and procedure for design and construction for the spent fuel storage racks. The staff also did not find the manufacturing process; special fabrication techniques; and the sequences used for constructing the fuel storage racks to reduce fabrication distortions and to provide accessibility for inspection. In accordance with SRP 3.8.4 Appendix D, and Appendix A to 10 CFR Part 50, General Design Criteria 1, 2, 4, 5, 61, 63, the applicant is requested to provide governing quality control requirements and procedure and any special fabrication and construction techniques used for constructing the fuel storage racks.	**DCD** **Yes** PRA **No** Technical Specifications **No** Technical/Topical/ Environmental Reports **Yes**	2.3
47	The 10 CFR Part 50, Appendix A, General Design Criteria (GDC) 1, 2, 4, 5, 63, and 10CFR 52.80(a) provide the regulatory requirements for the design of the new and spent fuel storage facilities. Standard Review Plan (SRP) Sections 9.1.2 and 3.8.4, Appendix D describes specific SRP acceptance criteria for the review of the fuel racks that are acceptable to meet the relevant requirements of the Commission's regulations identified above. In DCD Tier 1 Subsections 2.7.4.1.1 and 2.7.4.2.1, the new and the spent fuel racks respectively, are stated as “non-safety related, but seismic Category I for integrity of the spent fuel assemblies”. SRP Section 3.8.4, Appendix D states that “The Regulatory Guide 1.29, “Seismic Design Classification” classifies spent fuel pool racks as seismic Category I structures. Spent fuel pool racks should be treated as safety-related components for determining	DCD **Yes** PRA **No** Technical Specifications **No** Technical/Topical/ Environmental Reports **Yes**	2.3.3

	Quality Assurance requirements (10 CFR Part 50, Appendix B) and periodic condition monitoring requirements (10 CFR 50.65 “Maintenance Rule”)”. In accordance with SRP 3.8.4 Appendix D, and Appendix A to 10 CFR Part 50, General Design Criteria 1, 2, 4, 5, 61, 63, the applicant is requested to provide justification for treating the racks as non-safety related components and provide the basis for determining the Quality Assurance requirements (10 CFR Part 50, Appendix B) and periodic condition monitoring requirements (10 CFR 50.65 “Maintenance Rule”)” for the racks.		
50a	Title 10 of the Code of Federal Regulations (10 CFR) Part 50, Appendix A, General Design Criteria 4 requires SSCs to be designed and fabricated to accommodate the effects of environmental conditions during normal, off normal, and accident conditions. On November 13th 2015 the applicant provided docketed responses to eight of the ten items of concern that were sent as part of a request for a July 29th, 2015 public meeting on DCD Tier 2, FSAR Section 9.1.1 (ML15317A525). On Issue #4 (AI 9.24.4) the applicant provided the staff with the following: Information of the welding, cleanness and general fabrication sequence of fuel rack is as follows; 1) Welding Welding information for fabrication of fuel rack is as follows; (1) Welding materials shall be selected and controlled to contain between 8 and 25 percent ferrite, as determined by Subsection NB-2433 of the ASME Code. Electrodes shall conform to ASME SFA 5.4 or 5.9, Type 308. Commonly, for avoidance of sensitization of austenitic stainless steel, Type 308L is used as electrodes. (2) Austenitic stainless steel items shall not be heated above 177°C (350°F) (except during welding), unless they are subsequently given a full solution anneal at temperatures recommended for the individual types of stainless steel followed by water quenching or spraying from the solution heat treating temperature to below 427°C (800°F) (or black metal) within three minutes. 2) Cleanness (1) All internal and external surfaces shall be thoroughly cleaned of scale, dirt, chips, nonadherent weld spatter (which can be removed by power wire brushing), oil, grease, organic matter, loose particles, and all other potentially harmful materials. Adherent weld spatter on the interior surface of a fuel storage location shall be removed, such that the function of the mock fuel assembly inspection gage is not hindered by weld spatter. (2) Components, parts and subassemblies, that will have crevices or inaccessible surfaces after assembly, shall be cleaned prior to assembly. Acidic materials shall not be used on items containing crevices or inaccessible areas where complete drainage, neutralization, or removal of residuals cannot be accomplished. (3) Cleaning of corrosion-resistant materials shall be in accordance with ASME NQA-1 to the extent specified herein. The surfaces of cleaned components shall, as a minimum, meet the requirements of ASME NQA-1, Part II,	DCD **Yes** PRA **No** Technical Specifications **No** Technical/Topical/ Environmental Reports **Yes**	2.3 2.3.4 2.3.5

	Subpart 2.1, Class C. 3) General fabrication sequence General fabrication sequences for new and spent fuel racks are as follows; (These sequences present the fabrication process of major parts for racks) • General fabrication sequence for new fuel rack • Step 1: Fabricating the box. • Step 2: Fabricating the base plate for assembling with box. • Step 3: Fabricating the support for shoring up the fuel rack weight. • Step 4: Assembling the base plate with support. (called support assembly) • Step 5: Assembling the box with support assembly. • General fabrication sequence for spent fuel rack • Step 1: Fabricating the box. • Step 2: Fabricating the sheathing plate for fastening the location of neutron absorbing material and protecting the neutron absorbing material. • Step 3: Assembling the box with neutron absorbing material and sheathing plate. (called box assembly) Location of neutron absorbing material is between box and sheathing plate. Welding among each item is as follows: • Box and sheathing plate : Resistance weld (Spot weld)/Intermittent fillet weld • Box and neutron absorbing material : No weld • Sheathing plate and neutron absorbing material : No weld • Step 4: Fabricating the base plate for assembling with box assembly. • Step 5: Fabricating the support for shoring up the fuel rack weight. • Step 6: Assembling the base plate with support. (called support assembly) • Step 7: Assembling the box assembly with support assembly. There are two methods to install liner plates in spent fuel pool; (1) Wall-paper Type (floors): Liner plates are field welded to stainless steel embedment strips in the concrete. (2) Form Type(walls): Liner plates (with its anchorage system) are field welded together as a complete unit or shop welded together as a module at the SSLP assembly filed shop which act initially as form work during concrete placement of walls and subsequently as a leak tight membrane. Add this information to the SAR or technical report APR1400-H-N-NR-14012.		2.3 Figures 2-11 to 2-15 Outside scope of technical report (i.e., SFP topic not fuel rack)